Continuous Assessment of Epileptic Seizures with Wrist-worn Biosensors

by

Ming-Zher Poh

Bachelor of Science in Electrical and Computer Engineering
Cornell University (2005)
Master of Science in Electrical Engineering and Computer Science
Massachusetts Institute of Technology (2007)

Submitted to the Harvard-MIT Division of Health Sciences and Technology
in partial fulfillment of the requirements for the degree of

Doctor of Philosophy in Electrical and Medical Engineering

at the

MASSACHUSETTS INSTITUTE OF TECHNOLOGY

September 2011

Author .....
Harvard-MIT Division of Health Sciences and Technology
September 2011

Certified by .....
Rosalind W. Picard
Professor of Media Arts and Sciences
Thesis Supervisor

Accepted by .....
Ram Sasisekharan
Director of Harvard-MIT Division of Health Sciences and Technology

Continuous Assessment of Epileptic Seizures with Wrist-worn Biosensors

by

Ming-Zher Poh

Submitted to the Harvard-MIT Division of Health Sciences and Technology
on September 2011, in partial fulfillment of the
requirements for the degree of
Doctor of Philosophy in Electrical and Medical Engineering

Abstract

Epilepsy is a neurological disorder characterized predominantly by an enduring predisposition to generate epileptic seizures. The apprehension about injury, or even death, resulting from a seizure often overshadows the lives of those unable to achieve complete seizure control. Moreover, the risk of sudden death in people with epilepsy is 24 times higher compared to the general population and the pathophysiology of sudden unexpected death in epilepsy (SUDEP) remains unclear. This thesis describes the development of a wearable electrodermal activity (EDA) and accelerometry (ACM) biosensor, and demonstrates its clinical utility in the assessment of epileptic seizures.

The first section presents the development of a wrist-worn sensor that can provide comfortable and continuous measurements of EDA, a sensitive index of sympathetic activity, and ACM over extensive periods of time. The wearable biosensor achieved high correlations with a Food and Drug Administration (FDA) approved system for the measurement of EDA during various classic arousal experiments. This device offers the unprecedented ability to perform comfortable, long-term, and in situ assessment of EDA and ACM.

The second section describes the autonomic alterations that accompany epileptic seizures uncovered using the wearable EDA biosensor and time-frequency mapping of heart rate variability. We observed that the post-ictal period was characterized by a surge in sympathetic sudomotor and cardiac activity coinciding with vagal withdrawal and impaired reactivation. The impact of autonomic dysregulation was more pronounced after generalized tonic-clonic seizures compared to complex partial seizures. Importantly, we found that the intensity of both sympathetic activation and parasympathetic suppression increased approximately linearly with duration of post-ictal EEG suppression, a possible marker for the risk of SUDEP. These results highlight a critical window of post-ictal autonomic dysregulation that may be relevant in the pathogenesis of SUDEP and hint at the possibility for assessment of SUDEP risk by autonomic biomarkers.

Lastly, this thesis presents a novel algorithm for generalized tonic-clonic seizure detection with the use of EDA and ACM. The algorithm was tested on 4213 hours (176 days) of recordings from 80 patients containing a wide range of ordinary daily activities and detected 15/16 (94%) tonic-clonic seizures with a low rate of false alarms ($\leq$ 1 per 24 h). It is anticipated that the proposed wearable biosensor and seizure detection algorithm will provide an ambulatory seizure alarm and improve the quality of life of patients with uncontrolled tonic-clonic seizures.

Thesis Supervisor: Rosalind W. Picard
Title: Professor of Media Arts and Sciences

Thesis Committee

Thesis Supervisor
Rosalind W. Picard, Sc.D.
Professor of Media Arts and Sciences
Massachusetts Institute of Technology

Thesis Chair
John V. Guttag, Ph.D.
Dugald C. Jackson Professor of Computer Science and Engineering
Massachusetts Institute of Technology

Thesis Reader
Richard J. Cohen, M.D., Ph.D.
Whitaker Professor in Biomedical Engineering
Massachusetts Institute of Technology

Thesis Reader
Tobias Loddenkemper, M.D.
Assistant Professor of Neurology
Harvard Medical School

Acknowledgments

"Many are the plans in a person's heart, but it is the LORD's purpose that will prevail." Proverbs 19:21

Upon re-reading my graduate school statement of intent written six years ago, I realized how different my experience ended up being compared to what I had envisioned it to be. The beginning was rough as I struggled with work and a sense of emptiness despite being admitted into the Ph.D. program of my dreams. But I soon learned that true satisfaction and joy can only come from the Lord for He is the one who gives meaning and purpose to my life. By God's grace, my overall experience at MIT has been fantastic, one that has certainly helped me grow in many ways. So above all, I thank God for guiding me every step of the way, and for all the blessings in my life.

I want to express my deepest gratitude to my supervisor, Prof. Rosalind Picard, for being such an amazing mentor. It was Roz who gave me the opportunity to enter to wonderful, wacky world of the Media Lab. She trusted me from the very beginning and gave me so much freedom to explore and pursue ideas that interested me. Furthermore, Roz was always happy to share her godly wisdom and to support me in prayer. I couldn't have asked for a better advisor.

I am sincerely grateful to my thesis committee including Prof. John Guttag, Prof. Richard Cohen and Dr. Tobias Loddenkemper for helping me improve and achieve my research goals. John kindly chaired the committee and was a constant source of encouragement and advice. Richard brought along insight and expertise in physiologic signal analysis. Tobi was my primary collaborator at Children's Hospital who was a joy to work with and he taught me so much about epilepsy.

I would like to thank my other collaborators who contributed greatly to this work. In particular, Dr. Claus Reinsberger for performing the video-EEG analysis and teaching me about the autonomic nervous system, Dr. Eun-Hyoung Park for setting up and maintaining the data transfer process, Lolli Fleming for handling all the IRB issues and Dr. Joseph Madsen for helping us get the study up and running at Children's Hospital.

I'm grateful to all my labmates from the Affective Computing group. In particular, I thank Hyungil Ahn for showing me the ropes from day one, Yuta Kuboyama for being a great friend and sharing lunch breaks, Ehsan Hoque for improving my ping-pong skills,

Kyunghee Kim for helping me with the Heartphones project, Javier Hernandez for sharing his knowledge on SVMs, and Daniel Bender for being an awesome group administrator. I'm grateful to Daniel McDuff for his friendship and happy that we ended up as roommates and labmates. I'm also thankful to Jackie Lee for his encouragement as we worked towards completing our theses and defences together, as well as for his infectious entrepreneurial spirit. It's been a pleasure to get to know Rana el Kaliouby, Matthew Goodwin, Richard Fletcher, Shani Daily, Hoda Eydgahi, Micah Eckhardt, Rob Morris, Elliott Hedman and Akane Sano. I thank the Media Lab community as a whole, for creating a family-like atmosphere and making the lab one of the best places to work at.

Special thanks to the UROPs I've had the privilege of mentoring including Nicholas Swenson, Shubhi Goyal, Mangwe Sabtala and Andrew Goessling. In particular, Nick always was eager to learn and full of enthusiasm in his work.

Graduate school can be such a lonely experience without friends. So I'm thankful for all my friends at MIT including my HST mates Sukant Mittal, Yongkeun Park, Euiheon Chung and Benjamin Diop. Sukant and I went through the ups and downs of graduate life together and I'm glad to have a friend like him. My friends from the GCF have been a tremendous source of support. In particular, I thank Adekunle Adeyemo, Samuel Perli, David Kwabi, John Lee, Po-Ru Lo, Daniel McDuff, Eric Jones, Sze Zheng Yong and Louis Tee for being like brothers to me.

I cannot fully express how grateful I am for my parents. Mum and Dad have always been there to encourage me and never stopped praying for me. This thesis is dedicated to them in recognition of their love and support all these years. I thank my sisters, Jen and Lisa for cheering me on all the way. Lastly, my deepest thanks goes to Yukkee, who shared my burdens, gave me confidence and more importantly, for being a loving wife. I love you.

Contents

1 Introduction **23**

1.1 Epilepsy 23

1.1.1 Seizures 24

1.1.2 Treatment of Epilepsy 24

1.1.3 Mortality in Epilepsy 25

1.2 Sudden, Unexpected Death in Epilepsy 25

1.2.1 Risk Factors and Pathophysiology of SUDEP 26

1.3 Seizure Prediction and Detection 28

1.3.1 Seizure Detection Using Wearable Biosensors 29

1.4 Overall Aims 30

1.5 Thesis outline 31

2 Autonomic Alterations in Epilepsy **33**

2.1 Autonomic Nervous System 33

2.2 Heart Rate Variability 34

2.2.1 Regulation of Heart Rate Variability as a Predictor of Sudden Death 34

2.2.2 Potential Autonomic Mechanisms in SUDEP 36

2.3 Electrodermal Activity 37

2.3.1 Electrodermal Activity in Epilepsy 38

3 A Wearable Electrodermal Activity and Accelerometry Biosensor **41**

3.1 Introduction 41

3.2 Related Work 43

3.3 System Design 44

3.3.1 Circuit Design 44

3.3.2 Sensor Module 46
3.3.3 Packaging 47
3.4 Experimental Methods 49
3.4.1 Participants 49
3.4.2 Physiological Measurements 50
3.4.3 Physical Task 51
3.4.4 Cognitive Task 51
3.4.5 Emotional Task 52
3.4.6 Long-term In Situ Experiment 52
3.4.7 Data Analysis 52
3.5 Results 52
3.5.1 EDA Increases During Stressor Tasks 52
3.5.2 Recordings of Proposed System are Highly Accurate and Strongly Correlated with FDA System 54
3.5.3 Distal Forearm is a Viable EDA Recording Site 56
3.5.4 Long-term In Situ EDA Recordings Reveal Patterns in Autonomic Arousal 57
3.6 Discussion 58
3.7 Conclusion 61

4 Autonomic Footprints of Epileptic Seizures **63**
4.1 Introduction 63
4.2 Experimental Methods 65
4.2.1 Patients and Seizures 65
4.2.2 Wearable EDA Biosensors 65
4.2.3 Recordings 66
4.2.4 EEG Analysis 66
4.2.5 EDA Analysis 66
4.2.6 ECG Analysis: Time-frequency Mapping of Heart Rate Variability . 67
4.2.7 Statistical Analysis 68
4.3 Results 68

4.3.1 Autonomic Footprints Reveal Critical Window of Severe Imbalance after Tonic-Clonic Seizures 69
4.3.2 Comparison Between Complex Partial and Generalized Tonic-Clonic Seizures 74
4.3.3 Correlations Between Heart Rate, Sympathetic EDA and Parasympathetic HF Power 74
4.3.4 Magnitude of Autonomic Imbalance in Tonic-Clonic Seizures is Strongly Correlated with Post-Ictal Generalized EEG Suppression 75
4.3.5 Binary Outcome Analysis for Prolonged Post-Ictal EEG Attenuation 79
4.4 Discussion 80

5 Convulsive Epileptic Seizure Detection Using Electrodermal Activity and Accelerometry 85

5.1 Introduction 85
5.2 Related Work 88
5.3 Methods 90
5.3.1 Wearable EDA and ACM Biosensor 90
5.3.2 Patients and Seizures 90
5.3.3 EEG/ACM/EDA Analysis 91
5.3.4 Seizure Detection Architecture 91
5.3.5 Data Reduction 91
5.3.6 Feature Extraction 93
5.3.7 Support Vector Machines 97
5.3.8 Model Selection and Testing Methodology 98
5.4 Results 102
5.4.1 Performance Comparison of Seizure Detection Modes 102
5.4.2 Physiological Signal Fusion Improves Performance 103
5.4.3 False Alarms in Patients with No GTC Seizures 104
5.5 Discussion 105

6 Conclusions 111

6.1 Thesis Contributions 111
6.2 Other Relevant Contributions 113

6.3 Future Work 114
6.3.1 Home-based, Ambulatory Studies 114
6.3.2 Off-line Seizure Detection and Classification 114
6.3.3 Detection of Complex Partial Seizures/Subclinical Seizures 115
6.3.4 Responsive, Closed-Loop Devices 115
6.4 Outlook 116

A Supplementary Information on Design and Evaluation of Wearable Biosensor **117**

B Supplementary Information on Clinical Study **123**

C Supplementary Information on Autonomic Footprints of Epileptic Seizures **127**

D Supplementary Information on Convulsive Epileptic Seizure Detection **137**

List of Figures

1-1 *Outline of thesis aims.* 31

3-1 *(A) Circuit for EDA measurements. Computed profiles for the (B) voltage and (C) current flow across skin for a range of typical skin conductance values.* 45

3-2 *Overview of the EDA sensor system architecture. The device is capable of recording measurements onto an on-board flash memory card (data logging), wirelessly transmitting data to a remote site (data forwarding) and performing real-time analysis (data processing).* 46

3-3 *EDA sensor module. The device has a modular design and is shown with an optional radio transceiver mounted on top.* 47

3-4 *The wearable EDA sensor. (A) Final packaging in an attractive and inconspicuous wristband. (B) Disposable Ag/AgCl electrodes attached to the underside of the wristband. (C) The wearable EDA sensor can be worn comfortably on the wrist for long periods of time and during daily activities.* 48

3-5 *The experimental setup. Measurements were recorded from (I) right fingers with the Flexcomp system, (II) left fingers with the proposed sensor module, (III) right distal forearm with the proposed sensor module using Ag/AgCl electrodes and (IV) left distal forearm with the proposed sensor module using conductive fabric electrodes.* 50

3-6 *Example of a slide for the Stroop word-color matching test* 51

3-7 *EDA waveforms during (A) physical activity, (B) cognitive stressors and (C) emotional stressors (a horror movie clip). Measurements were recorded from (I) right fingers with the Flexcomp system, (II) left fingers with the proposed sensor module, (III) right distal forearm with the proposed sensor module using Ag/AgCl electrodes and (IV) left distal forearm with the proposed sensor module using conductive fabric electrodes.* 53

3-8 *Distributions of correlation coefficients between EDA measurements from bilateral fingers (I and II in Fig. 4) under (A) physical ($n = 13$), (B) cognitive ($n = 15$) and (C) emotional ($n = 13$) stressors. Each experiment was separated into baseline, task and recovery conditions for correlation. The median values of the correlation coefficients, $\tilde{r}$, are also presented for each condition.* 54

3-9 *Accuracy of the proposed sensor in fixed resistance measurements. Error bars represent 1 S.D. Inset: Computed sensitivity of the proposed sensor showing increasing quantization error at higher EDA values.* 55

3-10 *Distributions of correlation coefficients between EDA measurements from distal forearms (conductive fabric electrodes on the left distal forearm and Ag/AgCl electrodes on the right distal forearm) and ipsilateral fingers under (A) physical ($n = 13$), (B) cognitive ($n = 15$) and (C) emotional ($n = 13$) stressors. Each experiment was separated into a baseline, task and recovery conditions for correlation. The median values of the correlation coefficients, $\tilde{r}$, along with the performance indices (proportion of correlation coefficients geq 0.5), π, are also presented for each condition. Dashed lines indicate $r = 0.5$.* 56

3-11 *Long-term in situ EDA recordings. Continuous skin conductance measurements were recorded for seven days in a natural home environment. Daily EDA waveforms displayed are normalized (Scale bar on the right side indicates original values).* . . 58

4-1 *Long-term electrodermal activity (EDA) recordings obtained from a wearable biosensor. In this example of a 24 h continuous EDA recording from a single patient, four secondarily generalized tonic-clonic seizures (GTCS) were captured. Vertical red lines denote EEG seizure onset. Inset: The wearable biosensor consists of an inconspicuous wristband with an integrated sensor module that can be worn comfortably for long periods of time and during daily activities. The underside of the wristband is shown to reveal standard dry Ag/AgCl electrodes used for EDA measurements.* . 69

4-2 *Histogram of the onset times for the complex partial seizures (CPS) and secondarily generalized tonic-clonic seizures (GTCS) in this study. The occurrence times for both seizure types were distributed throughout the day and night.* 71

4-3 *Changes in autonomic activity after individual epileptic seizures. Examples of alterations in electrodermal activity (EDA), R-R intervals (RRI) along with time-frequency mapping of the RRI during peri-ictal segments of 75 min. (A) A small increase of EDA is observed with a decrease in RRI (i.e. increase in heart rate) during this complex partial seizure (CPS). There is also a brief reduction of the high frequency spectral component (HF, 0.15 - 0.4 Hz) of RRI during the post-ictal period that reappears after approximately 5 min. (B) A large surge in EDA is visible after this secondarily generalized tonic-clonic seizure (GTCS) accompanied by a drop in RRI. Note the reduction in RRI variability during the post-ictal period and the dramatic reduction of the high frequency power. Vertical red lines denote EEG seizure onset and offset.* 72

4-4 *Autonomic footprints of epileptic seizures. High-resolution profiles of autonomic alterations computed every minute during a peri-ictal period of 3 h for (A) complex partial seizures and (B) secondarily generalized tonic-clonic seizures. Each post-ictal measurement epoch was sequentially compared to the baseline level taken as the average of the entire 60 min pre-ictal period. Epochs in red indicate statistical significance after accounting for multiple comparisons using the False Discovery Rate controlling procedure ($p < 0.05$; paired, two-sided Wilcoxon signed rank test). Post-ictal levels of EDA were higher for 9 min after complex partial seizures ($n = 22$). Heart rate was also higher lasting 3 min ($n = 16$). HF power was continuously reduced for approximately 55 min ($n = 16$). Strikingly, the first 56 min after tonic-clonic seizures was associated with marked increases in EDA ($n = 12$) and heart rate ($n = 10$), as well as profound reduction in HF power ($n = 10$). Persistent tachycardia was observed for 40 min; heart rate and HF power levels recovered after 100 min. (C) EDA during the pre-ictal period was marginally similar between seizures ($p = 0.05$; Mann-Whitney-Wilcoxon test [MWW]), but was higher in tonic-clonic seizures during the first 60 min of the post-ictal period ($p = 0.004$; MWW). (D) There was no difference in pre-ictal HF power between seizures ($p > 0.5$; MWW), whereas post-ictal HF power was lower in tonic-clonic seizures ($p = 0.033$; MWW).* 73

4-5 *Correlation coefficients between EDA vs HR and HF vs HR during the (A) pre-ictal and (B) post-ictal period of complex partial seizures.* 75

4-6 *Correlation coefficients between EDA vs HR and HF vs HR during the (A) pre-ictal and (B) post-ictal period of generalized tonic-clonic seizures.* 75

4-7 *Post-ictal generalized EEG suppression (PGES) following a secondarily generalized tonic-clonic seizure. An example of a tonic-clonic seizure abruptly terminated and replaced by flattening of EEG signals in all channels.* 76

4-8 *Morphology of EDA changes relative to the onset/offset moments of PGES. The gray shaded areas represent the ictal period while the red shaded areas correspond to PGES. Seizures 9 and 11 did not exhibit PGES upon termination.* 77

4-9 *Relationship between degree of post-ictal autonomic disturbance and post-ictal generalized EEG suppression (PGES) in secondarily generalized tonic-clonic seizures (GTCS). Scatter plots of PGES duration vs (A) EDA response amplitude, (B) log-transformed area under rising portion of EDA curve and (C) maximum percentage HF power change. EDA response amplitude was strongly positively correlated with PGES (Pearson* $r = 0.81, p = 0.003; n = 11$*), as was the area under rising portion of EDA curve (*$r = 0.83, p = 0.002; n = 11$*). The reverse direction of relationship was observed for maximum percentage HF power change, which was strongly negatively correlated with PGES (*$r = -0.87, p = 0.002; n = 9$*). (D) The association between EDA response amplitude and PGES in GTCS on a patient-specific level showed close agreement in trends. Patient 2 had four GTCS events (top) and patient 5 had three GTCS events (bottom). (E) GTCS with higher SUDEP risk (PGES >* 20 *s) had a higher EDA response amplitude (*$p = 0.01$*; Mann-Whitney-Wilcoxon test [MWW]). (F) The maximum percentage decrease in HF power was greater in GTCS with higher SUDEP risk (*$p < 0.05$*; MWW).* 78

5-1 *Overview of seizure detection architecture.* 92

5-2 *Time-frequency mapping of the ACM signal during a tonic-clonic seizure (63 s long). The first 20 s do not contain much movement energy because the seizure starts off as a complex partial seizure before secondarily generalizing and affecting the motor cortex. The power distribution during the tonic clonic phase (after 20 s) is concentrated at frequencies above 2 Hz.* 94

5-3 *Example of recurrence plots for various events. Time series of net acceleration (top) along with the corresponding recurrence plot (bottom) during (A) a tonic-clonic seizure epoch (B) playing catch with a ball (C) shaking dice and (D) flapping hands.* 95

5-4 *Features extracted from a 10 s EDA epoch. Dotted line represents the least squares line fit. Green circles indicate measurement points that were greater than the previous point. Red squares indicate start and stop of the epoch.* 97

5-5 *ROC of the non-patient-specific (blue circles) and semi-patient-specific seizure (red squares) detectors.* 103

5-6 *Semi-patient-specific seizure detection performance. (A) Number of GTC seizures detected per patient. (B) Number of false alarms per 24 h per patient. (C) Latency of detection for each GTC seizure. *Seizure 10 (Patient 4) was not detected by the algorithm.* 104

5-7 *ROC of the semi-patient-specific seizure detector using solely ACM features (blue circles) and using both ACM and EDA features (red squares).* 105

5-8 *Histogram of False Alarm rates across 73 patients with no GTC seizures.* 106

A-1 *Layout of the EDA and ACM sensor board.* 118

A-2 *Individual EDA recordings of each participant during a physical task involving cycling. Measurements were made from (I) right fingers with Flexcomp, (II) left fingers with MIT sensor, (III) right distal forearm with MIT sensor using Ag/AgCl electrodes and (IV) left distal forearm with MIT sensor using conductive fabric electrodes* 119

A-3 *Individual EDA recordings of each participant during a cognitive task including a mental arithmetic test (MAT) and Stroop word-color matching test . Measurements were made from (I) right fingers with Flexcomp, (II) left fingers with MIT sensor, (III) right distal forearm with MIT sensor using Ag/AgCl electrodes and (IV) left distal forearm with MIT sensor using conductive fabric electrodes* 120

A-4 *Individual EDA recordings of each participant during an emotional task consisting watching a horror movie clip. Measurements were made from (I) right fingers with Flexcomp, (II) left fingers with MIT sensor, (III) right distal forearm with MIT sensor using Ag/AgCl electrodes and (IV) left distal forearm with MIT sensor using conductive fabric electrodes* 121

B-1 *Data collection from patients with epilepsy staying at the long-term monitoring unit at Children's Hospital Boston. Continuous video, electroencephalographic (EEG), electrocardiographic (EKG), electrodermal activity (EDA) and 3-D accelerometry (ACM) recordings were obtained throughout the stay. Patients were not constrained to remaining in the bed as the EEG recording system was ambulatory (backpack). Video frames shown depict patients wearing the wrist-worn biosensors and performing a variety of daily activities* 124

B-2 *Summary of data collected from clinical study performed from Jan to September 2009. (A) 94 patients were enrolled and 80 provided over 12 hours of complete EDA and ACM recordings. (B) Due to a server crash, only 64% of those patients had complete EEG-EKG-video recordings. (C) 11 patients experienced at least one complex partial seizure (CPS) or generalized tonic-clonic (GTC) seizure. 7 patients experienced at least one GTC seizure.* 125

B-3 *Example of a 24-hour recording from an 11-year-old female with refractory epilepsy. A single complex partial seizure and two GTC seizures that occurred during the monitoring period were accompanied by an increase in EDA.* 126

C-1 *Peri-ictal EDA recordings (sympathetic) of individual complex partial seizures (CPS). Red lines denote seizure onset and offset* 128

C-2 *Peri-ictal heart rate recordings of individual complex partial seizures (CPS). Red line denotes CPS.* 129

C-3 *Time-frequency mapping of heart rate variability of individual complex partial seizures (CPS). Two main spectral components can be observed. The high frequency (HF: 0.15 - 0.4 Hz) component reflects vagal modulation of the heart rate; the low frequency (LF: 0.04 - 0.15 Hz) reflects a complex mixture of sympathetic and parasympathetic modulation. Black lines denote seizure onset and offset.* 130

C-4 *Peri-ictal high-frequency heart rate variability power (HF: 0.15-0.4 Hz; parasympathetic) of individual complex partial seizures (CPS). Red line denotes CPS.* . . . 131

C-5 *Peri-ictal EDA recordings(sympathetic) of individual generalized tonic-clonic seizures (GTCS). Red lines denote seizure onset and offset* 132

C-6 *Peri-ictal heart rate recordings of individual generalized tonic-clonic seizures (GTCS). Red line denotes GTCS.* 133

C-7 *Time-frequency mapping of heart rate variability of individual generalized tonic-clonic seizures (GTCS). Two main spectral components can be observed. The high frequency (HF: 0.15 - 0.4 Hz) component reflects vagal modulation of the heart rate; the low frequency (LF: 0.04 - 0.15 Hz) reflects a complex mixture of sympathetic and parasympathetic modulation. Black lines denote seizure onset and offset.* . . 134

C-8 *Peri-ictal high-frequency heart rate variability power (HF: 0.15-0.4 Hz; parasympathetic) of individual generalized tonic-clonic seizures (GTCS). Red line denotes GTCS.* 135

D-1 *Electrodermal activity (EDA) and net acceleration recordings of individual generalized tonic-clonic seizures (GTCS) from seven patients included for seizure detection. This recordings are zoomed-in to highlight the ictal period. See Fig. D-2 for a broader view of the EDA changes surrounding each seizure.* 138

D-2 *Electrodermal activity (EDA) recordings of individual generalized tonic-clonic seizures (GTCS) from seven patients included for seizure detection. Note: One new patient (patient 3) was included in this study so the numbering and ordering of seizures are different compared to Fig. C-5 from the previous study.* 139

D-3 *Time-frequency mapping of the net acceleration recordings of individual generalized tonic-clonic seizures (GTCS) from seven patients included for seizure detection.* . 140

D-4 *SVM parameter tuning for non-patient-specific seizure detection: Grid-search for optimal pair of C and γ values based on cross-validation of F-measure for (leave-one-patient-out using both EDA and ACM features).* 141

D-5 *SVM parameter tuning for semi-patient-specific seizure detection: Grid-search for optimal pair of C and γ values based on cross-validation of F-measure for (leave-one-seizure-out using both EDA and ACM features).* 142

D-6 *SVM parameter tuning for semi-patient-specific seizure detection: Grid-search for optimal pair of C and γ values based on cross-validation of F-measure for (leave-one-seizure-out using only ACM features).* 143

List of Tables

4.1 Clinical Characteristics of Patients 70

5.1 Comparison of Wrist-worn Convulsive Seizure Detectors 108

Chapter 1

Introduction

1.1 Epilepsy

Approximately 50 million people worldwide are affected by epilepsy [206], one of the most common serious neurological disorders that has potentially deadly consequences. Epilepsy is a disorder of the brain characterized predominantly by an enduring predisposition to generate epileptic seizures – transient manifestations of abnormal, excessive or synchronous neuronal activity in the brain [62]. In America, the prevalence of epilepsy is estimated as 3 million with around 200,000 new cases diagnosed each year [55]. Among all medical conditions, it is as common as lung or breast cancer. Moreover, death from seizure-related causes is comparable with breast cancer; up to 50,000 deaths occur every year in America [36].

Epilepsy is not one condition, but a variety of disorders reflecting underlying brain dysfunction that may result from many different causes. In children and young adults, epilepsy is often attributed to birth trauma, congenital abnormalities or genetic disorders affecting the brain. In middle-aged adults and the elderly, strokes, tumors and cerebrovascular disease are more often the underlying causes [103]. Nonetheless, more than half of the time the underlying cause is unknown. Epilepsy imposes huge physical, psychological, social and economic burdens on individuals and their families. Due to the fear, misunderstanding and the resulting social stigma and discrimination surrounding epilepsy, many people with epilepsy suffer in silence, afraid to be found out [206]. This is particularly true in the developing world where 80% of the burden of epilepsy falls.

1.1.1 Seizures

An epileptic seizure is defined as "a transient occurrence of signs and/or symptoms due to abnormal excessive or synchronous neuronal activity in the brain" [62]. The diagnosis of epilepsy requires only one epileptic seizure along with an enduring alteration in the brain capable of giving rise to other seizures. Many types of seizures exist and accurate classification is important for prescribing the appropriate therapy.

In 1981, the International League Against Epilepsy (ILAE) formulated an international classification of epileptic seizures that divided seizures into two major classes: partial seizures and generalized seizures [79]. This classification is based on clinical and electroencephalographic (EEG) observations of the extent to which the brain is affected by the ictal discharges. Recently, the ILAE revised the terminology and concepts for organization of seizures [20], but no major changes were introduced. According to this latest proposal, focal seizures are perceived as originating within neural networks from only one side of the brain. They may affect a distinct region or be widely distributed. Moreover, focal seizures may originate in cortical or subcortical structures. On the other hand, generalized seizures are thought to originate within rapidly recruiting bilaterally distributed networks. These networks can include cortical and subcortical structures and do not necessarily involve the entire cortex.

1.1.2 Treatment of Epilepsy

Over a dozen antiepileptic drugs (AEDs) are available to treat epilepsy. These drugs typically seek to prevent the development of seizure activity by decreasing neuronal excitation or increasing inhibition. One approach is to modify electrical conduction along neurons by blocking certain ion channels (e.g. sodium, calcium or potassium channels) in the cell membrane. Alternatively, the drugs can target the chemical transmission between neurons by affecting the neurotransmitter interactions (e.g. GABA, glutamate) at the synapses. Nonetheless, up to 36% of patients have inadequate control of seizures with drug therapy [92].

For people with medically intractable seizures, some may be candidates for surgery such as those who have partial seizures. Epilepsy surgery can be performed only if the seizure origination point can be localized and the surgery to remove that part of the brain

will not significantly alter its normal function. As such, people with generalized seizures are not candidates for surgery. The ketogenic diet is another treatment option that is used primarily in children. This high-fat diet is designed to mimic the biological effects of starvation, but the exact mechanisms of seizure inhibition are unknown. For this treatment to work, a rigid diet must be followed that requires extraordinary dedication and discipline from both the child and family. Another approach for treating epilepsy is to use vagus nerve stimulation (VNS). VNS involves surgically implanting a battery-powered device akin to a cardiac pacemaker under the skin in the chest. The device is connected to the vagus nerve in the left side of the neck and can be adjusted to periodically stimulate the vagus nerve. This therapy has been shown to be an effective treatment for epilepsy in some patients, but its mechanism also remain unknown.

1.1.3 Mortality in Epilepsy

People with epilepsy have mortality rates two to three times higher than the general population [65, 118]. Some excess mortality is partly related to the underlying disorder causing epilepsy such as cerebrovascular disease, respiratory disorders and cancer. In America, up to 50,000 of deaths each year are direct seizure-related consequences, such as accidents (e.g. trauma or drowning), suicide, status epilepticus and sudden unexpected death in epilepsy (SUDEP) [36]. Status epilepticus is a condition in which epileptic seizure activity continues or is repeated without the person regaining consciousness for an extended period of time. It is a medical emergency that can lead to permanent injury or death. In adolescents and young adults, the most common direct seizure-related cause of death is SUDEP [65].

1.2 Sudden, Unexpected Death in Epilepsy

> *"She rose from Dinner about four o'clock in better health and spirits than she appeared to have been in for some time; soon after which she was seized with one of her usual Fits, and expired in it, in less than two minutes, without uttering a word, a groan, or scarce a sigh. This sudden and unexpected blow, I scarce need add has almost reduced my poor Wife to the lowest ebb of Misery."* [1]

This is one of the earliest accounts of sudden death as a result of a seizure and was written in 1773 by George Washington, the first US president, concerning his 17 year old

stepdaughter with refractory epilepsy [47]. SUDEP is defined as a sudden, unexpected, witnessed or unwitnessed, non-traumatic and non-drowning death of a patient with epilepsy, with or without evidence of a seizure (excluding documented status epilepticus), in which postmortem examination does not reveal a toxicological or anatomical cause for death [123]. It is the leading cause of death in patients with chronic uncontrolled epilepsy and although a relatively rare event, the risk of sudden death in people with epilepsy is 24 times higher compared to the general population [61]. The incidence rate of SUDEP in people with epilepsy ranges from 0.1 to 2.3 per 1,000 person-years (calculated as incidence proportion divided by number of years) [183]. Patients with refractory epilepsy are at higher risk (1.1 to 6.0 per 1,000 person-years) [11,118,124,125] and the highest rates fall on epilepsy surgery candidates or patients who fail to achieve complete seizure control after surgery, reaching 6.3 to 9.3 per 1000 person-years [39,130,170].

The circumstances of deaths in SUDEP cases bear remarkable similarities; death appears to occur during or shortly after a seizure and often occurs at home (in bed or by the bed) during the night [177]. Although the deaths are largely unwitnessed, evidence of a recent seizure is frequently found, such as a bitten tongue/lip, urinary incontinence, signs of having fallen off the bed and a disrupted environment [126]. Moreover, in most, but not all witnessed cases of SUDEP, patients died shortly after a generalized tonic-clonic seizure (within minutes rather than hours) [93, 94, 190]. One of the most frequent complaints of parents of SUDEP victims is that they were not informed of this fatal possibility. Many struggle with the thought that knowing about the risk of SUDEP beforehand possibly could have helped them prevent it. Nonetheless, there remains much debate among clinicians whether the risk of SUDEP should be discussed with all patients. Because SUDEP is a relatively rare phenomenon, the primary concern is on the potential to cause harm to the patient by disclosing information that was not actively sought, where the knowledge of SUDEP does not significantly alter management or outcome [30].

1.2.1 Risk Factors and Pathophysiology of SUDEP

Unlike many disorders that can be prevented by avoidance or correction of risk factors, the currently known risk factors for SUDEP are not as easily modifiable for many patients [169]. Nonetheless, knowledge of the clinical profile of SUDEP can guide studies into its pathophysiological mechanisms as well as help identify patients at risk. The risk factors

consistently associated with SUDEP include poor seizure control, antiepileptic drug (AED) polytherapy, and a long duration of epilepsy [177]. Five out of six studies analysing seizure frequency reported that the frequency of generalized tonic-clonic seizures was a significant risk factor [189]. Although polytherapy with AEDs was a risk factor in several studies, the absence of treatment with AEDs was also a strong risk factor in the largest case control study [94].

The pathophysiology of SUDEP remains unclear. As SUDEP is a category and not a condition, it may represent more than one entity and different mechanisms may operate in different individuals. In most cases, SUDEP is triggered by a generalized tonic-clonic seizure [189]. Only eight SUDEP cases have been reported during EEG monitoring. Seven of the SUDEP events occurred after a secondarily generalized tonic-clonic seizure and in the single case that occurred after a complex partial seizure, the patient had experienced two secondarily generalized tonic-clonic seizures (one hour apart) in the two hours prior to the terminal seizure. Notably, seven out of eight cases reported abrupt interruption of ictal activity replaced by severe suppression of the EEG that failed to recover in the fatal seizure [14, 23, 99, 104, 115, 144]. Four of the reports suggested electrical shutdown of the brain as the primary mechanism [23,98,104,115]. One case postulated that death was due to asphyxia secondary to obstructive apnea in the setting of post-ictal EEG suppression [144]. Two other reports attributed the deaths to hypoxemia leading to eventual cardiac failure, although the primary mechanism was not clarified [14]. Another SUDEP case was related to seizure-induced ventricular fibrillation as seen on the electrocardiogram (ECG) followed by terminal asystole in a patient with a past history of myocardial infarction and angina [40]. On the other hand, in two monitored cases of near SUDEP, either postictal central apnea or ictal obstructive apnea was suspected to be the primary dysfunction that led to cardiac arrest [168, 186]. Recently, a third near SUDEP case reported ventricular tachycardia and fibrillation after a secondarily generalized tonic-clonic seizure in a patient with epilepsy who had no underlying cardiac disease [56].

It is likely that no single mechanism can explain all cases of SUDEP. The pathophysiology of SUDEP appears to be multifactorial and identifying the primary cause of death is challenging. In general, three major domains of potential SUDEP mechanisms have been identified: cardiac, respiratory and autonomic [169]. These mechanisms may not be independent of each other and many potential mechanisms are in more than one domain,

especially in both cardiac and autonomic domains. As such, Surges *et al.* proposed a "fatal coincidence" hypothesis, suggesting that SUDEP is likely caused by the periictal coincidence of several precipitating factors that form a chain of events that culminates in sudden death [177].

1.3 Seizure Prediction and Detection

Patients with epilepsy often describe seizures as occurring "like a bolt from the blue" which accentuates the apparent sudden, unforeseen way in which seizures tend to strike [120]. This represents one of the most disabling aspects of the disease [54], especially for those unable to achieve complete seizure control. It can lead to an intense feeling of helplessness that has a strong impact on the everyday life of a patient. In addition, abrupt episodes of staring, loss of muscle control or loss of consciousness can pose a serious injury risk and can even be life-threatening if they occur while the patient is driving, crossing a busy street, bathing, swimming or climbing stairs. Therefore, a method capable of forecasting the occurrence of seizures could significantly improve the quality of life for epilepsy patients [53].

For many years, epileptic seizures were thought to strike abruptly but there is now mounting evidence that seizures develop minutes to hours before clinical onset. Clinical findings corroborating the existence of a pre-seizure state include a significant increase in blood flow in the epileptic temporal lobes minutes before seizure onset [16, 204], increase in cerebral oxygenation hours before the ictal event [2], increase in blood oxygen level dependent functional MRI (fMRI) signals [58] as well as changes in RR intervals on the ECG minutes before seizure onset [134]. Since Viglione and colleagues pioneered the visionary work on predicting epileptic seizures in the 1970s, much of the work in seizure prediction has focused on extracting characteristic features that are predictive of an impending seizure from intracranial electroencephalogram (EEG) signals [198]. Nonetheless, there is awareness that single quantitative techniques are unlikely to predict seizures in all patients. In recent years, seizure prediction work has diversified and there is an increasing interest in methods for forecasting seizures from other physiological or non-physiological variables [106].

Irrespective of whether seizures can be robustly predicted, a device that can detect seizures and trigger an alarm has important utility. Since seizures often cause loss of consciousness, most patients have trouble accurately reporting the occurrence of seizures.

Treatment decisions are primarily based on seizure frequency [43], thus inaccurate self-reports can lead to ineffective therapy. A seizure detection device would provide objective measurements for quantification of seizure frequency. More importantly, because most deaths are unwitnessed, supervision and attention to recovery after a seizure may be important in SUDEP prevention [93]. If a parent or caregiver is alerted when a seizure occurs, especially during sleep, the patient can receive timely treatment if injured, be placed in the recovery position and avoid airway obstruction that could be fatal. One study in a residential school for children with epilepsy who were closely supervised at night and monitored after a seizure reported that deaths occurred with students on leave or after they left, but not at the school [124]. Another large case-control study found that sharing a bedroom with someone capable of giving assistance and special precautions such as regular checks throughout the night or using a listening device were all protective factors [94].

1.3.1 Seizure Detection Using Wearable Biosensors

Although neuronal signals are the most obvious candidate for seizure detection, an EEG-based approach has its disadvantages. To obtain high-resolution data, recordings need to be intracranial, which is highly invasive and not likely to have widespread applicability. Even if the quality of recordings from surface-based electrodes is improved, the technical requirements for the implementation of a portable EEG recorder are challenging. Furthermore, much effort will be needed to design a wearable electrode system that is not obstructive, unwieldy or stigmatizing.

Wrist-worn or leg-worn sensors are appealing because patients can avoid intracranial procedures and they have the freedom to remove the device at any point in time. For example, accelerometers placed on the trunk and limbs have been used to detect motor seizures based on patterns in physical activity [129]. The autonomic nervous system is an attractive alternative that may provide a sensitive and easily measured index of central dysregulation because autonomic output reflects the sum of a wide number of central systems with a host of central inputs [18]. Therefore, it is likely that seizures can be detected from autonomic efferents that often accompany them. Many patients are aware of periods when seizures are more likely, although they can rarely specify an exact time when seizures will happen [106]. Sleep deprivation, emotional, somatic and intellectual stress have also been reported to provoked stress convulsions, supporting the notion that stress plays a role in facilitating

epileptic seizures [68, 70]. Cardiac autonomic activity as measured by heart rate variability (HRV) has been used to detect neonatal seizures [116]. HRV analysis has also been utilized for forecasting generalized seizures in rats and complex partial seizures humans by applying an unsupervised fuzzy clustering algorithm [89].

Using physiological signals other than EEG may not offer the same sensitivity or specificity for seizure detection, but the convenience and comfort of an unobtrusive device cannot be overlooked. In a survey of over 90 patients with epilepsy, almost 80% could not accept having to wear scalp EEG electrodes to obtain seizure warnings, but more than 50% could imagine wearing a device of the size of a Walkman on a long-term basis [159]. A wearable device that is non-stigmatizing and comfortable is more likely to be adopted by patients during their daily lives.

1.4 Overall Aims

Epileptic seizures can result in events that are potentially fatal, including accidents, status epilepticus and SUDEP. Combined EEG and video-monitoring remains the clinical standard for seizure detection but this technique is not practical for long-term outpatient monitoring or everyday use. A round-the-clock seizure monitoring system would allow tracking seizures for therapeutic purposes and prevent serious complications including death and neurological injury. Thus, there is a medical need for a reliable, comfortable, cost-effective, and non-stigmatizing seizure monitor suitable for everyday use. The specific aims of this thesis (shown in Figure 1-1) are:

- To develop a wrist-worn biosensor for long-term, continuous monitoring of electrodermal activity (EDA) as an index of sympathetic nervous system activity, and 3-D accelerometry (ACM) to measure movement patterns of the arm . The hypothesis is that a low-cost, compact, and non-stigmatizing device that can be worn comfortably will enable widespread, continuous measurements to be performed over days to months.

- To characterize autonomic alterations associated with epileptic seizures with the use of the wrist-worn EDA biosensor and time-frequency mapping of heart rate variability (HRV). The hypothesis is that epileptic seizures, generalized tonic-clonic seizure in

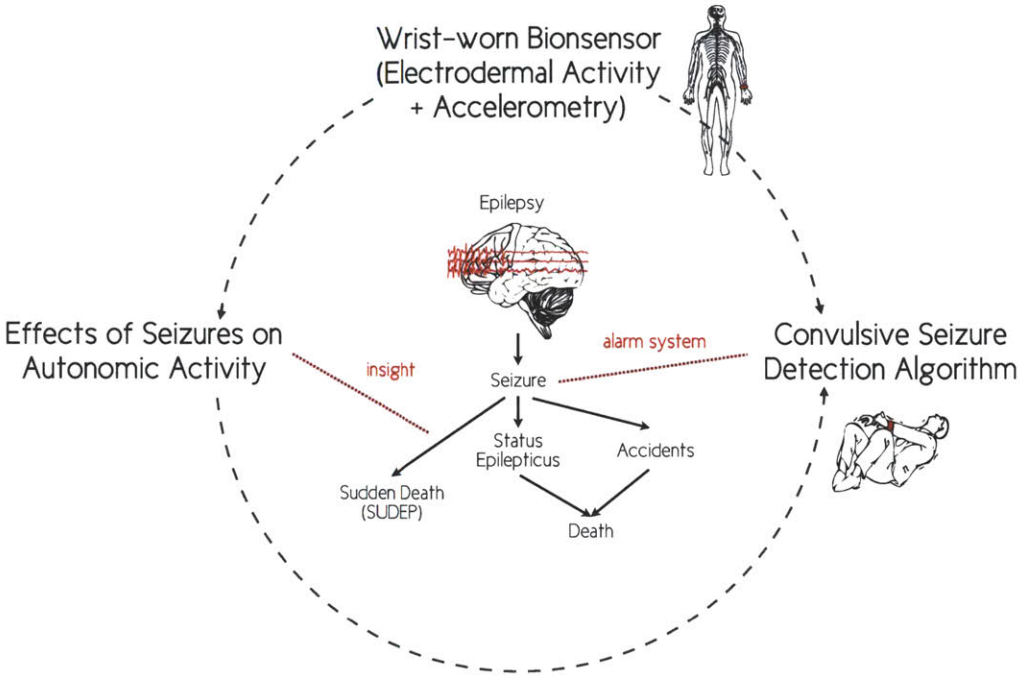

Figure 1-1: *Outline of thesis aims.*

particular, can induce an increase in EDA as a marker for sympathetic activity and reduce HRV indices of parasympathetic activity.

- To quantify the relationship between the intensity of seizure-induced autonomic imbalance and post-ictal EEG suppression, an objective surrogate marker under investigation by epileptologists for its possible relation to the risk of SUDEP. The hypothesis is that the duration of EEG suppression will correlate positively with the degree of sympathetic EDA increase and correlate negatively with the extent of parasympathetic HRV reduction.

- To develop an algorithm for automatic detection of generalized tonic-clonic seizures with the use of the wrist-worn biosensor. The hypothesis is that tonic-clonic seizures can be detected using EDA and ACM signals.

1.5 Thesis outline

The outline of the remainder of this thesis is as follows:

Chapter 2 provides background information on the autonomic nervous system and approaches to quantify activity using heart rate variability (HRV) and EDA. Existing information in the literature regarding autonomic activity in patients with epilepsy is also presented.

Chapter 3 presents a novel, unobtrusive, nonstigmatizing, wrist-worn integrated biosensor for long-term, continuous measurements of EDA and ACM along with the first demonstration of long-term, continuous assessment of EDA outside of a laboratory setting. This chapter includes performance evaluation of the biosensor against a Food and Drug Administration (FDA) approved system for the measurement of EDA during various classic arousal experiments. The choice of electrode material is also discussed.

Chapter 4 describes high-resolution characterization of autonomic alterations of epileptic seizures using the wearable EDA biosensor and time-frequency mapping of HRV. A comparison between the autonomic impact of complex partial and generalized tonic-clonic seizures is performed. The possibility that autonomic biomarkers could serve as biomarkers for SUDEP risk is examined by quantifying the relationship between the degree of autonomic disturbance and post-ictal generalized EEG suppresion, a surrogate marker of SUDEP risk.

Chapter 5 presents a novel algorithm for automated detection of generalized tonic-clonic seizures using the wearable biosensor. The utility of EDA as a supplementary signal to ACM for seizure detection is evaluated. Performance of the algorithm is tested on recordings taken over 176 days from 80 patients.

Chapter 6 summarizes this thesis and proposes future work.

Chapter 2

Autonomic Alterations in Epilepsy

2.1 Autonomic Nervous System

The autonomic nervous system (ANS) is the control system responsible for maintaining homeostasis of the body through regulation of visceral functions including functions of the heart muscle, smooth muscles, secretory glands and hormone secretion. The peripheral component of the ANS is composed of two functionally and anatomically distinct divisions – the sympathetic and parasympathetic nervous systems. While the parasympathetic nervous system promotes restoration and conservation of energy, the sympathetic nervous system stimulates increased metabolic output to deal with external challenges. As such, increased sympathetic activity elevates heart rate, blood pressure, and sweating, as well as redirects blood from the intestinal reservoir toward skeletal muscles, lungs, heart, and brain in preparation for motor action. The brain controls the ANS via a complex neural network called the central autonomic network. The central autonomic network comprises the insular cortex, anterior cingulate gyrus, amygdala, hypothalamus, prefrontal cortex, periaqueductal gray matter, parabrachial complex, nucleus of the tractus solitarius, and ventrolateral medulla [18]. Several of these structures, such as the insular cortex, prefrontal cortex and cingulate gyrus have recognized seizure potential, thus providing direct connections between epileptic seizures and ANS activity [160].

Autonomic symptoms during epileptic seizures are mediated by an activation of the central autonomic network and range from subtle manifestations to severe, even life-threatening events [15]. Autonomic signatures such as flushing, sweating and piloerection often accompany partial seizures and auras [15,108,109]. In contrast, GTCS are associated with severe

increases in blood pressure and changes in heart rate and cardiac conduction [157]. Seizure-induced autonomic dysfunction can have serious clinical consequences and potentially fatal effects when the cardiovascular or respiratory systems are involved [46].

2.2 Heart Rate Variability

The heart is one of the most important target organs of the ANS. Sympathetic innervation of the heart arises from the cervical and upper thoracic sympathetic ganglia, whereas parasympathetic innervation is mediated via the vagus nerve originating from the medulla oblongata. Sympathetic activation increases conduction, excitability and contractility of the heart. In contrary, parasympathetic activation decreases these cardiac functions.

Heart rate variability (HRV), a measure of beat-to-beat alterations in the heart rate, provides a measure of the cardiac autonomic modulation because they are mediated by autonomic inputs to the sinoatrial (SA) node [110]. Analysis of HRV can be performed in the time and frequency domains to obtain information regarding the influence of parasympathetic or mixed sympathetic and parasympathetic modulation. Vagal modulation can be quantified by analyzing oscillations at respiratory frequencies (also known as respiratory sinus arrhythmia; 0.15 – 0.4 Hz) that are mediated solely by the parasympathetic system and are abolished by atropine infusion [6, 142]. Although there is a consensus that HF power reflects vagal modulation of the heart rate, sympathetic modulation cannot be easily uncoupled. It has been claimed that power in the low frequency range (LF, 0.04 - 0.15 Hz) reflects primarily sympathetic modulation of heart rate and that the LF/HF ratio reflects the sympathovagal balance but this is highly controversial as beta blockade does not reduce, but rather increases LF power [32] and direct cardiac sympathetic blockage via epidural anesthesia has no effect on it [76].

2.2.1 Regulation of Heart Rate Variability as a Predictor of Sudden Death

Studies of HRV in patients with epilepsy suggest a decrease in parasympathetic tone and/or an increase in sympathetic tone in the inter-ictal state [177]. In patients with temporal lobe epilepsy, interictal HRV was reported to be reduced compared to healthy controls [148, 188], particularly at night, which is when SUDEP occurs most frequently [94]. Moreover,

HRV was found to increase after epilepsy surgery [74], suggesting that HRV is related to seizure control. Since most SUDEP cases occur shortly after a seizure, peri-ictal autonomic alterations might be more relevant to its pathophysiology. In a study of 12 patients, an increase of parasympathetic activity was observed during the pre-ictal period followed by a rapid fall 30 s before the onset of temporal lobe complex partial seizures (CPS), raising the possibility of predicting impending seizures based on hallmark autonomic alterations prior to their clinical presentation [134]. These findings have yet to be replicated and a separate study of 10 patients reported elevated parasympathetic activity prior to GTCS but not CPS [45]. On the other hand, low frequency heart rate oscillations (0.01 to 0.1 Hz) lasting 2-6 minutes postictally that could indicate neuroautonomic instability were observed in five female patients [7]. Recently, HRV was found to be significantly lowered postictally (measured 5 min after seizure offset) in GTCS compared to CPS in 25 patients [175]. Another study of 31 patients also reported that postictal HRV was lower in GTCS compared to CPS, supporting the notion that GTCS has a greater impact on autonomic function [191]. The authors observed that HRV was lower at two time points measured after GTCS onset (10-15 min and 5-6 hours) which suggests long-term postictal autonomic disturbance, but it is worth noting that continuous measurements were not taken in between. Overall, these studies indicate that there is a window of disorganized autonomic neural function in the postictal state and there is a need to investigate the duration and dynamics of this disturbance.

A number of studies have shown that decreased HRV is a consistent predictor of cardiac mortality and sudden cardiac death, independent of disease status [171]. These studies have included apparently healthy middle-aged adults who had Holter recordings prior to their sudden death [119] as well as patients who died suddenly while wearing a Holter monitor [112]. Furthermore, a report of progressive decrease in HRV in two patients with eventual sudden death within two years of the first recording suggests that long-term HRV monitoring can identify patients at high risk of sudden death [122]. Interestingly, a recent case study described a patient who underwent repeated measures of vagus-mediated HRV, which progressively deteriorated prior to SUDEP [146]. Another recent study of 19 patients found an association between vagus-mediated HRV and an inventory of clinical SUDEP risk factors [44]. Thus, it is reasonable to postulate that decreased HRV could be a potential risk factor for SUDEP.

2.2.2 Potential Autonomic Mechanisms in SUDEP

Death typically results from failure of one of the two major electrical systems of the body – the brain or the heart [97]. For example, the brain may fail to send out impulses from the respiratory centers, causing respiratory failure and subsequent death. Dysfunctional signalling from the brain to the heart may also cause it to enter a fatal arrhythmia. On the other hand, the heart may enter an arrhythmia on its own that causes sudden death. Central apnea and malignant arrhythmia are the only obvious etiologies that would leave no traces at autopsy [82].

A cat model for SUDEP suggests that ictal and interictal discharges result in abnormal sympathetic neural discharges monitored from postganglionic cardiac sympathetic branches and may lead to cardiac arrhythmia by altering ventricular automaticity and excitability [96]. The sympathetic nervous system can play an important primary pathogenic role as a trigger of ventricular tachyarrhythmias and sudden cardiac death in patients [150]. In a case study of a sheep with sudden cardiac death, an outburst of cardiac sympathetic nerve activity leading to ventricular fibrillation (VF) was observed post myocardial infarction [81]. A recent study using a canine model of sudden death demonstrated a direct temporal sequence between spontaneously enhanced sympathetic neural activity and the onset of ventricular arrhythmias [209]. Two ambulatory dogs died suddenly during recording and in both cases increased sympathetic neural activity preceded the onset of VF. On the other hand, there is also evidence that excessive parasympathetic outflow can also trigger death. In a rat model for epilepsy, non-convulsive seizures were accompanied by massive co-activation of sympathetic and parasympathetic activity [151]. None of the animals that died showed evidence of VF, but most exhibited significant sinus bardycardia and/or arrhythmia in the form of atrioventricular (AV) nodal block.

In patients with epilepsy, there is evidence that GTCS is associated with significant sympathetic activation. Plasma catecholamines rise sharply within 30 minutes of GTCS and are attributed to generalized sympathetic neural and adrenal activation [165]. The increase in epinephrine may, in some patients, be large enough to cause arrhythmias. Moreover, impaired vagal function as suggested by reduced HRV [175,191] may result in an increase in ventricular automaticity, making the heart vulnerable to arrhythmias. Malignant arrhythmias such as VF have been reported in a documented case of SUDEP [40] and have also

been observed in a near SUDEP case [56].

On the other hand, a massive increase in central sympathetic drive could trigger neurogenic pulmonary edema. Enlarged and dilated hearts along with pulmonary edema are common findings in postmortem studies of SUDEP patients [185]. Antemortem observations of post-ictal pulmonary edema have also been reported in both definite [178] and near-SUDEP incidents [139]. Although the degree of pulmonary edema observed postmortem is usually not expected to cause death [167], high-levels of sympathetic activity can also cause transient dilatation of ventricular walls after tonic-clonic seizures [102, 172]. This stress-induced cardiomyopathy can lead to left ventricular dysfunction and decreased cardiac output, thus further compromising the supply of oxygen and leading ultimately to death. Recently, a fatal case of this stress-induced cardiomyopathy in a woman with epilepsy was reported and could be one of the mechanisms of SUDEP [172].

2.3 Electrodermal Activity

Electrodermal activity (EDA) is a sensitive index of sympathetic nervous system activity. Sympathetic postganglionic fibers consisting of non-myelinated class C nerve fibers surround eccrine sweat glands and their activity modulates sweat secretion [152]. Although postganglionic sympathetic transmission is usually adrenergic, human eccrine sweat glands receive predominantly cholinergic innervation, with acetylcholine as the primary neurotransmitter. Nonetheless, sparsely distributed adrenergic fibers have also been found in proximity to sweat glands [162]. Both cholinergic and adrenergic stimulation induce secretory activity, with cholinergic stimulation producing the larger effect. Presently, there is no evidence that sweat glands receive parasympathetic innervation. Since sweat normally vaporizes so quickly in the absence of sudorisecretory impulses, additional sweat inhibition is unlikely to reduce the amount of sweat significantly [26].

Sweat is a weak electrolyte and good conductor. The filling of sweat ducts results in many low-resistance parallel pathways, thereby increasing the conductance of an applied current. Changes in skin conductance at the surface, or more generally, in EDA, reflect activity within the sympathetic axis of the ANS and provide a sensitive and convenient measure of assessing alterations in sympathetic arousal associated with emotion, cognition and attention [37]. Stress is generally defined as a disruption of the autonomic balance

involving a state of high sympathetic activation. Since EDA is solely determined by the activity of the sympathetic branch of the ANS which is predominant in stress states, tonic EDA parameters may be regarded as suitable measures of ANS activity induced by stress [26]. On the other hand, it remains controversial whether the sweat glands at palmar and plantar sites participate in thermoregulatory sweating [91].

Based on results from human and animal studies, two sources of central EDA control may exist. The hypothalamus, which is the main regulator of sweat secretion and thermoregulatory center, plays a major role in eliciting ipsilateral EDA under the direct influence of limbic structures. These influences appear to stem from antagonistic actions of the amygdala (excitatory) and hippocampus (inhibitory) [207, 208]. Autonomic responses in the skin such as sweating, piloerection and vasomotor changes can thus be elicited by various emotional states via the Papez circuit in the limbic system [136]. The second cerebral source comprises the basal ganglia along with premotor cortical areas that exhibit mainly contralateral influences on EDA [156].

2.3.1 Electrodermal Activity in Epilepsy

So far, autonomic alterations in epilepsy have mostly been studied using indirect parameters such as heart rate, respiratory rate and blood pressure changes that are dually modulated by both divisions of the ANS. Assessment of cardiac autonomic function by HRV alone is limited by its poor delineation of parasympathetic and sympathetic activity [166]. As such, the relative influence of parasympathetic or sympathetic system is not well characterized. The additional use of EDA can potentially provide more insight given its specificity for sympathetic activity.

The use of EDA in the context of epilepsy is rare in the literature. In 1958, Van Buren measured the plantar skin resistance of 13 patients with temporal lobe epilepsy during induced partial seizures [194]. The procedures used to precipitate seizures (e.g. hyperventilation, metrazol administration) usually resulted in low skin resistance long before the clinical manifestation of the seizure such that further ictal skin resistance changes might be minimal or absent. Nonetheless, some preictal decrease in skin resistance was observed in 18 out of 20 of the induced seizures. The postictal state was not considered. In a study of infantile spasms, Frost and colleagues noted that a slow skin potential occurred following two seizures in a 8-month old baby [69]. No further details were provided regarding the

timing or amplitude of the skin potential changes that accompanied the seizures. Nagai and colleagues investigated the effect of EDA biofeedback training on seizure frequency in patients with epilepsy [121]. They reported that biofeedback training significantly reduced seizure frequency, highlight the potential therapeutic value of EDA biofeedback for patients with treatment drug-resistant epilepsy.

Chapter 3

A Wearable Electrodermal Activity and Accelerometry Biosensor

3.1 Introduction

Electrodermal activity (EDA) is a sensitive index of sympathetic nervous system activity. Due to the lack of sensors that can be worn comfortably during normal daily activity and over extensive periods of time, research in this area has traditionally been limited to lab settings or artificial clinical environments. In this chapter, we describe a novel, unobtrusive, non-stigmatizing, wrist-worn integrated sensor and present, for the very first time, a demonstration of long-term (multi-day), continuous assessment of EDA outside of a lab setting.

In general, regulation of physiological states of arousal is achieved by a balance of activity within sympathetic and parasympathetic subdivisions of the autonomic nervous system (ANS). While the parasympathetic nervous system promotes restoration and conservation of bodily energy, the sympathetic nervous system stimulates increased metabolic output to deal with external challenges. As such, increased sympathetic activity (sympathetic arousal) elevates heart rate, blood pressure and sweating as well as redirects blood from the intestinal reservoir toward skeletal muscles, lungs, heart and brain in preparation for motor action. Sympathetic postganglionic fibers consisting of non-myelinated class C nerve fibers surround eccrine sweat glands and their activity modulates sweat secretion [152]. Since sweat is a weak electrolyte and good conductor, the filling of sweat ducts results in

many low-resistance parallel pathways, thereby increasing the conductance of an applied current. Changes in skin conductance at the surface, or more generally in to as EDA, reflect activity within the sympathetic axis of the ANS and provide a sensitive and convenient measure of assessing alterations in sympathetic arousal associated with emotion, cognition and attention [37].

Stress is generally defined as a disruption of the autonomic balance involving a state of high sympathetic activation. Given that EDA is solely determined by the activity of the sympathetic branch of the ANS which is predominant in stress states, tonic EDA parameters may be regarded as suitable measures of ANS activity induced by stress [26]. The hypothalamus, which is responsible for ANS activity, plays a major role in eliciting ipsilateral EDA under the direct influence of limbic structures [26]. These influences appear to stem from antagonistic actions of the amygdala (excitatory) and hippocampus (inhibitory) [207, 208]. Autonomic responses in the skin such as sweating, piloerection and vasomotor changes can thus be elicited by various emotional states via the Papez circuit in the limbic system [136]. In addition, it is widely recognized that attention-grabbing stimuli and attention demanding tasks also evoke increased EDA responses [51, 193].

Despite improvements in measuring equipment since the discovery of electrodermal phenomena more than 100 years ago [60, 180, 199], much of the research in this area is limited to observational measurements performed over short periods of time in lab settings or artificial clinical environments. The need for monitoring patients over extensive periods of time has stimulated interest in wearable unobtrusive devices that can be worn during normal daily activity to gather physiological data over periods of several weeks or months [25]. Long-term monitoring of EDA will allow the observation of patterns of sympathetic arousal and regulation at a significantly longer time scale (days to months) compared to existing studies (minutes to hours) and could potentially reveal previously unobservable trends. In addition, long-term measurements taken in a person's natural home environment also provide a clearer picture of the persons physiological state than a short period of assessment in an unnatural clinical setting [154]. Clinically, wearable EDA sensors can be used in psychopathology, dermatology and neurology for diagnostic purposes and therapy evaluation. Potential clinical applications include screening for cystic fibrosis [205], classification of depressive illnesses [117], prediction of functional outcome in schizophrenia [155], discrimination between healthy and psychotic patients [181], characterization of sympathetic

arousal in autism [72], early diagnosis of diabetic neuropathy [48] and providing biofeedback in treating chronic hyperhidrosis [49], epileptic [121] and psychogenic non-epileptic [143] seizures.

To achieve widespread, continuous and long-term assessment of EDA, there is a need for a sensor that not only is low-cost, compact, and unobtrusive, but also comfortable to wear and non-stigmatizing to the user. In this chapter, we present a novel solution in the form of a wearable and fully integrated EDA and accelerometry sensor that fulfills these characteristics. The study focuses on comparing the performance of the proposed system with an FDA-approved EDA measurement system during classic arousal experiments involving physical, cognitive and emotional stressors. We first validate the performance of the proposed sensor during EDA measurements from traditional palmar recording sites. In addition, we study the use of the ventral side of the distal forearms as a recording site for EDA measurements that is non-encumbering. We also investigate how the choice of electrode material affects performance by compare the use of conductive fabric electrodes to standard Ag/AgCl electrodes. Finally, we present a weeklong recording of EDA during daily activity. To the best of our knowledge, it is the first demonstration of long-term, continuous EDA assessment outside of a lab setting.

3.2 Related Work

At present, ambulatory EDA devices are often composed of a processing unit/analog-to-digital converter (A-D) and external probes that reduce comfort levels. Commercial sensor systems at the time this work began included FlexComp [187], SenseWear [24], QPET [29] and Vitaport [184]; they offer high quality EDA recordings but their current bulky form factors and high prices limit their widespread use for long-term ambulatory studies. Similarly, Tronstad et al. [192] proposed a portable logger for EDA long-term measurements, but its size is still considerably too large ($157 \times 95 \times 33$ mm) to be practical for continuous monitoring or to be considered a wearable device. In other designs [12, 100], the placement of electrodes on the fingers or palms is encumbering and highly susceptible to motion or pressure artifacts [147]. A recent proposal to measure EDA unobtrusively through imaging means [161] offers much promise, but the measurements carry substantial noise and quantification remains difficult.

Over the years, the Affective Computing group has devoted much effort into developing wearable EDA sensors suitable for ambulatory measurements resulting in the Galvactivator [140], HandWave [173] and iCalm sensors [57, 64]. The most recent iCalm design was a low-power wireless EDA sensor using the IEEE 802.15.4 wireless standard and represented a significant advancement. However, there were several drawbacks to the capabilities of the system that made it unsatisfactory for long-term clinical studies. Firstly, the iCalm relied entirely on a radio module for data forwarding to a base station (typically a laptop). This constrained users to staying within the wireless range of a base station and resulted in frequent loss of data due to dropped radio packets. In clinical studies of rare and unpredictable events such as epileptic seizures, it is necessary to have continuous measurements available round-the-clock. Moreover, the timing information of the recorded signals in the original iCalm were based on time stamps generated by the base station which was unreliable due to unpredictable radio transmission latency. Since the iCalm only contained an analog vibration/tilt sensor, it was not suitable for precise measurements of motor activity in three axes. To enable a very low-operational duty cycle and long battery life, the iCalm transmitted data at a low rate of 2 Hz, which is inadequate for measurement of rapid events. Another challenge in the design of wearable sensors is robustness and durability. The construction of the iCalm was not robust enough for unsupervised and continuous use over long periods of time. Furthermore, the sensor unit and connecting wires were not concealed and these could act as distractions.

This chapter presents a solution to the issues above. With the exception of the analog skin conductance circuitry, the design and construction of the wearable EDA and accelerometry biosensor described here are original. Recently, a commercial system based on this work was launched [3].

3.3 System Design

3.3.1 Circuit Design

For exosomatic measurements of EDA by direct current (DC), the constant current or constant voltage method is commonly used. However, these traditional methods face difficulty in amplifying the EDA signal since inter- and intra-individual variations in tonic skin conductance levels (SCL) result in a large dynamic range [26]. On the other hand, the phasic

skin conductance responses (SCR) are relatively small. In order to achieve a sufficiently high resolution of the SCRs over a dynamic range of SCLs without having to uncouple the two components, we employed an automatic bias control method using two operation amplifiers as shown in Figure 3-1a.

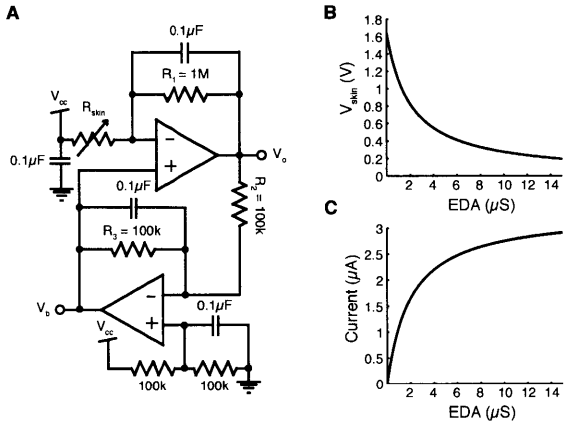

Figure 3-1: *(A) Circuit for EDA measurements. Computed profiles for the (B) voltage and (C) current flow across skin for a range of typical skin conductance values.*

The first stage comprises an active low-pass filter (cutoff frequency $f_c = 1.6$ Hz) with variable gain. To increase the dynamic range of measurements, the bias V_b of the first operational amplifier is determined by the feedback from the output of the second stage integrator V_o (time constant $\tau = 10$ ms). The applied voltage across the skin decreases in a non-linear fashion with increasing skin conductance (Figure 3-1b). Although the current flow through the skin increases non-linearly with skin conductance (Figure 3-1c), the current density is well below the recommended limit of 10 μA/cm^2 [52]; thus, there is minimal risk of damaging sweat glands. Within a range of skin conductance between 0.1 and 15 μS, the average voltage applied is 0.47 V and the average current flow is 2.37 μA. Overall, the skin resistance R_{skin} can be calculated as follows:

$$\frac{V_{cc} - V_b}{V_b - V_o} \tag{3.1}$$

EDA measured as skin conductance can be obtained simply by taking the inverse of Equation 3.1.

3.3.2 Sensor Module

The overall system is illustrated in Figure 3-2 1. DC is applied to the stratum corneum via surface contact dry electrodes for exosomatic measurements of EDA. To achieve a wide dynamic range of skin conductance measurements, the analog conditioning circuitry utilizes non-linear feedback automatic bias control with low-power operational amplifiers (LTC6081 by Linear Technology). A triple-axis accelerometer (ADXL330 by Analog Devices, Inc.) is also included for physical activity measurements. Accelerometry is a low-cost, flexible and accurate method for the analysis of posture and movement.

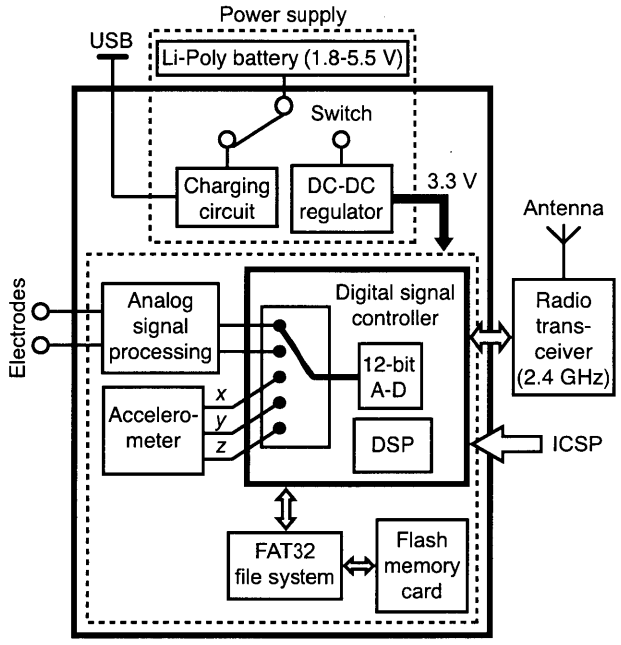

Figure 3-2: *Overview of the EDA sensor system architecture. The device is capable of recording measurements onto an on-board flash memory card (data logging), wirelessly transmitting data to a remote site (data forwarding) and performing real-time analysis (data processing).*

A digital signal controller (dsPIC30F2012 by Microchip Technology, Inc.) acts as the control center that can be programmed on-board through an In-Circuit Serial Programming (ICSP) interface. Digital signal controllers (DSC) combine the control attributes of a microcontroller (MCU) and computation capabilities of a digital signal processor (DSP), thus allowing application specific real-time complex analysis on-board. The analog signals are sampled at 32 Hz via an A-D with 12-bit resolution on the DSC. Power is drawn from a single lithium polymer battery with a nominal voltage of 3.7 V and a capacity of 1100 mAh. The battery can be recharged directly from a USB port by an on-board single cell Li-

Ion battery charger (LTC4062 by Linear Technology). A step-up/step-down charge pump (LTC3240 by Linear Technology) produces a fixed, regulated output of 3.3 V for the DSC and peripheral components.

In order to enable continuous measurements of EDA and physical activity without the constraint of staying within range of a base station, a data logging system is available on board. Using a separate microcontroller with dedicated firmware to implement a FAT32 file system (uALFAT by GHI Electronics, LLC) that communicates with the DSC through a UART (universal asynchronous receiver/transmitter) interface, data can be written to removable flash memory card. A 2G microSD card provides enough storage capacity for up to 28 days of continuous measurements with a sampling rate of 32 Hz. If it is desirable for the data to be accessible to the wearers caregiver for analysis and interpretation, or if the wearer chooses to share his/her recordings, the proposed system can also operate as a data forwarding device with the use of a 2.4 GHz transceiver module (nRF2401A by Sparkfun Electronics). In this mode, real-time measurements can be displayed on a PC equipped with a separate transceiver module for immediate analysis. The complete electronic module ($20 \times 30 \times 5$ mm) is shown in Figure 3-3. The layout of the sensor board is shown in Appendix A (Figure A-1).

Figure 3-3: *EDA sensor module. The device has a modular design and is shown with an optional radio transceiver mounted on top.*

3.3.3 Packaging

User comfort is a major consideration in the design of any wearable device intended for long-term and continuous use. Regardless of the capabilities of a wearable system, users will not be inclined to wear them on a daily basis over a period of days or weeks if the sensors are bulky and cumbersome. In view of this, we integrated the electronic module

into a regular wristband made out of terrycloth, resulting in a comfortable, attractive and lightweight wearable sensor (Figure 3-4). Since all electronics and wiring are concealed within the wristband, the resulting device is also inconspicuous, non-stigmatizing and allows for discrete monitoring of EDA. Furthermore, the electronic module can be easily detached when the user desires to wash the wristband.

Figure 3-4: *The wearable EDA sensor. (A) Final packaging in an attractive and inconspicuous wristband. (B) Disposable Ag/AgCl electrodes attached to the underside of the wristband. (C) The wearable EDA sensor can be worn comfortably on the wrist for long periods of time and during daily activities.*

To date, there is no generally accepted standardization with respect to electrodermal recording sites [26]. The electrodes are commonly placed on the palmar surface of the hand, the most popular sites being the medial and distal phalanges of the fingers and the thenar and hypothenar eminences. However, since both hands are often needed for manipulation, placement of electrodes on these sites is highly susceptible to motion artifacts and interferes with daily activities. Thus, we decided to use the ventral side of the distal forearms as our recording sites. We chose to use Ag/AgCl disc electrodes with contact areas of 1.0 cm^2 (Thought Technology Ltd.) for our recordings as recommended in the literature [66]. These

electrodes are disposable and can be snapped onto or removed from the wristband with ease (Figure 3-4b).

Overall, the complete wearable EDA sensor is compact ($70 \times 70 \times 20$ mm), lightweight (40.3 g) and the components used can be purchased off the shelf for approximately $150. In contrast, a commercial system such as the Flexcomp Infiniti (Thought Technologies Ltd.) measures $130 \times 95 \times 37$ mm, weighs 200 g and costs $6000 for the data acquisition unit and an additional $275 for an EDA sensor.

3.4 Experimental Methods

3.4.1 Participants

Data were collected from 26 participants between the ages of 18-56 during three separate experiments (physical task, cognitive task and emotional task) each consisting of a baseline, task and recovery period. Some participants underwent two consecutive experiments (order of experiments was not fixed) so there was overlap between the recovery period of the first experiment and baseline of the second experiment. This study (#0801002576) was approved by the Massachusetts Institute of Technology Committee On the Use of Humans as Experimental Subjects (COUHES). Informed consent was obtained from all participants prior to the beginning of the research session. 16 participants (eight females, eight males) were enrolled in a physical task, 15 participants (nine females, six males) underwent a cognitive task and 13 participants (eight females, five males) were subjected to an emotional task. Due to battery failure on the Flexcomp (one person) and motion-corrupted data (one person), full-length recordings were not available for two participants during the cognitive task, but uncorrupted sections were included in analysis. We excluded data from three participants in the physical task due to failure to turn the proposed sensor on (one person), disconnection of finger electrodes from the Flexcomp during task (one person) and motion-corrupted finger data (one person).

In addition, one participant volunteered to wear the proposed sensor for a long-term experiment to measure EDA in situ.

3.4.2 Physiological Measurements

EDA was measured as skin conductance changes using either the proposed system or a gold standard, commercially available and FDA-approved device (Flexcomp Infiniti, Thought Technologies Ltd) at four different recording sites (Figure 3-5). Ag/AgCl electrodes embedded in hook-and-loop fastener bands were secured around the medial phalanges of the index and middle fingers bilaterally. The electrodes on the right fingers were connected to the Flexcomp Infiniti (which served as our control) while the electrodes on the left fingers were connected to the proposed sensor module for EDA measurements. A wearable EDA sensor (wristband) was placed on each distal forearm with the sensor module on the right connected to Ag/AgCl electrodes, and the sensor module on the left connected to stretch conductive fabric (silver plated 92%, nylon 8%, surface resistance $< 1\ \Omega$/sq, contact area of 3.5 cm^2) that was sewn into the wristband in the place of the Ag/AgCl electrodes. Electrodes for both wristbands were in contact with the ventral side of the distal forearms. There was no pretreatment of recording sites and no conductive gel was applied to the electrodes. The clocks for the proposed sensors and the Flexcomp were synchronized prior to the start of each experiment and the time was recorded at the beginning and end of each condition. The sampling frequency for all signals was fixed at 32 Hz.

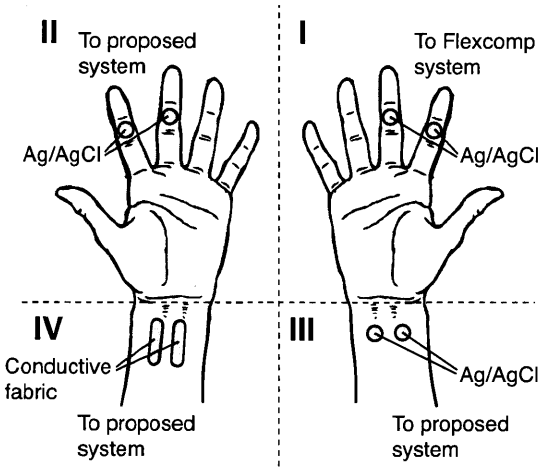

Figure 3-5: *The experimental setup. Measurements were recorded from (I) right fingers with the Flexcomp system, (II) left fingers with the proposed sensor module, (III) right distal forearm with the proposed sensor module using Ag/AgCl electrodes and (IV) left distal forearm with the proposed sensor module using conductive fabric electrodes.*

3.4.3 Physical Task

During the baseline period, participants were asked to sit quietly on the seat of a recumbent bicycle (Precor USA, Inc.) and relax for 10 min. Participants were then asked to pedal as fast as they could for a duration of 5 min at a fixed resistance of level 7. After the cycling task, participants were asked to remain seated for a recovery period of 10 min.

3.4.4 Cognitive Task

Participants were seated in a darkened and sound-dampened room facing a large screen and briefly oriented to their surroundings. At the start of the experiment, participants sat quietly for 10 min to obtain a baseline recording. Participants were then asked to follow instructions on the screen for a cognitive task. On-screen instructions requested them to perform serial subtractions in intervals of seven, starting with a four-digit number and to deliver their responses vocally for a 3 min period. A countdown timer was visible to the participants and a buzzer was sounded for each mistake in subtraction. The mental arithmetic task was followed by a Stroop word-color matching test. A slide consisting of color words (red, blue, green, brown and purple), each printed in a color differing from the color it named was displayed on the screen 3-6 and participants were asked to read the names of the colors serially as quickly as possible in 1 min. Once again, a countdown timer was visible and participants were alerted to errors by a buzzer. At the end of 1 min, the task was repeated again with a second slide that had the words printed in the reverse order. After completion of the task, participants were asked to remain seated and to relax for a recovery period that lasted 10 min.

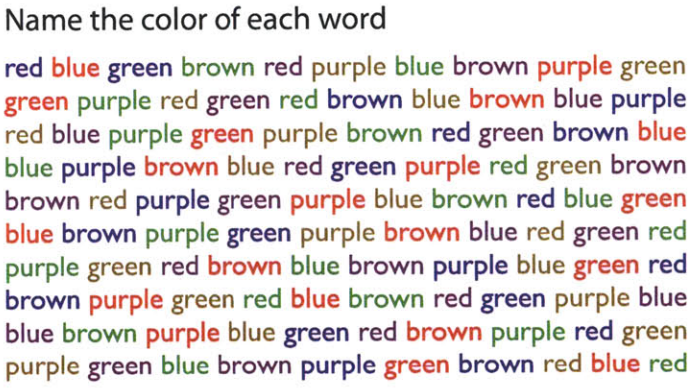

Figure 3-6: *Example of a slide for the Stroop word-color matching test*

3.4.5 Emotional Task

Similar to previous task, participants were seated in a darkened and sound-dampened room facing a large screen and briefly oriented to their surroundings. At the start of the experiment, participants sat quietly for 10 min to obtain a baseline recording. After establishing a baseline, participants were informed by an investigator that a horror movie would be played and waited in anticipation for 1 min. A 5 min clip from the movie 28 Days Later involving scenes of chaos, violence and disturbing images was then shown. At the end of the movie clip, participants were asked to remain seated and relax for a recovery period that lasted 10 min.

3.4.6 Long-term In Situ Experiment

A healthy volunteer (19 year-old male) wore the proposed sensor with Ag/AgCl electrodes on his left distal forearm 24/7 for a week to measure long-term EDA during daily activities. He was given the option to stop participating in the experiment at any moment and to remove the wristband at any time he chose. After a period between 24 to 30 hours, the volunteer removed the micro-SD card to download the data and also replaced the battery. This was repeated daily for a total of seven days.

3.4.7 Data Analysis

All data files were analyzed using custom software written in MATLAB (The MathWorks, Inc.). The raw EDA signals were filtered with a 1024-point lowpass filter (Hamming window, cutoff frequency of 3 Hz) to reduce motion artifacts and electrical noise. Pearsons correlation coefficients and the corresponding p-values were calculated for the filtered recordings from the different sites and systems as a measure of similarity between signals.

3.5 Results

3.5.1 EDA Increases During Stressor Tasks

All participants reported that the wearable EDA sensors (wristbands) felt comfortable throughout the duration of the study. Examples of typical EDA signals measured during the three different experiments are presented in Figure 3-7. Individual graphs for each

participant can be found in Appendix A (Figures A-2 to A-4).

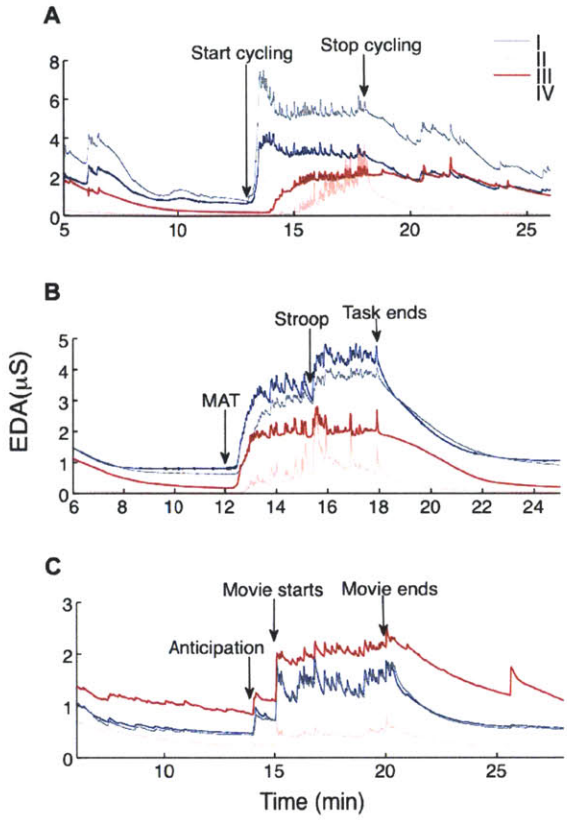

Figure 3-7: *EDA waveforms during (A) physical activity, (B) cognitive stressors and (C) emotional stressors (a horror movie clip). Measurements were recorded from (I) right fingers with the Flexcomp system, (II) left fingers with the proposed sensor module, (III) right distal forearm with the proposed sensor module using Ag/AgCl electrodes and (IV) left distal forearm with the proposed sensor module using conductive fabric electrodes.*

In all three experiments, skin conductance gradually decreased to a plateau during the initial relaxation period to establish a baseline. During the physical task, skin conductance increased as the participant was cycling (Figure 3-7a). In the course of the cognitive task experiment (Figure 3-7b), the start of the mental arithmetic test (MAT) was followed by a steep rise in skin conductance level that remained elevated throughout the test. Skin conductance increased to a higher level during the Stroop word-color matching task in 73.3% of participants. Multiple skin conductance responses (SCRs) were also evident during the tasks. From Figure 3-7c, we see that an SCR was generated when the investigator informed the participant that a horror movie would be played. At the start of the movie, the skin conductance level surged upward and remained high with multiple SCRs throughout the movie. When the tasks ended and the participant was asked to relax, skin conductance

decreased steadily to near baseline in all three experiments.

From Figure 3-7, we also see that recordings from our sensor modules on the fingers (II) and distal forearm with Ag/AgCl electrodes (III) are in very close agreement with recordings from the Flexcomp on the fingers (I). Overall, recordings on the wrist with conductive fabric electrodes (IV) produced the lowest skin conductance measurements in 86.7% of participants during the cognitive task and 84.6% of participants during the emotional task. However, the fabric electrodes produced highest readings towards the end of the physical task and during the subsequent recovery period in 46.2% of participants.

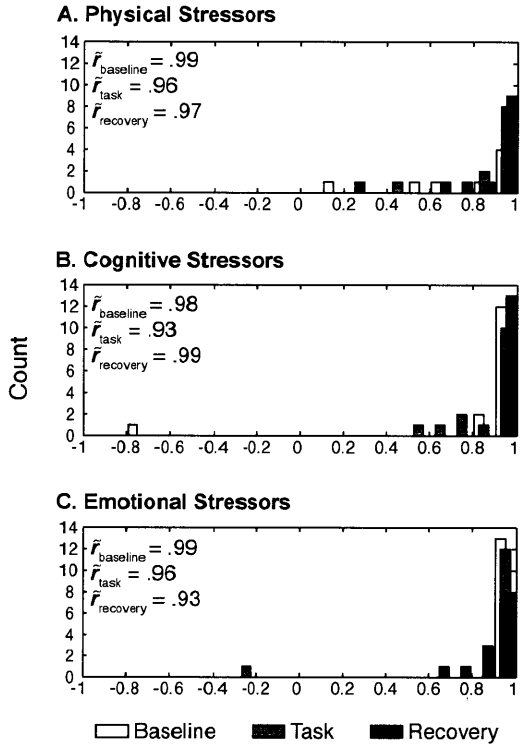

Figure 3-8: *Distributions of correlation coefficients between EDA measurements from bilateral fingers (I and II in Fig. 4) under (A) physical ($n = 13$), (B) cognitive ($n = 15$) and (C) emotional ($n = 13$) stressors. Each experiment was separated into baseline, task and recovery conditions for correlation. The median values of the correlation coefficients, $\tilde{r}$, are also presented for each condition.*

3.5.2 Recordings of Proposed System are Highly Accurate and Strongly Correlated with FDA System

To evaluate the performance characteristics of our sensor module, we correlated the measured EDA signals by the proposed device with the Flexcomp from the left and right fingers

respectively (I and II in Figure 3-5) during the baseline, task and recovery conditions for all three experiments. The resulting histograms of the correlation coefficients, r, are displayed in Figure 3-8 ($p < 0.0001$ for all observations). Since some of the distributions were slightly negatively skewed and the mean is not robust to outlying observations, we chose to use the median $\tilde{r}$ as the measure of central tendency. Overall, recordings from the proposed system and the Flexcomp were stongly correlated ($0.93 \leq \tilde{r} \leq 0.99$) during the baseline, task and recovery period for all three experiments.

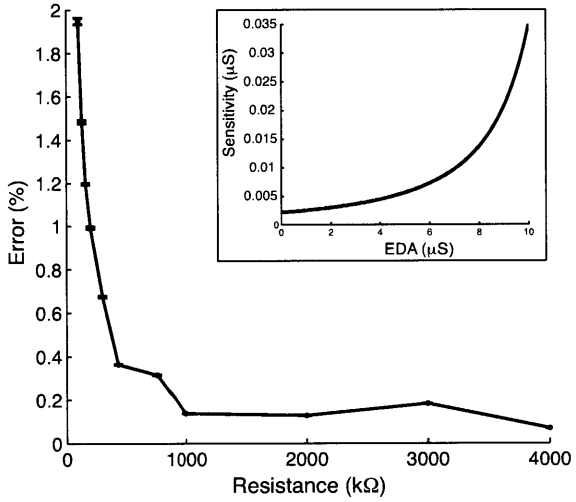

Figure 3-9: *Accuracy of the proposed sensor in fixed resistance measurements. Error bars represent 1 S.D. Inset: Computed sensitivity of the proposed sensor showing increasing quantization error at higher EDA values.*

To test the accuracy of the proposed system, we measured a series of 1% fixed resistors representative of typical skin resistance values (0.1-4.0 MΩ) with the proposed device and compared our readings to that of a digital multimeter (0.5% accuracy). The resulting error plot and computed sensitivity of the proposed system is presented in Figure 3-9. The measurement error of our device was higher at lower resistance values, which is likely due to the increasing quantization error at higher conductance values (Figure 3-9 inset). Within the tested range of resistances, the mean measurement error was found to be small ($0.68 \pm 0.64\%$). Across a range of typical skin conductance values, the mean sensitivity of the proposed device ($0.01 \pm 0.01\mu$S) was comparable to that of the Flexcomp (0.01 μS).

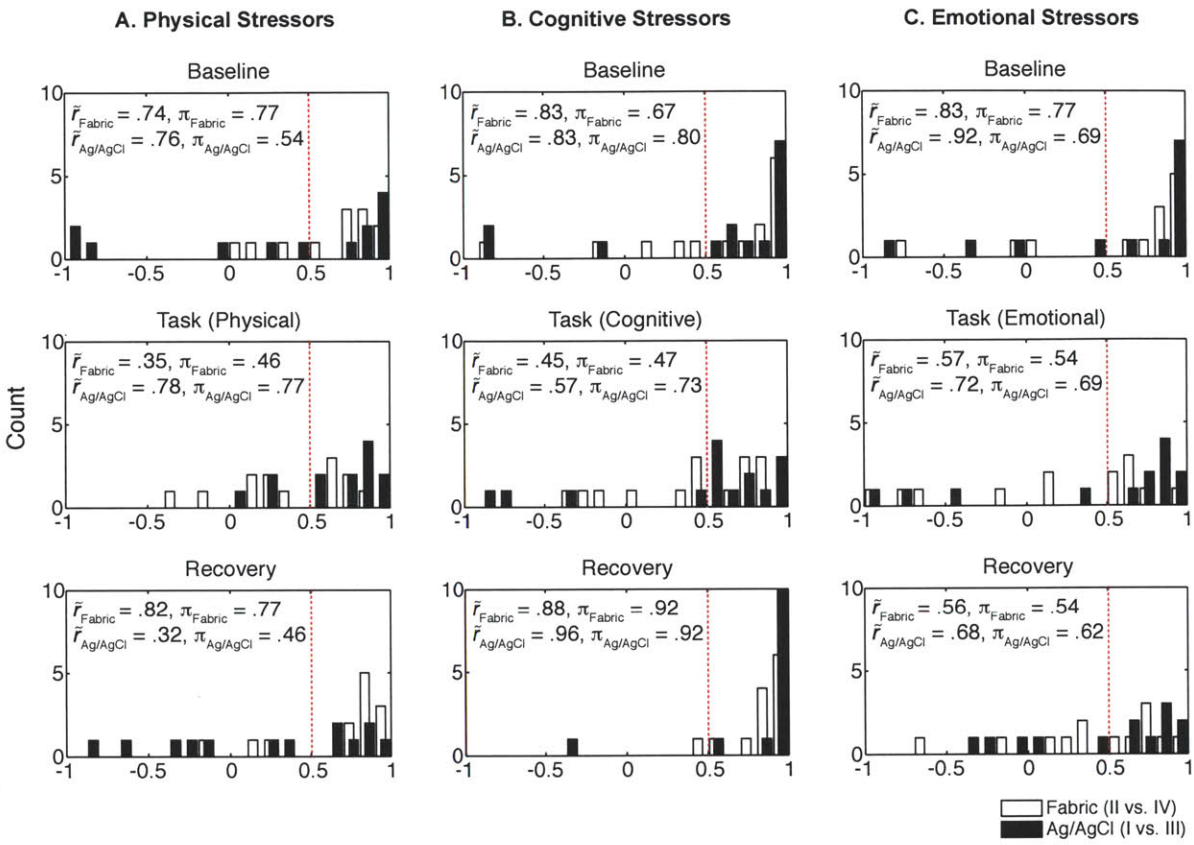

Figure 3-10: *Distributions of correlation coefficients between EDA measurements from distal forearms (conductive fabric electrodes on the left distal forearm and Ag/AgCl electrodes on the right distal forearm) and ipsilateral fingers under (A) physical ($n = 13$), (B) cognitive ($n = 15$) and (C) emotional ($n = 13$) stressors. Each experiment was separated into a baseline, task and recovery conditions for correlation. The median values of the correlation coefficients, $\tilde{r}$, along with the performance indices (proportion of correlation coefficients geq 0.5), π, are also presented for each condition. Dashed lines indicate $r = 0.5$.*

3.5.3 Distal Forearm is a Viable EDA Recording Site

To examine the degree to which distal forearm EDA activity parallels finger EDA activity (a traditional recording site), we correlated the EDA signals from the distal forearms with EDA signals from ipsilateral fingers (I and III, II and IV in Figure 3-5). Figure 3-10 presents the histograms of resulting correlation coefficients for the two different electrode types for all three experiments ($p < 0.0001$ for all observations).

In general, the distributions were negatively skewed with long tails to the left. Based on the median of the correlation coefficients $\tilde{r}$, correlation between the fingers and distal forearm was very strong ($0.76 \leq \tilde{r} \leq 0.96$) during the baseline and recovery periods for all but the physical and emotional recovery period with the Ag/AgCl electrodes. There

was also a strong correlation between the fingers and distal forearm during the physical ($\tilde{r} = 0.78$) and emotional ($\tilde{r} = 0.72$) tasks. During the cognitive task, the correlations were lower but remained moderately strong ($\tilde{r} = 0.57$).

By using Ag/AgCl electrodes on the right distal forearm and conductive fabric electrodes on the left distal forearm, we also compared the performance of the different electrode materials. Although the correlation between fingers and distal forearm was also very strong ($0.74 \leq \tilde{r} \leq 0.88$) during baseline and recovery periods with the conductive fabric electrodes, the correlation was weak during physical ($\tilde{r} = 0.35$) and cognitive tasks ($\tilde{r} = 0.45$) and moderately strong during the emotional task ($\tilde{r} = 0.57$). In addition, we herein define a performance index π to be the proportion of observations with moderately strong ($0.5 \leq r < 0.8$) to very strong ($r \geq 0.8$) correlation coefficients. Ag/AgCl electrodes yielded high performance for all three tasks ($0.69 \leq \pi \leq 0.77$) but for conductive fabric electrodes, the performance index was lower ($0.46 \leq \pi \leq 0.54$). From this perspective, the Ag/AgCl electrodes once again performed better than conductive fabric electrodes, particularly during the stressor task periods. Evidence from the analysis of correlation of EDA between fingers and distal forearms suggest that there are large interindividual differences with a small proportion (19%) of negative correlations.

3.5.4 Long-term In Situ EDA Recordings Reveal Patterns in Autonomic Arousal

The participant who wore the proposed sensor for a week reported no side effects or discomfort. From Figure 3-11, we see that long-term in situ recordings contain rich information about daily patterns of skin conductance modulation. For example, there is a consistent peak between the hours of midnight and 3 am corresponding to sleep activity. No skin conductance level drift was observable and the recordings were relatively artifact free, demonstrating the ability of the proposed sensor to continuously measure EDA during daily activities. The biggest advantage of the proposed wrist-worn Ag/AgCl sensor is the unprecedented ability to perform comfortable and long-term EDA measurements in situ, capturing differences in activities such as sleep, studying, lab-work, class-work, etc., without having to use gels or recalibrate baselines as the gel wears off and worry about whether levels are comparable.

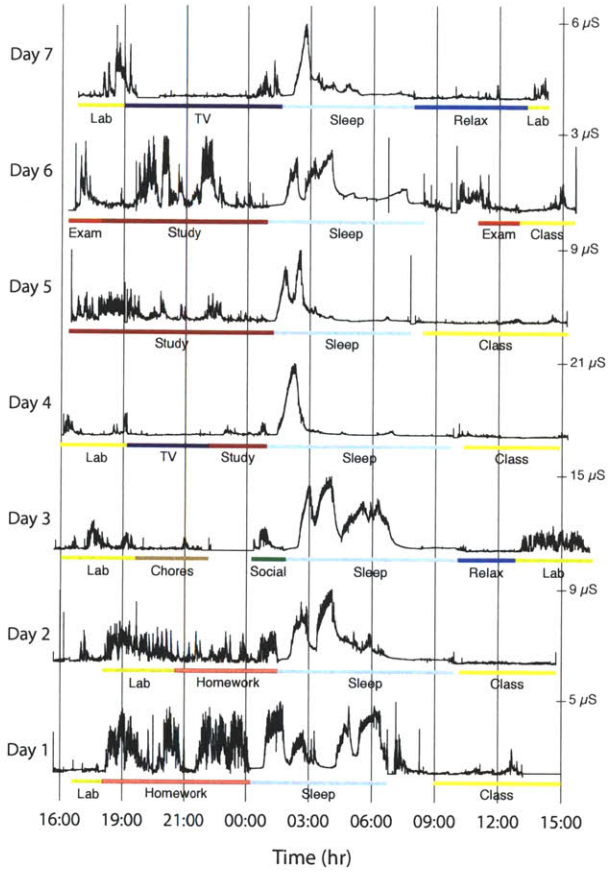

Figure 3-11: *Long-term in situ EDA recordings. Continuous skin conductance measurements were recorded for seven days in a natural home environment. Daily EDA waveforms displayed are normalized (Scale bar on the right side indicates original values).*

3.6 Discussion

As an index of sympathetic nervous system activity, EDA offers important insight into a broad spectrum of psychological and neurological disorders. The proposed sensor wristband provides a practical and comfortable new solution for widespread EDA assessment. Using Ag/AgCl electrodes, we found strong correlation between the proposed sensor wristband and an FDA-approved EDA measurement system across all tests. This capability for long-term EDA measurements both within and outside of a lab or clinical setting creates exciting opportunities for investigations that would otherwise have been difficult to implement.

It is not a trivial task to design experiments for performance comparison between different EDA sensors. Measurements of fixed resistors alone are insufficient and do not provide evaluation of the dynamic properties of the EDA sensors. Therefore, there is a need to

perform tasks that are well known to elicit changes in EDA while performing simultaneous measurements with the proposed system and an established system. However, both pairs of electrodes cannot be placed on the same recording site due to cross-talk interference. Due to the effect of habituation, which is characterized by decreasing reaction intensity with repeated stimulation, performing repeated measurements with the different sensors is also not a practical solution. This problem can be avoided by placing the different pairs of electrodes on bilateral recording sites, but there still exists issues concerning left-hand/right-hand differences in EDA [63,135]. Thus, it is important to point out the fact that even with identical sensors (e.g. Flexcomp) placed on bilateral sites, one should not expect to obtain identical measurements. With this caveat, we formulated the experimental setup described in III.B and depicted in Figure 3-5 with the goal of comparing the performance characteristics of the proposed EDA sensor with a "gold standard", FDA-approved and commercially available EDA measurement system (Flexcomp).

The three experiments performed were selected to capture a variety of EDA responses to classic stimuli. Furthermore, the cognitive experiment consisted of two separate tasks of differing complexity (mental arithmetic task and the Stroop word-color matching test) while the emotional experiment also elicited an anticipatory response prior to providing emotional stimuli. It is well known that stress can induce an increase in both tonic and phasic components of EDA. Our measured EDA recordings showed changes of skin conductance from baseline (at rest) in response to a stressor task and during recovery. As expected, skin conductance increased during physical strain as induced by intense exercise and emotional strain as induced by mental arithmetic, the Stroop word-color matching task and the horror movie clip. Although it is tempting to assume that each different EDA waveform represents either purely thermoregulatory or emotional sweating, it is worth noting that the responses are likely a combination of different sweating mechanisms. For example, sweating from physical exercise involves both thermal and mental sweating [91] and the rapid change from baseline at the start of the various stressor tasks presumably involves the orienting response. Therefore, these recordings merely demonstrate changes in EDA under different stressors. Emotional sweating (increased sweat gland activity as a concomitant of psychological and especially emotional states) has been observed mainly on palmar and plantar sites, but the specificity of emotional sweating remains in question [9]. Our findings indicate that the ventral sides of the distal forearms can also produce sweat responses to emotional stimuli.

The strong correlations between the proposed device and the Flexcomp, placed on the traditional measurement sites, indicate that our system functions as intended.

The wide distribution in correlation coefficients between the fingers and the dorsal forearm could be due to differences in sweat gland distribution or skin sudomotor innervation. Indeed, the two most commonly used dermatome maps present different spinal nerve innervations at the ventral side of the distal forearms. According to Fender [59], dermatomes of the ventral side of the distal forearms are continuous with the palmar sites (C6-C8), but Keegan and Garrett [87] describe the ventral side of the distal forearms as innervated by dermatomes C5, C6, C8 and T1. In addition, differences in moisture buildup between the skin-electrode interfaces could also contribute to the large variance of correlation coefficients. This was particularly evident at the end of the physical task, which resulted in negative correlation coefficients in 38% of participants (decreasing skin conductance at fingers but increasing skin conductance at distal forearms). There is a lack of evidence to suggest a dependence on age or gender. Nonetheless, the overall pattern of results suggests that the EDA measured from the distal forearms closely parallels EDA measured from the fingers.

Using conductive fabric as electrodes is an attractive option in designing wearable sensors as it potentially enables greater comfort. Although at rest and recovery, the conductive fabric electrodes performed somewhat similarly to conventional Ag/AgCl electrodes, it is important to take note that that they have weaker ability to measure EDA changes during stressor tasks. Given the stretchy nature of the conductive fabric, it is likely that the electrodes do not maintain their electrical properties when in contact with the user. Furthermore, the ability of fabric to absorb moisture and sweat also contributes to altering their electrical properties over time and is the likely reason for our results showing that the levels of EDA were usually higher after the physical exertion task for the conductive fabric electrodes than for the traditional Ag/AgCl electrodes (Figure A-2). In view of this, we recommend using standard Ag/AgCl electrodes for more sensitive analysis of EDA measurements.

Long-term assessment of EDA revealed interesting trends in the participants sympathetic modulation over a weeklong period. Intervals of elevated EDA frequently corresponded to times when the participant was studying, doing homework or taking an exam. This is possibly due to the increased cognitive stress associated with those activities. The

characteristic peaks occurring during sleep have been associated with slow wave sleep [85] and remain a subject for future studies. We found the sensor wristband to provide reliable and robust attachment of the electrodes to the skin, even in the presence of forearm motion during normal daily activities. Motion artifacts were typically observed only when the electrode-skin interface was disturbed such as when external pressure was applied against the electrodes or when the wearer readjusted the position of the electrodes.

3.7 Conclusion

We have presented a compact and low-cost wearable EDA sensor that enables comfortable long-term assessment of EDA. The novelty of our system consists in the use of the distal forearms as recording sites, the miniaturization of the sensor module as well as the design of a small wristband that allows for unobtrusive and non-stigmatizing continuous EDA measurements during everyday activities. Experimental outcomes using Ag/AgCl electrodes correlated strongly with the FDA-approved EDA measurement system.

To the best of our knowledge, we described the first detailed study indicating that the ventral side of the distal forearms is a viable alternative to the more popular palmar sites for EDA measurements across physical, cognitive and emotional stressors. Importantly, we also presented the first long-term recordings of EDA during daily activity outside of a lab or clinical setting. While palmar electrodes are encumbering, easily lost and frequently subjected to motion and pressure artifacts, the proposed wrist-worn sensor does not suffer anywhere near as much from these problems. Given the versatility of the proposed system that acts both as a data forwarding and data logging device, users are not constrained to stay within the range of a base station but instead have unrestricted continuous measurements regardless of location.

The importance of this work is the unprecedented ability to perform comfortable long-term and in situ assessment of EDA that the proposed system offers. Continuous long-term (multiple-day) EDA measurements during normal daily activity like that in Fig. 9 have, to our knowledge, not prior to this work been demonstrated in a practical way, and thus the new technology developed in this paper represents a significant advancement over existing systems. Investigations of long-term sympathetic nervous system activity can potentially add precious insight and enrich understanding of widespread neurological

conditions. Studies are currently underway to evaluate the use of the proposed EDA sensor in a variety of clinical applications, including autism, epilepsy and sleep disorders.

Chapter 4

Autonomic Footprints of Epileptic Seizures

4.1 Introduction

Sudden unexpected death in epilepsy (SUDEP) is the leading cause of death directly related to epilepsy, and is particularly prevalent in people with chronic epilepsy [164, 175, 189]. Although a relatively rare event, the risk of sudden death in young people with epilepsy is 24 times higher compared to the general population [61]. The incidence of SUDEP in the general epilepsy population ranges from 0.1 to 2.3 per 1000 person-years [101, 104], representing a tangible risk of SUDEP. People with pharmacologically refractory epilepsy are at even higher risk and the incidence rate can reach 6.3 - 9.3 per 1000 person-years in candidates for epilepsy surgery [39, 130]. The pathophysiological mechanisms of SUDEP are poorly understood although various seizure-induced mechanisms have been proposed, including cardiac arrhythmia [40, 56], central [168] and obstructive [144] apnea, pulmonary dysfunction [139, 185] and primary cerebral shutdown [23, 115]. These mechanisms may not be independent of each other and are likely interrelated, possibly through the autonomic nervous system. Case-control studies have provided insight into the clinical risk profiles and consistently indicate that SUDEP mainly occurs in the context of a generalized tonic-clonic seizure [75, 94, 131, 202]. However, it remains unclear what causal or contributory factors make tonic-clonic seizures a major risk factor and why in some cases a generalized tonic-clonic seizure becomes fatal unlike all other similar seizures in the past. One explanation

might be that the intensity of the seizure is a key factor in initiating a lethal vicious cycle of events [167].

Recently, a case-control study revealed that the duration of post-ictal generalized electroencephalographic (EEG) suppression was associated with SUDEP [104]. The period of post-ictal diffuse EEG attenuation was significantly prolonged in generalized motor seizures of the SUDEP group and the risk of SUDEP increased in direct proportion to duration of suppression. This is consistent with observations from published case reports of SUDEP that occurred during EEG monitoring; seven out of eight cases reported abrupt interruption of ictal activity replaced by severe suppression of the EEG that failed to recover in the fatal seizure [14, 23, 99, 104, 115, 144]. EEG features were not described in the eighth case [40]. Moreover, another case that was monitored at the time of a near SUDEP incident with successful cardio-respiratory resuscitation also involved marked suppression of the post-ictal EEG [168]. However, another study demonstrated the association between PGES and GTCS, but challenged the significance of PGES as an independent SUDEP biomarker [176]. This discrepancy could be due to the fact that the data studied were snapshots recorded a long time before the patients died of SUDEP. Given the inter-seizure variability of PGES for each patient and that a patients risk for SUDEP may evolve over time, measurements based on a couple of seizures may not be representative of a patients overall risk. If data on PGES could be collected over longer durations (e.g. weeks to months) from patients at home, this would lead to a better characterization of the utility of PGES as a biomarker for SUDEP.

Here, we describe a pilot study on the autonomic footprints left by different seizures types and the relationship between the seizure intensity, quantified as the degree of autonomic imbalance and post-ictal generalized EEG suppression, a surrogate biomarker for SUDEP. To gain a better understanding of the role of the sympathetic nervous system, we performed continuous measurements of electrodermal activity during peri-ictal periods of complex partial seizures and secondarily generalized tonic-clonic seizures using a novel wearable biosensor. Sympathetic postganglionic fibers innervate eccrine sweat glands and their activity is reflected in measurable changes in skin conductance at the surface [37, 153]. Therefore, modulation in skin conductance, or more generally speaking, in electrodermal activity (EDA), is a unique parameter that reflects purely sympathetic activity without parasympathetic antagonism [26, 37, 197, 203]. To assess parasympathetic activity, we per-

formed time-frequency mapping of heart rate variability. Heart rate variability, a measure of fluctuations in the interval between normal heartbeats mediated by autonomic inputs to the sinoatrial node, is an established measure of cardiac autonomic function [21, 110, 171]. Vagal modulation can be quantified by analyzing oscillations at respiratory frequencies (also known as respiratory sinus arrhythmia) that are mediated solely by the parasympathetic system and are abolished by atropine infusion [6, 142]. Here we present, for the first time, high-resolution characterization of sympathetic and parasympathetic alterations associated with seizures and show a critical window of autonomic imbalance after tonic-clonic seizures. Importantly, we found that the seizure intensity of tonic-clonic seizures, quantified as the magnitude of autonomic disturbance, was strongly correlated with post-ictal EEG suppression. These results raise the possibility that autonomic footprints of seizures could serve as biomarkers for the risk of SUDEP, as well as the possibility of a wearable device for round-the-clock monitoring to identify potentially dangerous seizures

4.2 Experimental Methods

4.2.1 Patients and Seizures

We recruited patients with epilepsy who were admitted to the long-term video-EEG monitoring (LTM) unit at Childrens Hospital Boston for characterization of events, pre-surgical evaluation or invasive monitoring for possible epilepsy surgery. Typically patients stayed for three to seven days at the LTM. All the participants provided written informed consent. This study was approved by the institutional review boards of Childrens Hospital Boston and Massachusetts Institute of Technology. We excluded patients who did not experience either a complex partial or secondarily generalized tonic-clonic seizure that was successfully captured during monitoring. We also excluded seizures that were not preceded by at least 60 min of non-ictal activity.

4.2.2 Wearable EDA Biosensors

The design and construction of the wrist-worn wearable EDA biosensor has been described in the previous chapter. Briefly, the sensor measures exosomatic skin conductance by applying direct current to the stratum corneum of the epidermis beneath measuring electrodes. To achieve a wide dynamic range of skin conductance measurements, the analog conditioning

circuitry utilizes non-linear feedback automatic bias control with low-power operational amplifiers. The sensor module also contains a tri-axis accelerometer for measurements of physical activity (actigraphy). All the electronic components were integrated into a wristband made out of terrycloth for comfortable and inconspicuous use. We used disposable Ag/AgCl disc electrodes with contact areas of 1.0 cm^2 for our recordings as recommended in the literature [66]. We use the ventral side of the distal forearms as recording sites as placement of electrodes on the forearm are less susceptible to motion artifacts and highly correlated to palmar recordings [141]

4.2.3 Recordings

EEG recordings were performed using conventional scalp EEG electrodes (10-20 system) with a sampling rate of 256 Hz or implanted intracranial electrodes at a sampling rate of 500 Hz (XLTEK, Oakville, ON, Canada). ECG was monitored concurrently from a modified lead-II with adhesive electrodes placed below the clavicles. For all the epilepsy work in this thesis, EDA recordings were recorded at 20 Hz and synchronized with the video/EEG/ECG recordings by generating technical artifacts at the beginning and end of each session for offline realignment. Each recording session lasted approximately 24 hours and batteries were replaced on a daily basis.

4.2.4 EEG Analysis

Video and EEG recordings were examined by two board-certified clinical neurophysiologists who were blinded to EDA, heart rate variability, and clinical information. Seizure type, ictal EEG localization, EEG seizure onset and offset, clinical seizure onset and duration of post-ictal generalized EEG suppression were determined. Post-ictal generalized EEG suppression was defined as the immediate post-ictal generalized decrease of EEG signals below 10 V in amplitude, not including muscle, movement, breathing, electrode or other artifacts [104].

4.2.5 EDA Analysis

EDA recordings were analyzed using custom written software in MATLAB (MathWorks Inc., Natick, MA). Raw EDA recordings were low-pass filtered (Hamming window, length = 1025, 3 Hz) to reduce motion artifacts and the filtered signals were used in all subsequent processing. For each seizure, the corresponding peri-ictal EDA recording from 60 min prior

to EEG seizure onset up to 120 min afterwards was segmented. To obtain the time profile of EDA alterations, a one-minute moving average window with zero overlap was applied to the pre- and post-ictal segments (e.g. each data point shown in Figure 4-4A and B is the average of 20 $\times$ 60 samples). To calculate the ictal EDA parameters, the segmented recordings were low-pass filtered (Hamming window, length = 1025, 0.01 Hz) to obtain the tonic component of EDA. The baseline was computed as the mean level over the entire 60 min pre-ictal period. Response latency was measured as the time from EEG seizure onset to the moment the filtered EDA signal exceeded two standard deviations (SD) above the pre-ictal baseline (EDA response onset). EDA response amplitude was determined as the difference between the response peak and pre-ictal baseline. Response end time was established as the time when the EDA response fell below 90% of the peak ictal amplitude. The area under the EDA response curve was calculated by integrating the EDA signal from the EDA response onset to the end time after subtracting the baseline. Area under the rising portion was taken as the integral from the EDA response onset to the peak response. The natural log-transformation was applied to all area calculations as the formation of the sum of products generates a value that increases and decreases in an exponential manner.

4.2.6 ECG Analysis: Time-frequency Mapping of Heart Rate Variability

All ECG recordings were analyzed using custom written software in MATLAB (MathWorks Inc., Natick, MA). ECG recordings were processed to remove noise as described by De Chazal and colleagues [41]. Baseline wander was removed by subtracting an estimate of the baseline obtained by two median filters. Power-line and high-frequency noise was then removed from the baseline-corrected ECG using a 12-tap low-pass filter (35 Hz) with equal ripple in the pass and stop bands. For each seizure, the corresponding peri-ictal filtered ECG signal from 60 min prior EEG seizure onset up to 120 min afterwards was segmented. The inter-beat interval (RRI) time series was formed by first employing automated QRS detecting using filter banks [4] and then manually examining the results to correct for false positives and missed beats. To remove artifacts such as ectopic beats, the RRI signal was filtered using the non-causal of variable threshold algorithm [200] with a tolerance of 20%. Next, the RRI signal was interpolated using a cubic spline at 4 Hz to obtain a uniformly sampled time series. The time profile of heart rate alterations was computed as with a one-minute sliding window with no overlap that was applied to the pre- and post-ictal

segments. For time-frequency analysis, baseline non-stationarities of the RRI series were removed by a detrending method based on a smoothness priors approach with the smoothing parameter [182]. The detrended RRI series was converted into an analytical signal using the Hilbert transform to remove negative frequencies. The smoothed pseudo Wigner-Ville (SPWV) time-frequency distribution with 1024 frequency bins was then computed using the analytical signal. We used a rectangular window (length = 121) for time-domain smoothing and a Gaussian window for frequency smoothing (length = 127). The parasympathetic mediated high frequency spectral component (HF) was extracted from the SPWV distribution by integrating the spectral powers between 0.15 and 0.4 Hz. The time profile of HF power alterations was obtained using a one-minute moving average window with no overlap that was applied to the pre- and post-ictal segments (Figure 4-4A and B). Pre-ictal baseline was determined by taking the mean value over the 30 min period right before EEG seizure onset. The minimum HF power level was also determined from the 30 min post-ictal period. The maximum percentage change in HF power was defined as:

$$\Delta HF_{max} = \frac{HF_{min} - HF_{baseline}}{HF_{baseline}} \times 100\% \tag{4.1}$$

4.2.7 Statistical Analysis

Statistical analyses were performed using the MATLAB statistics toolbox (MathWorks Inc., Natick, MA). Within seizure type comparisons of pre- and post-ictal measurements were performed using paired, two-sided Wilcoxon signed-rank tests (WSRT). To account for multiple comparisons, the resulting p values were adjusted using the False Discovery Rate controlling procedure [19]. Comparisons between seizure types and between SUDEP risk groups were made using unpaired, two-sided Mann-Whitney-Wilcoxon tests (MWW). The Pearson correlation coefficient was determined to measure the strength and direction of the linear relationship between the different pairs of variables. Each test was performed at a significance level of 0.05. Data are expressed as mean $\pm$ standard error (SE).

4.3 Results

We included 11 patients with refractory epilepsy in this study, all of which were candidates for epilepsy surgery. Clinical information for each patient is presented in Table 4.1. In

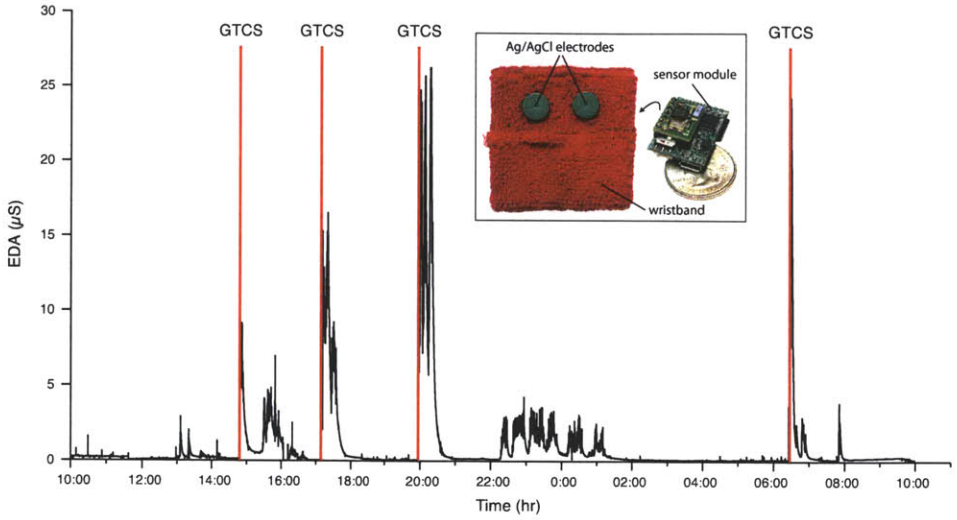

Figure 4-1: *Long-term electrodermal activity (EDA) recordings obtained from a wearable biosensor. In this example of a 24 h continuous EDA recording from a single patient, four secondarily generalized tonic-clonic seizures (GTCS) were captured. Vertical red lines denote EEG seizure onset. Inset: The wearable biosensor consists of an inconspicuous wristband with an integrated sensor module that can be worn comfortably for long periods of time and during daily activities. The underside of the wristband is shown to reveal standard dry Ag/AgCl electrodes used for EDA measurements.*

addition to combined video-EEG and electrocardiogram (ECG) monitoring, we successfully recorded over 1176 hours of EDA data with durations of 4.5 ± 0.8 days/patient (mean $\pm$ SD) using a wearable skin conductance biosensor (Figure 4-1). A total of 34 seizures comprising 22 complex partial and 12 secondarily generalized tonic-clonic seizures met the inclusion criteria described in the Methods section. The seizures occurred at different day- and nighttimes and during both awake and sleep states (Figure 4-2). Physiological recordings of each individual seizure are presented in Appendix C.

4.3.1 Autonomic Footprints Reveal Critical Window of Severe Imbalance after Tonic-Clonic Seizures

First, we examined the time courses of autonomic alterations in complex partial and secondarily generalized tonic-clonic seizures to identify differences that may contribute to tonic-clonic seizures being a major risk factor for SUDEP. We analyzed both EDA and electrocardiogram (ECG) recordings up to 60 min before EEG seizure onset and 120 min afterwards when possible. ECG recordings were not included for six complex partial seizures and one tonic-clonic seizure due to short post-ictal recordings (< 30 min), missing data, and signal corruption by artifacts. We chose time-frequency mapping based on the modified Wigner

Table 4.1: Clinical Characteristics of Patients

Patient no./sex	Age/epilepsy duration [years]	EEG seizure focus	MRI findings	Seizure frequency	AEDs	Duration of monitoring	Seizures included
1/m	15/13.5	Right>left posterior quadrant	Right occipital resection cavity (history of glioma)	2–4 CPS/week; 3 GTCS in life	LEV,LTG, MT,OXC	3 nights	2 CPS, 1 GTCS
2/m	17/1	Bifrontal	Frontal meningioma	1 GTCS/month	VPA	6 nights	4 GTCS
3/m	20/3	Left fronto-temporal	Normal	2–3 CPS/week; 0.5 GTCS/month	CBZ,LEV	5 nights	1 CPS, 2 GTCS
4/m	9/9	Left fronto-temporal	History of right thalamic hemorrhage	0.1–2 CPS/month	LTG,TGB, VPA	4 nights	1 GTCS
5/f	11/7	Multifocal	N.A.	N.A.	LEV,PHT, VPA	4 nights	2 CPS, 3 GTCS
6/m	16/15	Left fronto-temporal	Normal	1–2 CPS/month; 2 GTCS/year	GBP,LOR, LTG,ZNS	5 nights	1 GTCS
7/m	13/N.A.	Right central	Right fronto-parietal dysplasia	N.A.	DIA,LTG, PHT,TPM	4 nights	6 CPS
8/m	13/8	Left fronto-temporal	Absence of corpus collosum, dysmorphic ventricles, bifrontal transmantle gray matter heterotopia, small pituitary gland	1–2 CPS/month; 1 – 2 GTCS/year	CBZ,LTG	5 nights	5 CPS
9/f	6.5/3	Left hemisphere	N.A.	3 CPS/day	CBZ,LTG	5 nights	4 CPS
10/m	3/1	Multifocal	Normal	1–2 CPS/week; 4 GTCS in life	CLN,LEV, LTG,VPA	4 nights	1 CPS
11/f	9/5	Left temporal	Normal	2–3 CPS/week	LEV,VPA	4 nights	1 CPS

AED antiepileptic drugs; CBZ carbamazepine; CLN clonazepam; CPS complex-partial seizure; DIA diazepam; GBP gabapentin; GTCS secondarily generalized tonic-clonic seizure; LEV levetiracetam; LOR lorazepam; LTG lamotrigine; MT melatonin; MRI magnetic resonance imaging; N.A. information not available; OXC oxcarbazepine; PHT phenytoin; TPM topiramate; VPA valproic acid; ZNS zonisamide

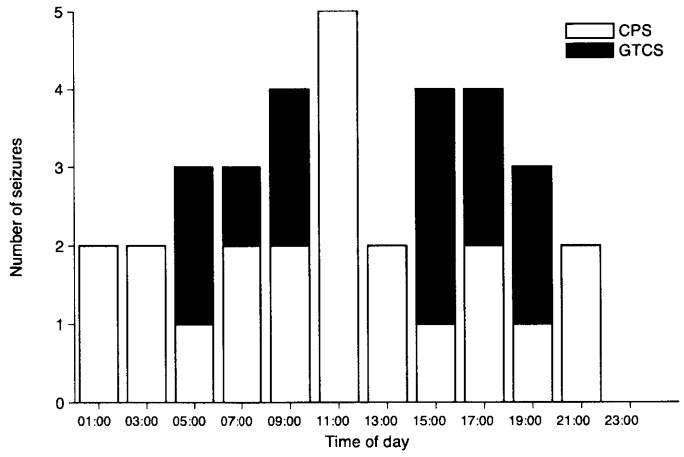

Figure 4-2: *Histogram of the onset times for the complex partial seizures (CPS) and secondarily generalized tonic-clonic seizures (GTCS) in this study. The occurrence times for both seizure types were distributed throughout the day and night.*

distribution for its high resolution and ability to detect rapid transients [133, 134]. Cardiac vagal activity was estimated by the power in the high frequency spectral component (HF, 0.15 - 0.4 Hz) of inter-beat (RR) interval oscillations that reflect parasympathetic modulation of the heart. Examples of changes in autonomic activity from a single seizure of each type are shown in Figure 4-3.

In 19/22 (86%) complex partial seizures, we observed an increase in EDA greater than two SD above the mean pre-ictal level, which we defined as an EDA response. All 12 (100%) generalized tonic-clonic seizures exhibited an EDA response. There was no difference between the latency from EEG seizure onset to EDA response onset between the two seizure types ($p > 0.1$; two-sided Mann-Whitney-Wilcoxon test [MWW]); the median latency for all seizures was 33.25 s.

By comparing the minute-to-minute evolution of post-ictal autonomic activity to the pre-ictal baseline (averaged over 60 min before seizure onset), we observed a period of autonomic disturbance after complex partial seizures (Figure 4-4A). Sympathetic-mediated EDA was significantly higher for the first 9 min before returning to baseline ($p < 0.05; n = 22$; two-sided Wilcoxon signed-rank test [WSRT]). Post-ictal heart rate was elevated for 3 min ($p < 0.05; n = 16$; WSRT). Parasympathetic-modulated HF power was persistently lower for approximately 55 min with sporadic brief periods of reduction afterwards ($p < 0.05; n = 16$; WSRT).

Strikingly, we found a period of severe and uninterrupted autonomic imbalance after

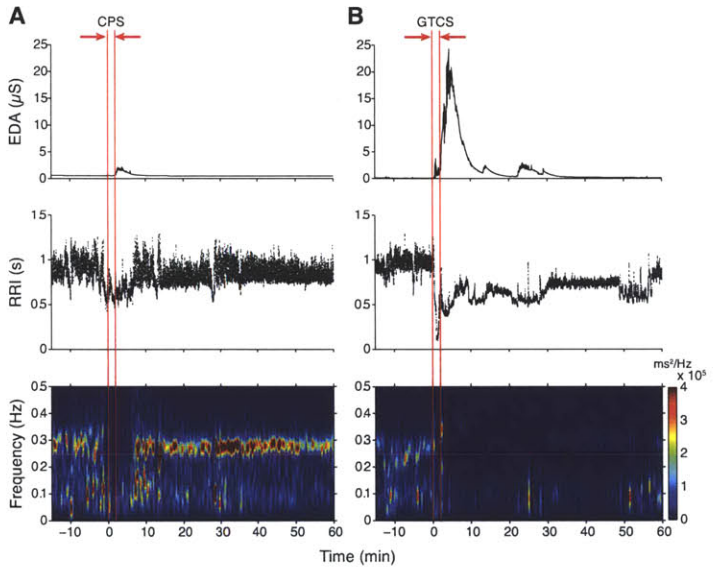

Figure 4-3: *Changes in autonomic activity after individual epileptic seizures. Examples of alterations in electrodermal activity (EDA), R-R intervals (RRI) along with time-frequency mapping of the RRI during peri-ictal segments of 75 min. (A) A small increase of EDA is observed with a decrease in RRI (i.e. increase in heart rate) during this complex partial seizure (CPS). There is also a brief reduction of the high frequency spectral component (HF, 0.15 - 0.4 Hz) of RRI during the post-ictal period that reappears after approximately 5 min. (B) A large surge in EDA is visible after this secondarily generalized tonic-clonic seizure (GTCS) accompanied by a drop in RRI. Note the reduction in RRI variability during the post-ictal period and the dramatic reduction of the high frequency power. Vertical red lines denote EEG seizure onset and offset.*

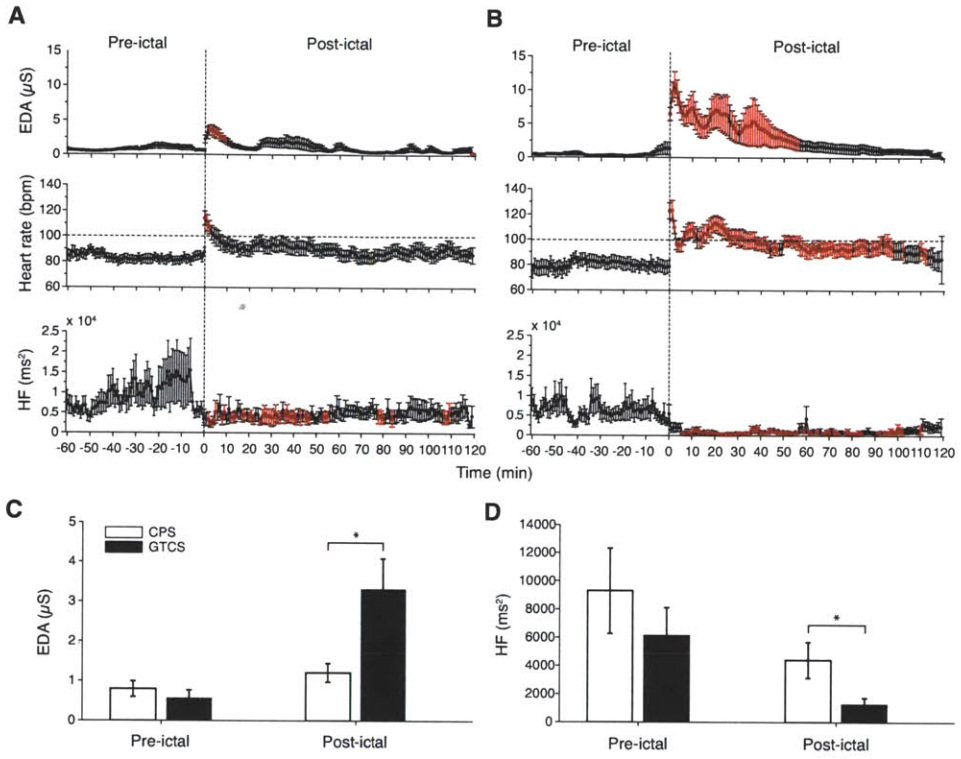

Figure 4-4: *Autonomic footprints of epileptic seizures. High-resolution profiles of autonomic alterations computed every minute during a peri-ictal period of 3 h for (A) complex partial seizures and (B) secondarily generalized tonic-clonic seizures. Each post-ictal measurement epoch was sequentially compared to the baseline level taken as the average of the entire 60 min pre-ictal period. Epochs in red indicate statistical significance after accounting for multiple comparisons using the False Discovery Rate controlling procedure ($p < 0.05$; paired, two-sided Wilcoxon signed rank test). Post-ictal levels of EDA were higher for 9 min after complex partial seizures ($n = 22$). Heart rate was also higher lasting 3 min ($n = 16$). HF power was continuously reduced for approximately 55 min ($n = 16$). Strikingly, the first 56 min after tonic-clonic seizures was associated with marked increases in EDA ($n = 12$) and heart rate ($n = 10$), as well as profound reduction in HF power ($n = 10$). Persistent tachycardia was observed for 40 min; heart rate and HF power levels recovered after 100 min. (C) EDA during the pre-ictal period was marginally similar between seizures ($p = 0.05$; Mann-Whitney-Wilcoxon test [MWW]), but was higher in tonic-clonic seizures during the first 60 min of the post-ictal period ($p = 0.004$; MWW). (D) There was no difference in pre-ictal HF power between seizures ($p > 0.5$; MWW), whereas post-ictal HF power was lower in tonic-clonic seizures ($p = 0.033$; MWW).*

generalized convulsions (Figure 4-4B). This period was characterized by profound elevation of EDA for 56 min ($p < 0.05; n = 12$; WSRT), increased heart rate lasting approximately 100 min ($p < 0.05; n = 10$; WSRT) with persistent tachycardia for 40 min and suppressed HF power unrelieved for approximately 100 min ($p < 0.05; n = 10$; WSRT). These findings suggest that the early post-ictal phase appeared to be dominated by sympathetic over-activation coupled with vagal suppression whereas the later phase seemed to be dominated by impaired vagal reactivation.

4.3.2 Comparison Between Complex Partial and Generalized Tonic-Clonic Seizures

We also probed the difference in magnitude of autonomic alterations between both seizure types. Pre-ictal levels (averaged over 60 min) of EDA and HF power were not different between seizure types; however, post-ictal EDA (averaged over 120 min) was significantly higher in tonic-clonic seizures compared to complex partial seizures ($p = 0.004$; MWW; Figure 4-4C), suggesting much higher sympathetic activation. In addition, post-ictal HF power was significantly lower in tonic-clonic seizures ($p = 0.033$; MWW; Figure 4-4D), suggesting much lower vagal influence. Therefore, autonomic activity after tonic-clonic seizures was impacted more severely and these alterations lasted longer compared to complex partial seizures.

4.3.3 Correlations Between Heart Rate, Sympathetic EDA and Parasympathetic HF Power

We examined the relationship between heart rate (HR), EDA and HF by calculating the Pearson correlation coefficient between HR and EDA as well as between HR and HF during both pre-ictal and post-ictal periods (60 min) for each individual seizure. In the pre-ictal period before complex partial seizures, there was no correlation between EDA and HR (median correlation coefficient $\tilde{r} = 0$) whereas HF and HR were negatively correlated ($\tilde{r}$ = -0.64). After complex partial seizures, the correlation between EDA and HR increased significantly ($\tilde{r} = 0.66$, $p < 0.05, n = 16$; WSRT). There was no significant difference in the correlation between HF and HR ($\tilde{r}$ = -0.62, $p = 0.38$). In the pre-ictal period before tonic-clonic seizures, there was also no correlation between EDA and HR (median correlation coefficient $\tilde{r} = 0$). HF and HR were negative correlated ($\tilde{r}$ = -0.15) but the correlation was

weaker compared to that of before complex partial seizures ($p < 0.005$). After tonic-clonic seizures, the correlation between EDA and HR trended upward ($\tilde{r} = 0.35, p = 0.098, n = 10$; WSRT). There was no significant difference in the correlation between HF and HR ($\tilde{r}$ = -0.09, $p = 0.91$).

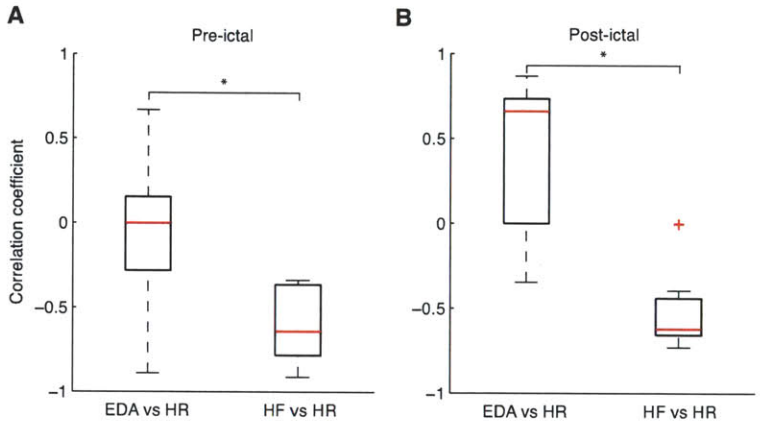

Figure 4-5: *Correlation coefficients between EDA vs HR and HF vs HR during the (A) pre-ictal and (B) post-ictal period of complex partial seizures.*

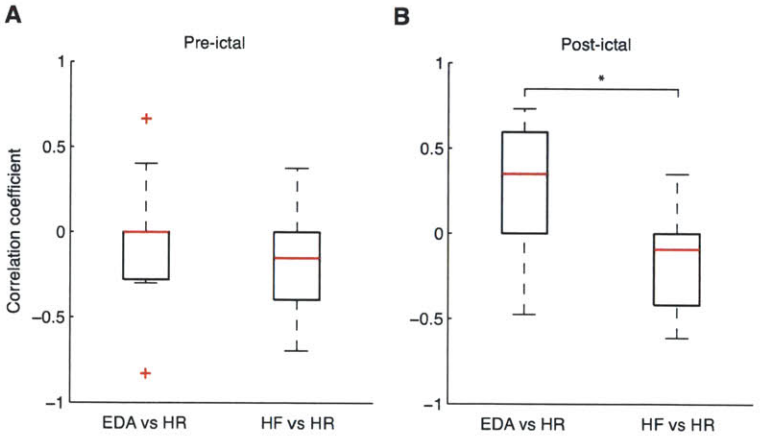

Figure 4-6: *Correlation coefficients between EDA vs HR and HF vs HR during the (A) pre-ictal and (B) post-ictal period of generalized tonic-clonic seizures.*

4.3.4 Magnitude of Autonomic Imbalance in Tonic-Clonic Seizures is Strongly Correlated with Post-Ictal Generalized EEG Suppression

To evaluate a possible link between seizure intensity and SUDEP, we examined the relationship between the autonomic impact and post-ictal EEG suppression in tonic-clonic seizures,

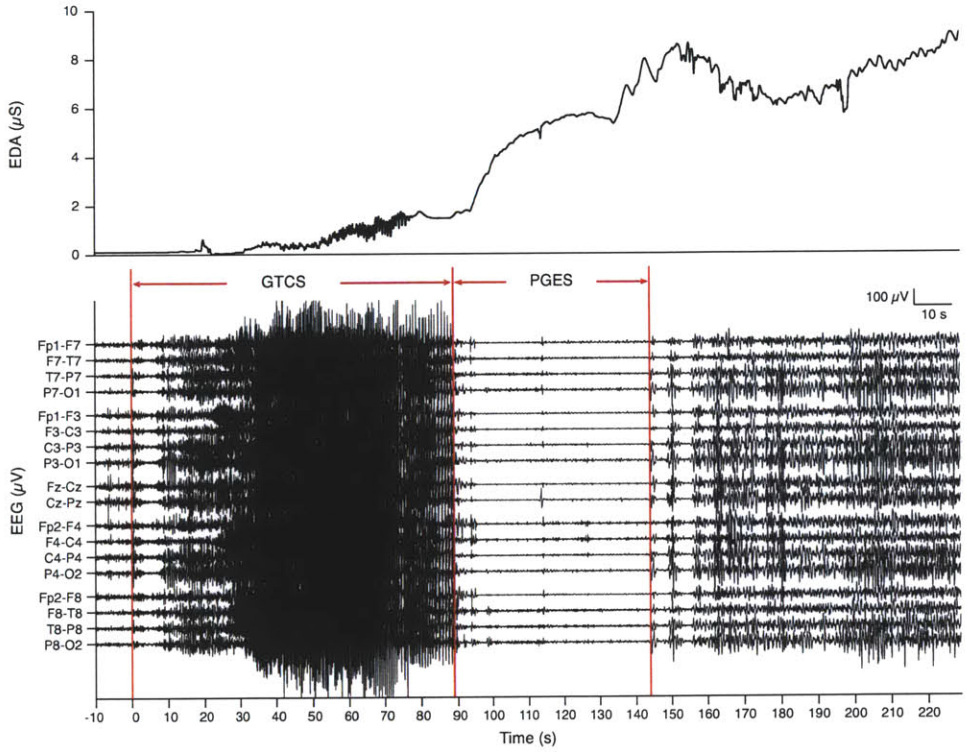

Figure 4-7: *Post-ictal generalized EEG suppression (PGES) following a secondarily generalized tonic-clonic seizure. An example of a tonic-clonic seizure abruptly terminated and replaced by flattening of EEG signals in all channels.*

a proposed biomarker of SUDEP risk. An example of generalized EEG suppression following a tonic-clonic seizure along with changes in EDA is shown in Figure 4-7. In general, the onset/offset moments of PGES appeared to coincide with a steep and smooth increase in EDA with a lack of high frequency responses 4-8. The duration of post-ictal EEG suppression could not be measured reliably in one seizure due to excessive corruption of the EEG signal by artifacts. Post-ictal EEG background attenuation was observed in 9/11 (81.8%) of the included tonic-clonic seizures. We quantified the magnitude of seizure-induced sympathetic activation by the amplitude of EDA response and area under the EDA response curve. We applied the log transformation to the area under the curve measurements to produce a linear change in the measurements. The impact on parasympathetic function was measured as the maximal percentage change in HF power during the post-ictal period compared to the pre-ictal baseline.

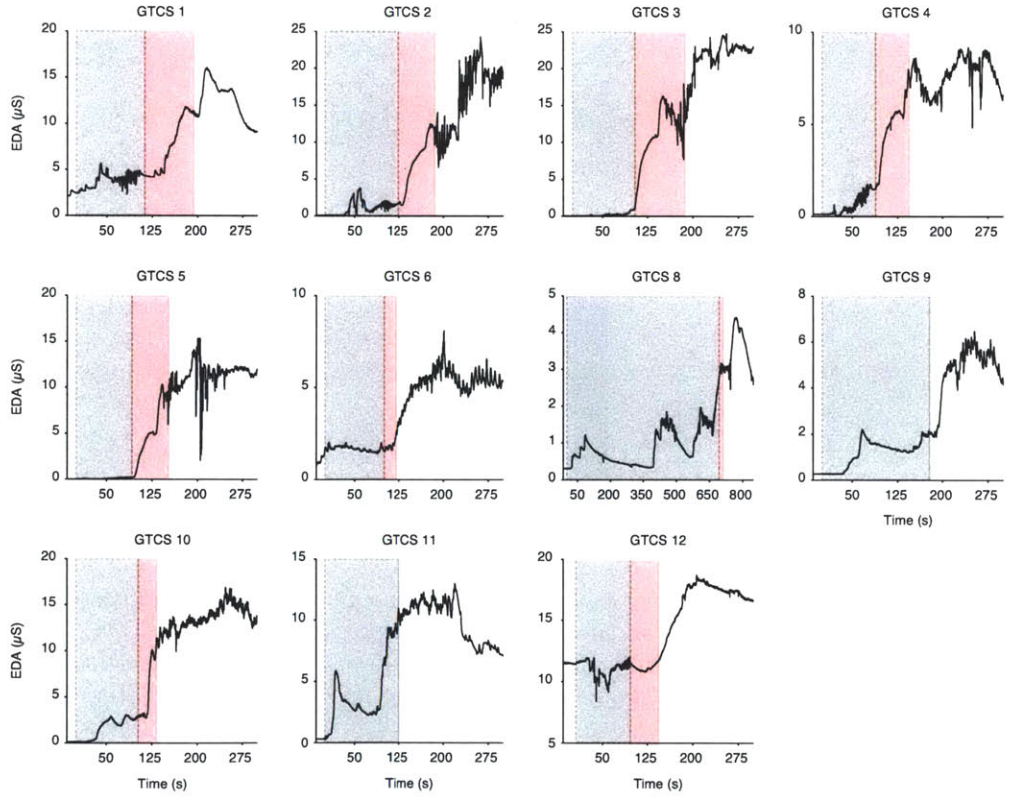

Figure 4-8: *Morphology of EDA changes relative to the onset/offset moments of PGES. The gray shaded areas represent the ictal period while the red shaded areas correspond to PGES. Seizures 9 and 11 did not exhibit PGES upon termination.*

Across all patients, we found that the amplitude of EDA response was strongly and pos-

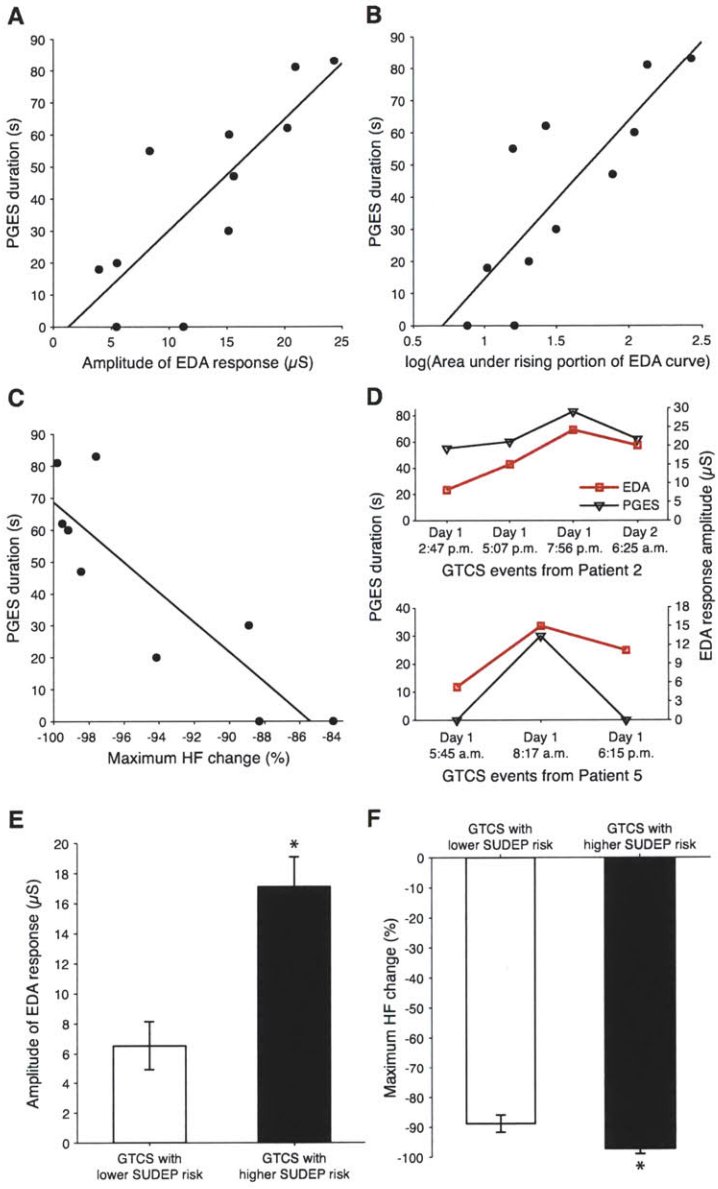

Figure 4-9: *Relationship between degree of post-ictal autonomic disturbance and post-ictal generalized EEG suppression (PGES) in secondarily generalized tonic-clonic seizures (GTCS). Scatter plots of PGES duration vs (A) EDA response amplitude, (B) log-transformed area under rising portion of EDA curve and (C) maximum percentage HF power change. EDA response amplitude was strongly positively correlated with PGES (Pearson* $r = 0.81, p = 0.003; n = 11$*), as was the area under rising portion of EDA curve (*$r = 0.83, p = 0.002; n = 11$*). The reverse direction of relationship was observed for maximum percentage HF power change, which was strongly negatively correlated with PGES (*$r = -0.87, p = 0.002; n = 9$*). (D) The association between EDA response amplitude and PGES in GTCS on a patient-specific level showed close agreement in trends. Patient 2 had four GTCS events (top) and patient 5 had three GTCS events (bottom). (E) GTCS with higher SUDEP risk (PGES >* 20 *s) had a higher EDA response amplitude (*$p = 0.01$*; Mann-Whitney-Wilcoxon test [MWW]). (F) The maximum percentage decrease in HF power was greater in GTCS with higher SUDEP risk (*$p < 0.05$*; MWW).*

itively correlated with the duration of EEG suppression ($r = 0.81, p = 0.003; n = 11$; Figure 4-9A). Similarly, the log-transformed area under the EDA curve was positively correlated with post-ictal EEG suppression ($r = 0.75, p = 0.008; n = 11$); the area under the rising portion of the EDA response particularly showed strong correlation ($r = 0.83, p = 0.002; n = 11$; Figure 4-9B). In contrast, the maximal percentage change in HF power was strongly and negatively correlated ($r = -0.87, p = 0.002; n = 9$; Figure 4-9C) with the duration of EEG suppression (i.e. a greater reduction of HF power was associated with a longer post-ictal EEG suppression). Notably, the post-ictal EEG suppression was not dependent on the total seizure duration ($p > 0.3, n = 11$) or on the duration of the generalized motor phase ($p > 0.3, n = 11$).

We also examined the relation between the EEG suppression duration and autonomic variables on a patient-specific level (within patients who had multiple tonic-clonic seizures) to see how sensitive the autonomic measures might be as an indicator of post-ictal EEG suppression. We observed that the trends in post-ictal EEG suppression and amplitude of EDA response amplitude after all four tonic-clonic seizures from Patient 2 were in close agreement (Figure 4-9D top). This similarity in trends was also present for all three tonic-clonic seizures in Patient 5 (Figure 4-9D bottom). The two tonic-clonic seizures from Patient 3 could not be compared because the duration of post-ictal EEG suppression could not be determined in one seizure (excessive corruption of the EEG signal by artifacts).

4.3.5 Binary Outcome Analysis for Prolonged Post-Ictal EEG Attenuation

Next, we divided the convulsive seizures into lower and higher SUDEP risk groups to assess the difference in autonomic impact between the two groups. For generalized motor seizures, post-ictal EEG suppression greater than 20 s is associated with a significant elevation of odds ratios for SUDEP [104] and this served as our threshold for grouping the seizures. We found that the EDA response amplitude was significantly higher in seizures with higher SUDEP risk ($p = 0.01$; MWW; Figure 4-9E). Moreover, seizures in the higher risk group also had a greater maximum reduction in HF ($p < 0.05$; MWW; Figure 4-9F).

4.4 Discussion

The present study is the first to quantify both sympathetic and parasympathetic autonomic disturbance after tonic-clonic seizures and to show a significant correlation of these alterations to the duration of post-ictal EEG suppression. We found that autonomic activity after tonic-clonic seizures was impacted more severely compared to complex partial seizures. Furthermore, this impact lasted up to 100 min. This critical period appears to involve sympathetic over-activation evidenced by a surge in EDA coupled with vagal withdrawal indicated by suppressed HF power in the early phase, and impaired vagal reactivation in the later phase. Importantly, the degree of both sympathetic activation and parasympathetic suppression increased approximately linearly with duration of post-ictal EEG suppression. Our results suggest that seizure intensity, as determined by magnitude of autonomic impact, could be an important factor in the pathophysiological mechanism of SUDEP.

While many studies have analyzed baseline (inter-ictal) alterations of autonomic function in patients with epilepsy [160], data on post-ictal autonomic alterations are limited despite evidence that they are among the most dangerous effects of seizures [46]. Prior studies on post-ictal autonomic modulation limited heart rate variability analysis to a single measurement taken during the early [7, 175] post-ictal period ($<$ 15 min) and in one case, during late [191] post-ictal period (5 - 6 h). As such, little is known about the time course of autonomic disturbance after seizures. Moreover, decoupling the relative influence of parasympathetic or sympathetic system is challenging because heart rate, like blood pressure and respiration rate, is controlled by both branches of the autonomic nervous system [197] and the two influences are not easily separated. While there is a consensus that HF power reflects vagal modulation of the heart rate, there is no clear cardiac measure of sympathetic modulation. It has been claimed that power in the low frequency range (LF, 0.04 - 0.15 Hz) reflects primarily sympathetic modulation of heart rate and that the LF/HF ratio reflects the sympathovagal balance but this is highly controversial as beta blockade does not reduce, but rather increases LF power [32] and direct cardiac sympathetic blockage via epidural anesthesia has no effect on it [76]. In contrast, EDA provides a sensitive index of sympathetic activity alone. This work appears to be the first attempt to characterize changes in EDA before, during and after epileptic seizures.

This study was able to leverage an innovation in bio-sensing that allows sympathetic EDA to be measured comfortably for long periods of time off the wrist. The findings here significantly expand current knowledge by presenting continuous, minute-by-minute profiles of both sympathetic and parasympathetic modulation up to 2 h after complex partial and secondarily generalized tonic-clonic seizures. Compared to complex partial seizures, generalized tonic-clonic seizures induced much higher and prolonged sympathetic activation and greater reduction of cardiac vagal influence compared to complex partial seizures. This difference in both the degree and duration of autonomic imbalance may in part explain why tonic-clonic seizures are a major risk factor for SUDEP. The high-resolution time course revealed what appears to be two-phases of post-ictal autonomic disturbance after tonic-clonic seizures. The first phase involved a prolonged sympathetic surge in EDA lasting approximately 65 min. This time course is in close agreement with changes in plasma concentrations of catecholamines that are maximally elevated in the first 10 minutes after tonic-clonic seizures and decline over 60 min to normal levels [165]. Together, these findings support the notion of a generalized sympathetic neural activation. On the other hand, the marked decrease in HF power implies a reduction of vagal control over the heart. Similarly, the persistent low HF power and delayed decrease in heart rate even after sympathetic levels are restored to baseline suggest impaired vagal reactivation in the second phase. Experimental [77] and clinical studies [112,119,122] have consistently shown that decreased vagal activity is associated with increased risk for cardiac mortality and sudden death, independent of disease status. A recent case study described a patient who underwent repeated measures of HF power, which progressively deteriorated prior to SUDEP [146]. Augmented vagal activity is protective against lethal arrhythmias [42,78,195] and decreased vagal modulation leading to an increase in ventricular automaticity could in turn make the heart susceptible to arrhythmias. The autonomic profiles uncovered in this study indicate that there exists a critical window of disordered autonomic regulation after seizures, especially tonic-clonic seizures, which may lead to increased vulnerability of a patient for sudden death.

The strong correlations between post-ictal EEG suppression and both sympathetic and vagal alterations that act in opposite directions provide the first evidence that post-ictal generalized EEG suppression is associated with the severity of autonomic disturbance in tonic-clonic seizures. Post-ictal generalized EEG suppression was shown to provide quan-

tification of SUDEP risk in a retrospective case-control study [104] and provided a surrogate marker for actual SUDEP. In conjunction with a recent report of association between vagus-mediated heart rate variability and an inventory of clinical SUDEP risk factors [44], our findings raise the possibility that autonomic activity could provide markers for SUDEP risk. We found that tonic-clonic seizures at higher risk for SUDEP had significantly higher sympathetic activation and greater vagal reduction compared to tonic-clonic seizures in the lower risk group. These results suggest that seizure intensity as measured by autonomic dysregulation may be factor in the pathogenesis of SUDEP. Prolonged EEG suppression may excessively inhibit different neuronal systems, such as parasympathetic centers or circuits, and result in unbridled sympathetic activation. In turn, sympathetic over-activity can play an important role as a trigger of ventricular tachyarrhythmias and sudden cardiac death [81,150,209], especially in the setting of impaired vagal reflexes that lower the threshold for ventricular fibrillation [22]. Indeed, SUDEP due to cardiac arrhythmia following a partial seizure has been witnessed once, albeit in an individual with a history of myocardial infarction [40]. Ventricular fibrillation after a secondarily generalized tonic-clonic seizure in a patient without underlying cardiac disease was also reported in a near-SUDEP event [56].

These findings must be considered in light of several limitations of the present study. First, due to the exploratory nature of the study, a relatively small number of patients and seizures were included. The limited number of patients also precluded us from comparing autonomic and EEG features in different seizure types within individual patients or selecting only one seizure per patient to reduce the effect of individual differences. There is a possibility of patient selection bias since the study group involved only patients with epilepsy severe enough to merit hospitalization, and are at higher risk for SUDEP. As SUDEP is a rare phenomenon and cannot be reasonably expected to occur during a monitoring situation, direct assessment of the risk of SUDEP is very challenging. Thus, we derived the risk for SUDEP from post-ictal EEG suppression, a surrogate marker that is possibly related to SUDEP risk.

The current results provide a promising outlook for patients with epilepsy. The possibility of autonomic biomarkers of seizure intensity or SUDEP risk is attractive for ambulatory monitoring without the need for continuous EEG measurements. It remains challenging to implement a-low-cost, wearable EEG recorder that is not unwieldy or stigmatizing. On the other hand, the wrist-worn EDA biosensor utilized in this study allows comfortable round-

the-clock monitoring without social awkwardness. With the onboard tri-axis accelerometer and wireless transceiver, it is possible to develop convulsive seizure detectors that can automatically alert caregivers in the event of a seizure [90, 107]. Furthermore, EDA parameters such as the amplitude of EDA response would provide caregivers with important information regarding the severity of the seizure and aid in the identification of seizures that require immediate medical attention. Our data suggest that the correlation between amplitude of EDA response and duration of EEG suppression amplitude also exists within seizures of a specific individual. Supervision and attention to recovery after a seizure may be important in SUDEP prevention because most deaths are unwitnessed [93]. A study in a residential school for children with epilepsy who were closely supervised at night and attended to after a seizure reported that deaths occurred with students on leave or after they left, but not at the school [125]. Another large case-control study found that sharing a bedroom with someone capable of giving assistance and special precautions such as regular checks throughout the night or using a listening device were all protective factors against SUDEP [94]. The findings here might help discriminate when a post-ictal period is likely to be life-threatening.

SUDEP in most cases is triggered by a generalized tonic-clonic seizure but it remains unknown what physiological contributory factors make this particular seizure fatal unlike all other seizures in the past. Our data reveal a window of significantly disordered autonomic regulation after tonic-clonic seizures that may create conditions for sudden death. These findings further establish a correlation between the degree of autonomic dysregulation and duration of EEG suppression following a tonic-clonic seizure. Since prolonged post-ictal EEG suppression was observed in patients who subsequently died of SUDEP, it will be of great interest to establish whether or not these autonomic footprints could provide reliable biomarkers to identify epilepsy patients who are at risk of SUDEP.

Chapter 5

Convulsive Epileptic Seizure Detection Using Electrodermal Activity and Accelerometry

5.1 Introduction

People with epilepsy often describe seizures as occurring "like a bolt from the blue" which reflects the apparent sudden, unforeseen way in which seizures tend to strike [120]. Abrupt episodes of staring, loss of muscle control or loss of consciousness can pose a serious injury risk and can even be fatal if, for example, they occur while the person is driving, crossing a busy street, bathing, swimming or climbing stairs. The danger of brain damage increases with seizure duration and seizures can progress to become status epilepticus, a life-threatening medical emergency in which the brain is in a state of persistent seizure. Moreover, sudden unexpected death in epilepsy (SUDEP), although a relatively rare event, tends to occur during or shortly after a seizure and the deaths are largely unwitnessed [177,183]. The apprehension and worry about injury, or even death, resulting from a seizure often overshadows the lives of those unable to achieve complete seizure control [54]. Many parents of children with epilepsy fear that their child might be seriously injured by seizures and the fear increases when they are unable to observe their children's seizures during sleep [84]. An unobtrusive device suitable for long-term, continuous monitoring and capable of automated detection of an ongoing seizure could have a significant positive impact on the everyday lives

of patients and families. Timely detection of an ongoing seizure and subsequent notification of caregivers would enable a patient to receive treatment if injured, or to be placed in the recovery position to avoid airway obstruction that could be fatal.

Combined electroencephalogram (EEG) and video-monitoring remains the gold standard for seizure detection in clinical routine. As such, the vast majority of work in automatic epileptic seizure detection has focused on analyzing the EEG [71,145,149,163]. Nonetheless, an EEG-based approach for a seizure detection alarm system has many practical disadvantages for long-term or everyday use. To obtain high-resolution data, the electrodes need to be placed on the surface of the brain or within its depths, involving a highly invasive procedure [106]. Non-invasive scalp EEG-based algorithms have achieved good performance [163], but the ambulatory EEG units available today are bulky and cumbersome. The technical requirements for the implementation of wearable EEG recorder are challenging and much effort will be needed to design a wearable electrode system that is not obstructive, unwieldy or stigmatizing [34]. In a survey of 141 patients with uncontrolled epilepsy from two different epilepsy centers, almost 80% of patients were opposed to wearing scalp EEG electrodes to obtain seizure warnings [159]. This strong aversion may be due to the discomfort associated with wearing scalp electrodes, the fear of stigmatization, or both. On the other hand, up to 55% of patients were willing to consider the use of a mobile device.

The special requirements for a seizure detector suitable for everyday use in terms of cost, comfort and social acceptance call for alternative sensing modalities. The clinical manifestation of a seizure depends on the location and extent of the propagation of the affected neurons. For seizures that result in motor accompaniments, video analysis of the movements can be used for seizure detection [86,105]. Nonetheless, it is difficult to detect movements under a blanket and these video-based approaches are limited to bedtime monitoring when the patient is within the camera's field of view. Similarly, sensor-embedded mattresses can be used to detect generalized tonic-clonic (GTC) seizures but cannot provide ambulatory monitoring [33]. Accelerometry (ACM) recordings have also been reported to be a valuable sensing method for detection of seizures with motor accompaniments [129] but few algorithms for automated detection have been proposed [17,38,80,128]. More importantly, these studies did not evaluate the rate of false alarms during normal daily movements, a critical parameter for any wearable seizure detector. Two recent clinical studies evaluated the use of wrist-worn device containing a three-dimensional accelerometer to detect GTC

seizures over long periods of monitoring, but the feature derivations and seizure detection algorithms were not described [90,107]. Another study reported promising results in a small training set, but lacked any independent test data for proper evaluation [158].

Epileptic seizures are often associated with changes in autonomic nervous system (ANS) functioning. These ictal autonomic symptoms range from subtle manifestations such as flushing, sweating and piloerection to severe increases in blood pressure and changes in heart rate and cardiac conduction [15,108,109,157]. They are not merely simple reactions to motor manifestations of seizures, but are mediated by an activation of the central autonomic network [15]. The various ictal clinical manifestations outlined represent alternative options to the EEG that can potentially be used for seizure detection. A multi-modal approach that combines two or more complementary physiological signals may lead to better discriminability. In the previous chapter, we showed that electrodermal activity (EDA), which reflects the modulation of sweat gland activity by the sympathetic nervous system, increased during both 86% of complex partial seizures and 100% of GTC seizures in a set of 34 seizures measured. However, no one has explored the utility of EDA in the context of seizure detection.

In this chapter, we describe a novel algorithm and device for seizure detection using a wearable EDA and ACM sensor that is suitable for round-the-clock monitoring. This method uses Support Vector Machines to construct semi-patient-specific classifiers for sensitive and specific detection of GTC seizures. We outline the steps involved in pre-processing the data, feature extraction and creating the models. The problem of seizure detection is posed as a supervised learning task in which the goal is to classify a time series segment as seizure or non-seizure based on extracted features from EDA and ACM recordings. We evaluate the performance of our algorithm on EDA and accelerometry data comprising a wide range of daily movements from epilepsy patients undergoing long-term monitoring in video-EEG units. We demonstrate how analysis of ictal autonomic changes in EDA can be used to supplement accelerometer-based motion analysis in order to enhance overall seizure detection performance.

5.2 Related Work

Accelerometry (ACM) is a practical and low-cost method of objectively monitoring human activity patterns [114]. It has been used in many clinical research areas such as performing activity recognition [13, 179], estimating metabolic energy expenditure [28], studying sleep and circadian rhythms [10, 83], detecting falls in the elderly [27] and assessing the severity of motor complications in Parkinson's disease [137]. In the context of epilepsy, the use of accelerometers for monitoring seizures was rare [69] until recent years. In 2005, Nijsen and colleagues first proposed the use of accelerometers as a sensing method for seizure detection [129]. Out of 897 seizures that were recorded, 428 (48%) of the seizures could be detected by visual analysis of the ACM patterns. Moreover, the authors observed that 95% of the 428 motor seizures contained stereotypical ACM patterns. Although visual analysis of ACM is labor intensive, this early work highlighted the potential value of ACM for detection of motor seizures.

Since then, investigators have started to develop automated seizure detectors based on ACM pattern analysis. Niijsen and colleagues presented an approach for automated detection of tonic seizures using ACM in 2009 [127]. Using linear discriminant analysis for classification, their algorithm detected 80% of the 27 tonic seizures from 18 patients. However, the positive predicted value (PPV), which is the proportion of detections that are true seizure events, was relatively low at 35%. In subsequent work, Niijsen and colleagues described a method for detecting myoclonic seizures also based on linear discriminant analysis using features derived from time-frequency analysis of ACM [128]. Four accelerometers were attached to a patient's wrists and ankles. 35 myclonic seizures from 21 patients were recorded and the Niijsen algorithm detected 80% of the seizures with a PPV of 15%.

Several investigators have focused on detecting nocturnal seizures of a patient in bed. Cuppens and colleagues introduced a simple method for motor seizure detection based on setting a threshold for the mean ACM energy [38]. This method achieved 92% sensitivity and 84% specificity on a validation set comprising 24 motor seizures from 3 patients. However, the performance was not evaluated on a test data set. Jallon used a Bayesian approach with hidden Markov models for statistical modeling of nocturnal seizures [80]. Based on a validation set composed of 46 seizures from 2 patients, the author reported a sensitivity of 89% and PPV of 65%. As was the case with the Cuppens study, no independent test data

was evaluated. Moreover, seizure occurrences were based on witness accounts and were not confirmed using video-EEG.

A major limitation of all the studies above is the lack of performance evaluation on long-term recordings containing a wide range of daily movements. In these works, the tested recordings were restricted to night time recordings (when patients were in bed and relatively inactive) or limited recordings of normal movements. Patel and co-workers highlighted the importance of assessing the rate of false alarms during routine daily activities in the development of a wearable seizure detector [138]. They proposed a method combining features from ACM and electromyography (EMG) and performed classification using a C4.5 decision tree. Based on evaluation on long-term data (48 hours) from a single patient with 3 seizure events, they reported an accuracy of 98%. It is worth noting that in unbalanced data sets (as is the case with rare seizure events) the overall accuracy can be misleading and is not an appropriate measure of performance. Another group reported that a Wii remote attached to the forearm could be used to detect four GTC seizures in three patients with 100% sensitivity and $\geq$ 88% specificity [158]. These results were based on visual determination of a suitable intensity threshold of the ACM signal for each seizure as well as a heuristically selected threshold for the time span in which the movement had to exceed the intensity threshold. As no independent data was tested, the generalizability of this simple thresholding method was not determined. Recently, Kramer and colleagues developed a seizure detection bracelet (EpiLert) and conducted a preliminary clinical trial [90]. The EpiLert detected 19 of 22 (91%) convulsive seizures from 15 patients and when tested on all 31 patients enrolled (including those who didn't experience seizures), it produced 8 false alarms during 1692 hours of monitoring. These results are very promising, but the authors did not disclose their method for feature extraction or classification methodology. Furthermore, the low false alarm rate could be because patients likely to have frequent seizure-like movements such as dystonic posturing, subtle behavioral automatism and pseudoseizures were excluded from testing. Another commercial wrist-worn motion detection device, the SmartWatch, was evaluated in a clinical study of 40 patients [107]. Out of the 40 patients, six had a total of eight GTC seizures and seven (88%) were detected by the SmartWatch. False alarms occurred 204 times over the duration of testing which was unspecified. Moreover, the seizure detection algorithm was not described.

5.3 Methods

5.3.1 Wearable EDA and ACM Biosensor

A complete description of the wearable EDA and ACM biosensor is described in Chapter 3. Briefly, the sensor measures exosomatic EDA (skin conductance) by applying direct current to the stratum corneum of the epidermis beneath measuring electrodes. To achieve a wide dynamic range of skin conductance measurements, the analog conditioning circuitry utilizes non-linear feedback automatic bias control with low-power operational amplifiers. In addition, the sensor module also contains a triaxis accelerometer for measurements of physical activity (actigraphy). A microcontroller digitizes the analog signals via a 12-bit A-D at a sampling frequency of 20 Hz. The data is then written to an onboard microSD card. We integrated the sensor module into a regular wristband made out of terrycloth, resulting in a comfortable and lightweight wearable sensor. Since all electronics and wiring are concealed within the wristband, the resulting device is inconspicuous, non-stigmatizing and allows for discrete monitoring of EDA. Furthermore, the electronic module can be easily detached when the user desires to wash the wristband.

We used dry Ag/AgCl disc electrodes with contact areas of 1.0 cm^2 for our recordings as recommended in the literature [66]. These electrodes are disposable and can be snapped onto or removed from the wristband with ease. Although the electrodes are commonly placed on the palmar surface of the hand (e.g. medial and distal phalanges of the fingers and the thenar and hypothenar eminences), we used the ventral side of the distal forearms as recording sites. Placement of electrodes on the forearm are less susceptible to motion artifacts and highly correlated to palmar recordings [141]. A 3.7 V lithium polymer battery with a capacity of 1100 mAh provides around 40 hours of operation; the battery can be recharged via a micro-USB cable.

5.3.2 Patients and Seizures

Over a period of eight months, we enrolled patients with epilepsy who were admitted to the long-term video-telemetry monitoring (LTM) unit at Childrenś Hospital Boston for assessment. The patients stayed at the LTM for 1-7 days for characterization of events or localization of the seizure onset zone in the setting of pre-surgical evaluation. EEG recordings were performed using conventional scalp electrodes (10-20 system) at a sampling

rate of 256 Hz or implanted intracranial electrodes at a sampling rate of 500 Hz (XLTEK, Oakville, ON, Canada). EDA sensor wristbands were placed on both wrists such that the electrodes were in contact with the ventral side of the forearms. EDA and ACM recordings were sampled at 20 Hz and synchronized with the video-EEG recordings by generating technical artifacts at the beginning and end of each session for offline realignment. Each recording session lasted approximately 24 hours and batteries were replaced on a daily basis.

5.3.3 EEG/ACM/EDA Analysis

Ictal video-EEG recordings were retrospectively reviewed by two board-certified clinical neurophysiologists who were blinded to the EDA data. Each GTC seizure was reviewed for both EEG and clinical ictal onset and offset times, EEG location and seizure semiology on video recordings. EDA and ACM recordings were analyzed using custom written software in MATLAB (The Mathworks, Inc.). Only recordings from one wearable biosensor were utilized for seizure detection (default choice was the right forearm unless data was unavailable or corrupted).

5.3.4 Seizure Detection Architecture

The various stages of the GTC seizure detector is depicted in Figure 5-1. A sliding window was used to extract 10 s epochs from both ACM and EDA recordings for each 2.5 s increment (75% overlap). The data was then pre-processed to removed non-motor and non-rhythmic epochs. Various features including time, frequency and non-linear features are extracted from remaining epochs of the ACM and EDA signals. Finally, each feature vector comprising features from both ACM and EDA signals was assigned to a seizure or non-seizure class using a Support Vector Machine. A seizure was declared after one feature vector was assigned to the seizure class.

5.3.5 Data Reduction

A GTC seizure typically lasts for 1-2 minutes whereas the patients were monitored continuously throughout their stay (days) in the hospital. As such, there is a vast amount of non-seizure data (forming the majority class), which causes the data set to be highly imbalanced. Thus, pre-processing of the data is important to decrease the computational workload as well as reduce the degree of data imbalance during supervised learning.

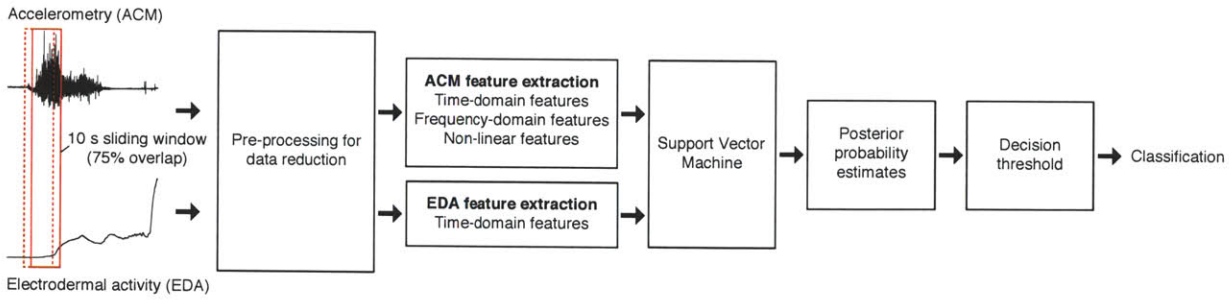

Figure 5-1: *Overview of seizure detection architecture.*

The first step was to divide the data into non-movement and movement events. We combined information from all three axes of the accelerometer to calculate the magnitude of the net acceleration, a as:

$$a = \sqrt{a_x^2 + a_y^2 + a_z^2} \tag{5.1}$$

A sliding window of 10 seconds with 75% overlap was used to calculate the standard deviation, σ of the acceleration epoch $(a_1, a_2, \ldots, a_N)$:

$$\sigma = \sqrt{\frac{1}{N-1}\sum_{i=1}^{N}(a_i - \mu)^2} \tag{5.2}$$

where

$$\mu = \frac{1}{N}\sum_{i=1}^{N} a_i \tag{5.3}$$

Epochs with σ below 0.1 g were automatically discarded from further analysis and treated as non-motor, and hence non-seizure events. The remaining epochs were detrended using a smoothness priors approach (smoothing parameter $\lambda = 300$) [182] and the discrete Fourier transform (DFT) was computed (200-point).

GTC seizures are composed of two primary phases – the tonic phase and the clonic phase. The tonic phase involves stiffening of the limbs and flexion or extension of the neck, back and extremities. During the clonic phase, muscles of the entire body start to contract and relax rapidly. These convulsions are manifest in the ACM signal as rhythmic activity typically above 2 Hz. Thus, each epoch was evaluated for important periods using an algorithm by Vlachos et al [201]. The underlying assumption is that the magnitudes of the coefficients of the DFT of a non-periodic time series are distributed according to an

exponential distribution.

$$f(x) = \lambda e^{\lambda x}$$

Important periods will have powers that deviate from the power content of the majority of the periods and can be identified by locating outliers according to an exponential distribution. As a result, we seek for infrequent powers by setting the probability p to a very low value to derive a power threshold T_p.

$$p = P(x \geq T_p) = e^{-\lambda T_p}$$

Solving for the power threshold,

$$T_p = -\frac{ln(p)}{\lambda} \tag{5.4}$$

For 99% confidence, we set $p = 0.01$ and λ is the reciprocal of the mean of the detrended acceleration signal power.

$$\frac{1}{\lambda} = \frac{1}{N}\sum_{i=1}^{N} a_i^2$$

Epochs with no frequency components that exceeded T_p were discarded and labelled as non-seizure events. Otherwise, $f_{dominant}$, the frequency component with the highest power beyond T_p was identified. If $f_{dominant} \geq 2$ Hz, the epoch was accepted for subsequent feature extraction.

5.3.6 Feature Extraction

A total of 19 features were computed to characterize each measurement epoch. These features were chosen to describe the time, frequency and phase space characteristics of the ACM signal as well as the temporal traits of the EDA signal.

Time-domain Analysis

To quantify the time-domain attributes of the ACM signal, we computed four different features. We calculated the mean, standard deviation, and root mean-squared of the net acceleration. In addition, we estimated the amount of force by accumulating the magnitude

of accelerometer data from each axis a_{mag} throughout the 10 s epoch.

$$a_{mag} = \int_{n}^{n+\Delta} |a_x(t)| + |a_y(t)| + |a_z(t)| dt \tag{5.5}$$

Spectral Analysis

The major energy band for daily activities falls between 0.3 and 3.5 Hz [174] whereas during GTC seizures the power is typically concentrated at frequencies above 2 Hz (Figure 5-2). To capture the spectral information of the net acceleration, we detrended the net acceleration using a smoothness priors approach (smoothing parameter $\lambda = 300$) [182] and computed the power spectral density using Welch's method (eight segments of equal length, 50% overlap, Hamming window). The entire frequency spectrum was divided into eight non-overlapping bands and the total integrated power within each spectral band was included as a feature (8 features). The dominant frequency within each epoch (across the entire 0 to 10 Hz band) along with its maximum power were also computed as features (2 features). Thus, a total of 10 spectral features were included for classification.

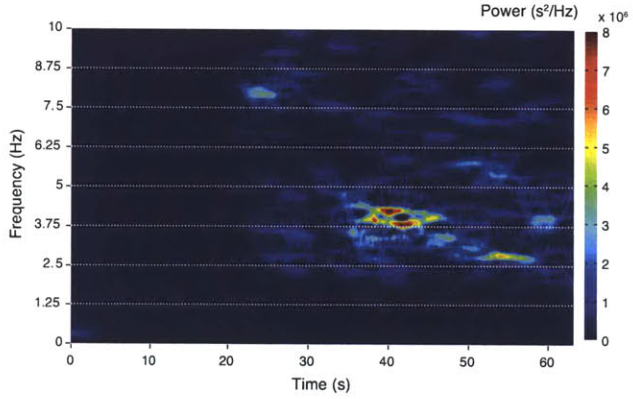

Figure 5-2: *Time-frequency mapping of the ACM signal during a tonic-clonic seizure (63 s long). The first 20 s do not contain much movement energy because the seizure starts off as a complex partial seizure before secondarily generalizing and affecting the motor cortex. The power distribution during the tonic clonic phase (after 20 s) is concentrated at frequencies above 2 Hz.*

Non-linear Analysis: Recurrence Quantitative Analysis

Recurrence plots provide a graphical method designed to locate hidden recurring patterns and compute non-linear dynamical measures [50]. This technique allows signals to be represented in state (phase) space by constructing embedded vectors $\vec{\mathbf{x}}(k)$ using the method of

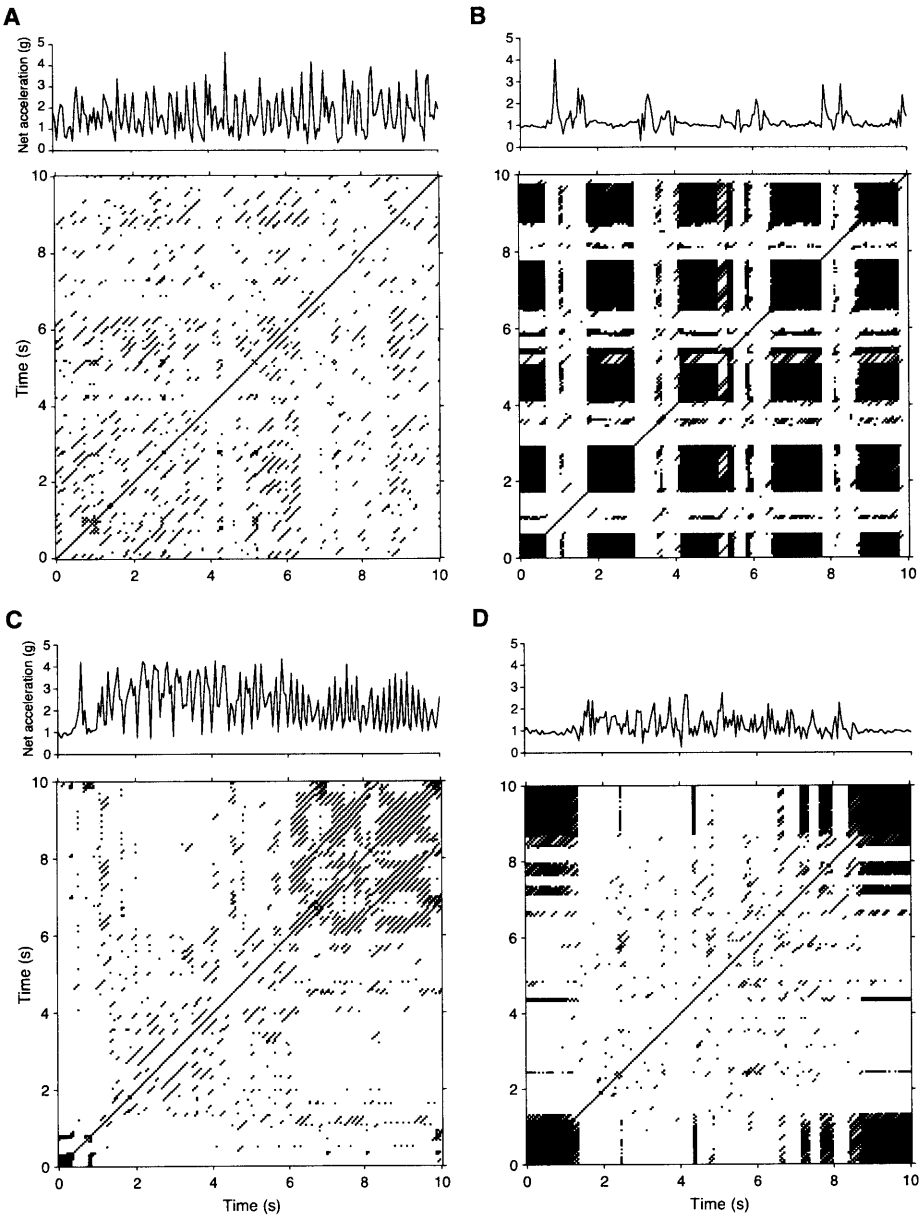

Figure 5-3: *Example of recurrence plots for various events. Time series of net acceleration (top) along with the corresponding recurrence plot (bottom) during (A) a tonic-clonic seizure epoch (B) playing catch with a ball (C) shaking dice and (D) flapping hands.*

time delays:

$$\vec{\mathbf{x}}(k) = \Big[x(k), x(k+d), \ldots, x(k+(m-1)d)\Big]^T$$

where m is the embedding dimension and d is the time delay.

Recurrence analysis was performed using the Recurrence Plot toolbox for Matlab [113]. The optimal parameter $m = 5$ was chosen as the embedding dimension where the amount of false nearest neighbors approached zero [88]. The delay $d = 1$ was calculated from the first minimum of the mutual information function [67]. The recurrence plot $\mathbf{R}(i,j)$ was then constructed by computing distances between all pairs of embedded vectors; a critical radius $\epsilon = 1$ was established to create a binary plot showing, for a given moment in time, the times at which the state space trajectory visited roughly the same area in the state space.

$$\mathbf{R}(i,j) = \Theta\Big(\epsilon - \Big|\Big|\vec{\mathbf{x}}(i) - \vec{\mathbf{x}}(j)\Big|\Big|\Big)$$

where $\Theta(x)$ is the Heaviside step function.

An example of a recurrence plot constructed from a seizure epoch is shown in Figure 5-3A. The short line segments parallel to the main diagonal suggest that the time series is deterministic. These small scale structures were quantified using recurrence quantification analysis [113]. The first feature included was the Shannon entropy $ENTR$ of the lengths of the diagonal lines, which reflects the complexity of the deterministic structure in the system.

$$ENTR = -\sum_{l=l_{min}}^{N} p(l) \ln p(l) \tag{5.6}$$

where $p(l)$ is the probability that a diagonal line has exactly length l estimated from the histogram $P(l)$ of the lengths l of the diagonal lines.

$$p(l) = \frac{P(l)}{\sum_{l=l_{min}}^{N} P(l)}$$

The second feature computed was laminarity LAM, the percentage of recurrence points which formed vertical lines. LAM is related with the amount of laminar phases in the system (intermittency).

$$LAM = \frac{\sum_{v=v_{min}}^{N} vP(v)}{\sum_{v=1}^{N} vP(v)} \tag{5.7}$$

where $P(v)$ is the histogram of the lengths v of the vertical lines.

To summarize, 16 ACM features were computed including 4 time-domain (mean, standard deviation, root mean-squared and accumulated magnitude), 10 spectral (dominant frequency, maximum power, and integrated power values from 8 non-overlapping frequency bands) and 2 non-linear features (entropy and laminarity).

EDA Analysis

First, the EDA recordings were lowpass filtered (Hamming window, length = 1025, 3 Hz) to reduce artifacts. Since GTC seizures are associated with an increase in EDA, we included three features extracted from each 10 s EDA epoch (Figure 5-4). We performed a linear least squares fit to the EDA segment and computed the slope as the first feature. The number of measurement points within the epoch that were greater than the previous point (i.e. $x(n) > x(n-1)$) was determined as the second feature. The third feature corresponded to the difference between the EDA measured at the start and end of the 10 s epoch.

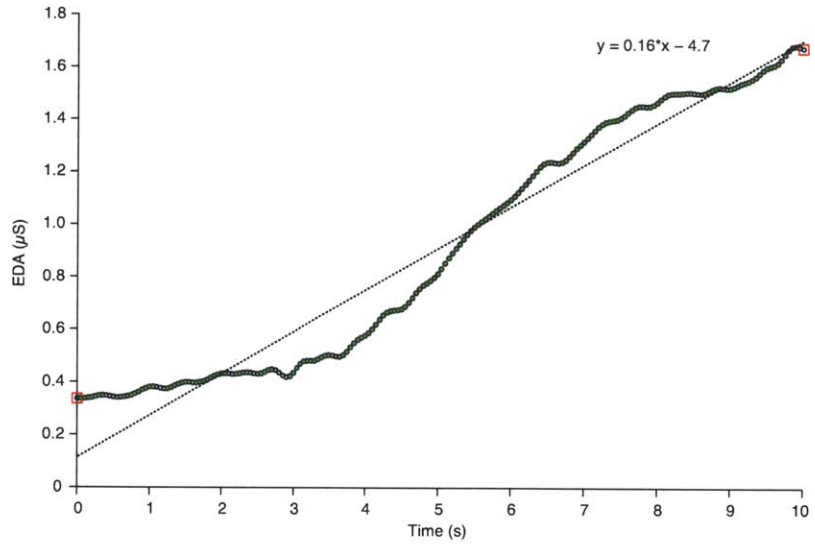

Figure 5-4: *Features extracted from a 10 s EDA epoch. Dotted line represents the least squares line fit. Green circles indicate measurement points that were greater than the previous point. Red squares indicate start and stop of the epoch.*

5.3.7 Support Vector Machines

Support Vector Machines (SVMs) are state-of-the-art binary classification methods that exhibit a remarkable resistance to overfitting and have shown excellent performance in complicated pattern recognition problems [31, 73]. An SVM can learn a decision boundary

in the form of a hyperplane that separates two classes. This hyperplane is selected such that the classification margin, which is the geometric distance between the hyperplane and the boundary cases of each class (i.e. the support vectors), is maximized for the best ability to accurately classify unseen data [132, 196]. Moreover, SVMs can map the original finite dimensional feature space into a much higher dimensional space through the use of a kernel function to improve the separability of the data.

An SVM is a good choice for the task of seizure detection because its unique learning mechanism allows it to perform well with moderately imbalanced data without any modifications [5]. Since an SVM only takes into account those instances that are close to the boundary for building its model, it is unaffected by negative instances far away from the boundary even if they are large in number. This is important given that the number of non-seizure instances far outnumber the seizure instances.

5.3.8 Model Selection and Testing Methodology

Designing the SVM algorithm for seizure detection consisted of a training phase, in which the model was learned on a subset of data and a testing phase, in which the model performance was evaluated on a different subset of data. We chose the Gaussian Radial Basis kernel function (RBF) as it provides non-linear mapping of the original feature vectors $\vec{\mathbf{y}}_\mathbf{i}$ into a higher dimensional space.

$$\text{RBF} : K(\vec{\mathbf{y}}_i, \vec{\mathbf{y}}_j) = \exp(-\gamma ||\vec{\mathbf{y}}_i - \vec{\mathbf{y}}_j||^2), \gamma > 0$$

Overall, the SVM model required two parameters to be chosen: the penalty ("soft margin") parameter of the error term C which specifies the trade-off between maximizing the classification margin and minimizing the training error, and the RBF kernel parameter γ which controls the curvature of the hyperplane. SVMs were implemented using LibSVM, a publicly available software library for support vector classification [35]. Each feature in the training data was linearly scaled to the range [0, 1] to assure commensurability of the various features before applying SVM. The same scaling template was applied to the testing data before performing classification.

Performance Metrics

The problem of seizure detection was posed as a supervised learning task in which the goal was to classify each 10 s epoch as seizure or non-seizure based on extracted features from EDA and ACM recordings. If any epoch between the start and end of a labelled seizure was correctly classified as a seizure event, the seizure was considered to be detected (true positive). If multiple epochs within the seizure duration were detected, these were treated as a single correct detection event. False detections that occurred within 30 s apart from each other were treated as a single false alarm.

We characterized the performance of our seizure detector using the following metrics:

- **Sensitivity** The percentage of recorded seizures that were identified by the detector.
- **False Alarms Per 24 h** Number of times over the course of a day (24 h) that the detector incorrectly declares a seizure.
- **Electrographic Detection Latency** The delay between EEG onset and detector recognition of seizure activity (first epoch classified as seizure).
- **Clinical Detection Latency** The delay between clinical (onset of physical or cognitive symptoms) onset and detector recognition of seizure activity. This was done based on video analysis and was not blinded to EEG since the visualizing software displayed both recordings concurrently. Note that the same neurophysiologists labelled both the EEG and clinical onset.

For model selection, values of C and γ are typically selected based on the best cross-validation accuracy. However, in learning imbalanced data, the overall classification accuracy is not an appropriate measure of performance since a trivial classifier that predicts every instance as the majority class (non-seizure) would achieve very high accuracy but be of little use. As such, we used the F-measure to evaluate the performance of the SVM while searching for the best pair of C and γ.

$$\text{F-measure} = 2 \times \frac{\text{Sensitivity} \times \text{PPV}}{\text{Sensitivity} + \text{PPV}}$$

where the positive predictive value (PPV) is the proportion of seizures declared by the

detector that were true seizure events.

$$\text{PPV} = \frac{\text{number of True Positives}}{\text{number of True Positives} + \text{number of False Alarms}}$$

Non-Patient-Specific Seizure Detection

We first examined the performance of a *non-patient-specific* or "generic" seizure detection algorithm that excludes all data from a test patient in the training phase. Since limited data was available, we implemented a *leave-one-patient-out* strategy to evaluate the performance.

The total number of patients with recorded GTC seizures is denoted by M_{SZ}. In this approach, the entire recording session from a single patient P_{test} was set aside for the testing phase. The remaining data from the other $M_{SZ} - 1$ patients was included in the training phase. The goal of the training phase was to identify appropriate values of C and γ for model selection. As it is not known beforehand which values of C and γ are best for a given problem, we performed a grid-search to evaluate various combinations of the parameters ($C = 2^{-5}, 2^{-3}, \ldots, 2^{11}; \gamma = 2^{-15}, 2^{-13}, \ldots, 2^{-1}$). To avoid selection of SVM parameters that would result in overfitting to the training set, the training data was again separated into two parts, of which data from a single patient was considered "unknown". Sequentially data from each "unknown" patient were tested using the classifier trained on the remaining $M_{SZ} - 2$ patients. As such, we performed $(M_{SZ} - 1)$-fold cross-validation for each possible combination of C and γ. The pair of C and γ that produced the highest average cross-validation F-measure was selected (see Appendix D for the values selected). Using the selected parameter values, the whole training set (data from all $M_{SZ} - 1$ patients) was trained again to generate the final classifier and tested on the data from the single patient P_{test} that had been set aside. This entire process was repeated with a re-training of the SVM in each round, such that data from each patient were excluded once for testing, and the remainder used as training data (M_{SZ}-fold cross-validation). Overall performance was determined by taking the average of the performance of all tested patients.

Semi-Patient-Specific Seizure Detection

To allow the SVM to learn from previous examples of seizures from the test patient if that patient had more than a single GTC seizure recording available, we also implemented a *leave-one-seizure-out* strategy to assess the performance of our seizure detection algorithm.

As the detector was not trained solely on data from a particular test patient but included examples from all other patients, this approach was *semi-patient-specific.*

We divided the data from the M_{SZ} patients into N_{SZ} seizure recordings and N_{NS} non-seizure recordings ($N_{NS} = 2N_{SZ}$). In this approach, one seizure recording R_{testSZ} along with two non-seizure recordings R_{testNS} were set aside for testing. The remaining data from the other $N_{SZ} - 1$ seizure and $N_{NS} - 2$ non-seizure recordings were used for training the SVM. A grid-search was performed to evaluate various combinations of the parameters ($C = 2^{-5}, 2^{-3}, \ldots, 2^{11}; \gamma = 2^{-15}, 2^{-13}, \ldots, 2^{-1}$). To avoid overfitting to the training set, the training data was again separated into two parts, of which data from a single seizure recording together with two non-seizure recordings were considered "unknown". Sequentially data from each "unknown" seizure and non-seizure recordings were tested using the classifier trained on the remaining $N_{SZ} - 2$ seizure and $N_{NS} - 4$ non-seizure recordings. As such, we performed $(N_{SZ} - 1)$-fold cross-validation for each possible combination of C and γ. The pair of C and γ that produced the highest average cross-validation F-measure was selected (see Appendix D for the values selected). Using the selected parameter values, the whole training set (data from all $N_{SZ}-1$ seizure and $N_{NS}-2$ non-seizure recordings) was trained again to generate the final classifier and tested on the data from the single seizure recording R_{testSZ} and two non-seizure recordings R_{testNS} that had been withheld. This entire process was repeated with a re-training of the SVM in each round, such that data from each seizure and non-seizure recording were excluded once for testing, and the remainder used as training data (N_{SZ}-fold cross-validation). Overall performance was determined by taking the average of the performance of all tested recordings.

Testing For Generalization of False Alarm Rate to New Group of Patients

To evaluate the generalization of the seizure detection algorithm in terms of its false alarm rate, we utilized recordings from M_{NS} patients who did not experience GTC seizures for testing. Data from all the M_{SZ} patients with GTC seizures were used to train the SVM. A grid-search was performed to evaluate various combinations of the parameters ($C = 2^{-5}, 2^{-3}, \ldots, 2^{11}; \gamma = 2^{-15}, 2^{-13}, \ldots, 2^{-1}$). To avoid overfitting, the leave-one-seizure-out approach was employed such that N_{SZ}-fold cross-validation was performed for each possible combination of C and γ. The pair of C and γ that produced the highest average cross-validation F-measure was selected. Using the selected parameter values, the whole training

set (entire data set from M_{SZ} patients with GTC seizures) was trained again to generate the final classifier and tested on the recordings from all M_{NS} patients that had been withheld.

5.4 Results

We included 80 patients in this study. A total of 16 secondarily GTC seizures were recorded from 7 patients. This includes all the patients with GTC seizures from Chapter 4 along with one new patient who had four GTC seizures (not included previously since EEG and video data lost). The seizures occurred at different day and night times as well as during both awake and sleep states. All 16 GTC seizures started as partial seizures that eventually generalized and resulted in tonic-clonic activity (data for each individual seizure presented in Appendix D - note that the seizure numbers). These 7 patients provided 688 h (29 days) of EDA and ACM recordings throughout their stay at the LTM (4.1 $\pm$ 1.2 days/patient). On average, the data reduction technique described in 5.3.5 reduced the amount of data by 98%. Moreover, the degree of imbalance between non-seizure and seizure epochs which was approximately 1500 to 1 before pre-processing was decreased to 50 to 1 (most recordings contained low amplitude, non-rhythmic motor activity). The remaining 73 patients who did not experience GTC seizures provided 3525 h (147 days) of recordings. Altogether, the total recordings available for analysis was 4213 hours (176 days). These recordings were obtained in a routine clinical environment and contained a wide range of activities of daily living.

5.4.1 Performance Comparison of Seizure Detection Modes

To visualize the performance of the non-patient-specific and semi-patient-specific seizure detection modes, we performed receiver operating characteristic (ROC) analysis (Figure 5-5). The ROC curves depict the trade-off between sensitivity and false alarm rate as the decision threshold is varied. At the optimal cut-off point that maximized sensitivity and minimized the false alarm rate (i.e. point nearest the top left-hand corner), the non-patient-specific detector achieved 88% (14/16 seizures detected) sensitivity with an average of 1 false alarm per 24 h. On the whole, the semi-patient-specific seizure approach improved the performance. At the optimal threshold, 15/16 (94%) seizures were detected with 1 false alarm per 24 h.

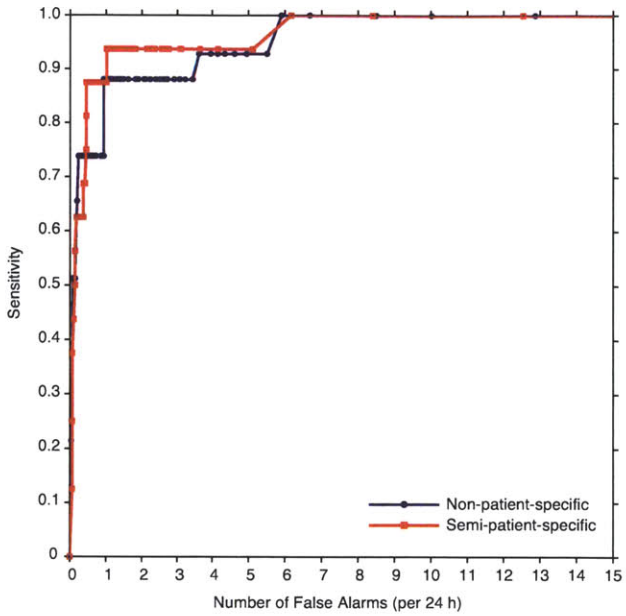

Figure 5-5: *ROC of the non-patient-specific (blue circles) and semi-patient-specific seizure (red squares) detectors.*

Figure 5-6a shows the true positive detections declared on each test patient under the semi-patient-specific mode. Only one seizure was missed (patient 4). There were 28 false alarms during the 688 hours of testing (0.98 per 24 h). The average false alarm rate across patients was 1.05 ± 0.71 per 24 h (Figure 5-6b). The electrographic and clinical latencies for each seizure are illustrated in Figure 5-6c. In all seizures, the electrographic onset preceded its clinical onset. Three seizures had a particularly long non-motor lead in (seizures 10, 11 and 12 in Figure C-1) and seizure 10 was missed completely. The median electrographic latency was 42.95 s; median clinical latency was 31.42 s.

5.4.2 Physiological Signal Fusion Improves Performance

To evaluate the utility of combining ACM and EDA, we compared the performance of two semi-patient-specific seizure detectors. One detector included features from both the ACM and EDA recordings (original feature set), and the other incorporated features from only the ACM recordings. Figure 5-7 illustrates the ROCs of the two different detectors. The overall performance was lower when only ACM features were included. The optimum performance achieved was 94% sensitivity with a higher average false alarm rate of 1.5 per 24 h compared to the detector utilizing both ACM and EDA features (1 per 24 h).

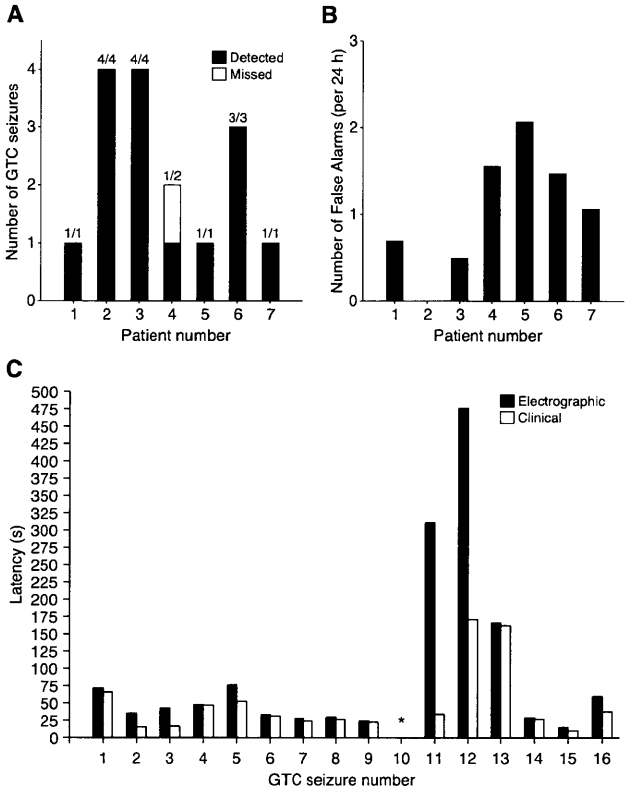

Figure 5-6: *Semi-patient-specific seizure detection performance. (A) Number of GTC seizures detected per patient. (B) Number of false alarms per 24 h per patient. (C) Latency of detection for each GTC seizure. *Seizure 10 (Patient 4) was not detected by the algorithm.*

5.4.3 False Alarms in Patients with No GTC Seizures

After training the SVM using data from the 7 patients with GTC seizures, we tested the seizure detection algorithm for false alarms on the 3525 h (147 days) recordings from the 74 patients who did not have GTC seizures. On average, each patient was tested over 48 ± 35 h of data. There were 102 false alarms during the 3525 hours of testing (0.69 per 24 h). The average false alarm rate across patients was 0.98 ± 2.61 per 24 h (Figure 5-8), which is similar to the rate observed in the 7 patients with GTC seizures. The majority of patients (77%) had less than one false alarm per 24 h. Out of the 73 patients, 46 (63%) did not raise any false alarms during the entire monitoring period, resulting in a median false alarm rate of zero. On the other hand, four patients had an unusually high rate of false alarms.

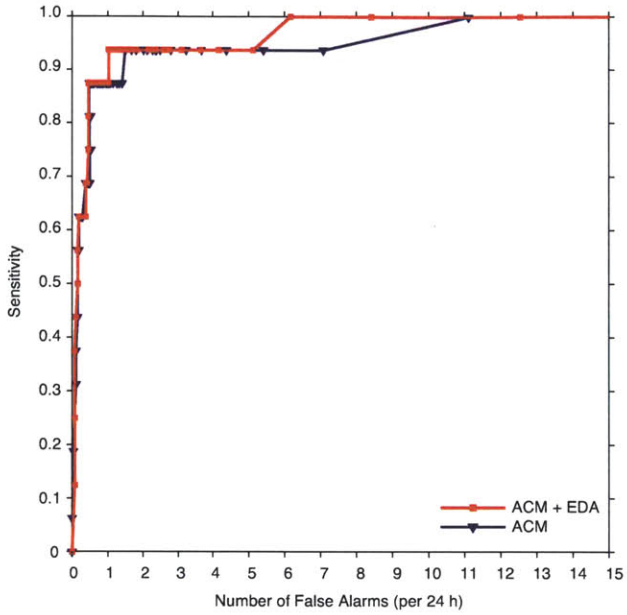

Figure 5-7: *ROC of the semi-patient-specific seizure detector using solely ACM features (blue circles) and using both ACM and EDA features (red squares).*

5.5 Discussion

In this chapter, we presented a novel sensor and algorithm for GTC seizure detection. The present study is the first to demonstrate the utility of EDA as a new physiological signal to supplement ACM signals for seizure detection. Moreover, we evaluated the algorithm on 80 patients containing a wide range of ordinary daily activities to test for false alarms. Since the EEG recording system was ambulatory (in the form of a backpack), patients were not constrained to staying in bed but could walk around the room, go over to a playroom nearby or leave the LTM for imaging studies and other tests. Overall, our algorithm achieved high sensitivity, detecting 15/16 (94%) of GTC seizures recorded from 7 patients and only triggered 130 false alarms over 4213 hours of recordings (0.74 per 24 h) from 80 patients.

An important property of this algorithm is its adaptability. We examined a non-patient-specific seizure (generic) detection mode to assess the baseline performance on unseen patients and compared it to an adaptive approach that included previous examples of seizures from the test patient in training. Our results indicate that the adaptive, or semi-patient-specific mode produced superior performance compared to the generic mode. Since the GTC seizure manifestation in ACM and EDA signals may vary from patient to patient, it is reasonable that an adaptive approach which takes advantage of the consistency of an individual

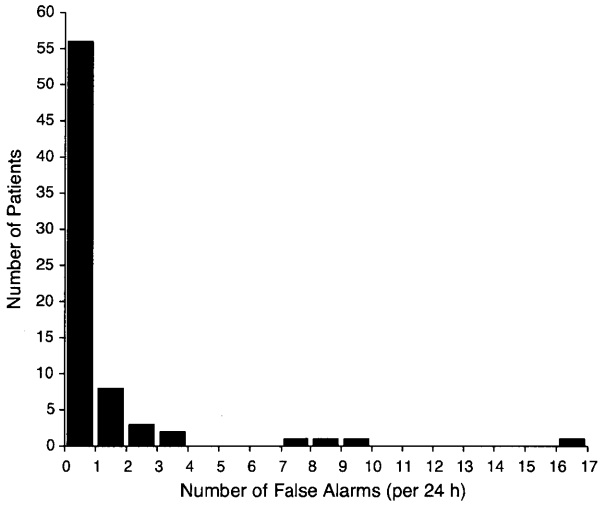

Figure 5-8: *Histogram of False Alarm rates across 73 patients with no GTC seizures.*

patient's unique seizure signature as well as typical non-seizure activity patterns improves performance. For practical use, the generic mode is important for a seizure detector to be of immediate use to every patient right "out of the box". As more examples of seizures are obtained over time, the algorithm can then improve and become more customized for each particular patient.

Another unique feature of our methodology is the use of EDA as an additional input signal for classification. Our study illustrates how a seizure detector that combines information extracted from both EDA and ACM recordings can perform better than a detector that only uses information extracted from ACM. Sympathetic postganglionic fibers innervate eccrine sweat glands and their activity modulates sweat secretion [152]; EDA refers to modulation in skin conductance and is a unique parameter that reflects purely sympathetic activity [26,37]. Several cortical structures with recognized seizure potential (e.g. the fontral cortex or cingulate gyrus) have direct or indirect connections with autonomic centers from the medulla oblongata [160] and electrical stimulation of such structures can induce changes in EDA [95,111]. In the previous chapter, we showed that epileptic seizures, GTC seizures in particular, can induce elevations in EDA reflecting strong ictal sympathetic discharges. Importantly, we showed how the amplitude of the EDA response is strongly correlated with the duration post-ictal EEG suppression, a biomarker for SUDEP risk. Thus, incorporating EDA measurements in a seizure detector can potentially improve detection performance as well as provide a quantitative measure of the autonomic impact for each seizure.

The proposed algorithm failed to detect one of the test seizurse because that seizure only produced mild motor convulsions and little change in the EDA signal (see seizure 10 in Figure D-1). Furthermore, the missed seizure was not similar to the other seizure example from the same patient (seizure 11). It is possible that with more training examples that resembled the missed seizure, the algorithm would have produced the correct classification. The relatively low number of seizure examples represents one of the limitations of this study, but the promising results should encourage further efforts in this direction. On the other hand, the extensive amount of non-seizure data allowed a good estimation of the false alarm rate. Based on analysis of the video recordings, the false alarms were typically triggered by forceful, rapid and rhythmic motions during activities such as dice shaking, hand flapping and juggling. In other instances, a patient was shaking a balloon and hitting a toy violently. During several occasions, the patients were out of sight from the video camera; thus, the activity associated with the false alarms could not be determined. Out of all 80 patients, only four patients had a relatively high amount of false alarms. In two cases, the high false alarm rates (8 and 16 per 24 h) occurred in patients with Autism Spectrum Disorders who exhibited frequent hand flapping, a behavioural automatism. Of note, ACM has been utilized for automated detection of stereotypical motor movements in such persons [8]. In the third case, the patient was engaged in vigorous motion-controlled gaming (Nintendo Wii) regularly throughout the monitoring duration (9 false alarms per 24 h). The fourth patient's video recordings were not available and therefore the cause of false alarms could not be determined. Again, more examples of these harder cases in the training set may improve the decision boundary and performance. Alternatively, the addition of another physiological signal such as heart rate or heart rate variability may provide better discriminability of these cases.

Previous work on non-EEG based wearable GTC seizure detectors have focused primarily on ACM as the input signal. Table 5.1 provides a comparison of the key features for each system. Schulc and colleagues utilized a Wii Remote mounted on the forearm using a stocking to detect four GTC seizures from three patients based on a visually determined intensity and duration threshold of the ACM signal [158]. However, the results have to be taken with caution as independent assessment of the algorithm was not performed on separate test data to determine whether the perfect sensitivity achieved was due to overfitting. Two commercial wrist-worn motion sensors, the SmartWatch and EpiLert have been

Table 5.1: Comparison of Wrist-worn Convulsive Seizure Detectors

Features	Schulc et al. [158]	SmartWatch Lockman et al. [107]	EpiLert Kramer et al. [90]	**MIT Wearable Biosensor**
Signals	ACM	ACM	ACM	**ACM + EDA**
Setup	Wii Remote on forearm	Wrist-worn motion sensor	Wrist-worn motion sensor	Wrist-worn biosensor
Number of patients tested	3	40 (6 with seizures)	31 (**15** with seizures)	**80** (7 with seizures)
Number of seizures tested	4	8	**22**	16
Duration of recordings tested	27 – 43 h	Unspecified	1692 h	**4213 h**
Algorithm described?	**Yes**, heuristic selection of thresholds for ACM intensity and time span	No	No	**Yes**, Support Vector Machine
Sensitivity	100%†(4/4)	88% (7/8)	91% (20/22)	**94%** (15/16)
False alarms	Not reported	204	**0.11 per 24 h***(8 in 1692 h)	0.74 per 24 h (130 in 4213 h)
Latency	Not reported	5–43 s	17 s (median)	31 s (median)

ACM accelerometry; EDA electrodermal activity
† Training results only (no independent testing performed).
* Patients with dystonic posturing, subtle behavioral automatism, and suspected pseudoseizures were excluded.

evaluated in separate clinical studies [90, 107]. The SmartWatch produced a large number of false alarms whereas the EpiLert had a very low rate of false detections (8 in 1692 h). One drawback of the EpiLert study is that patients expected to have a high incidence of seizure-like movements such as dystonic posturing, subtle behavioral automatism and pseudoseizures were excluded from testing, which could explain the low false alarm rate. These devices also employed proprietary algorithms that were not described. Our proposed seizure-detection methodology was tested on the largest number of patients and the results compare favorably with these studies.

Timely detection of seizures allows caregivers to monitor their severity and duration to determine whether immediate treatment is necessary. Case control studies have consistently indicated that sudden unexpected death in epilepsy (SUDEP) mainly occurs in the context of a GTC seizure [177, 189]. As most deaths are unwitnessed, supervision and attention to recovery after a seizure may be important in SUDEP prevention [93]. One study in a

residential school for children with epilepsy who were closely supervised at night and monitored after a seizure reported that deaths occurred with students on leave or after they left, but not at the school [124]. Another large case-control study found that sharing a bedroom with someone capable of giving assistance and special precautions such as regular checks throughout the night or using a listening device were all protective factors [94]. Moreover, since GTC seizures often cause loss of consciousness, most patients have trouble accurately reporting the occurrence of seizures. Treatment decisions are primarily based on seizure frequency [43], thus inaccurate self-reports can lead to ineffective therapy. A seizure detection device would provide objective measurements for quantification of seizure frequency. We anticipate that the proposed wearable biosensor and seizure detection algorithm will enable ambulatory, round-the-clock monitoring and improve the quality of life of patients with uncontrolled GTC seizures.

Chapter 6

Conclusions

6.1 Thesis Contributions

The overall goal of my research was to design and evaluate a wearable electrodermal activity (EDA) and accelerometry (ACM) biosensor, as well as to demonstrate its clinical utility in the assessment of epileptic seizures. The resulting thesis has the following contributions:

- I have designed, built and evaluated a low-cost, unobtrusive, nonstigmatizing, wrist-worn sensor that can provide comfortable and continuous measurements of EDA and ACM over extensive periods of time. The device is capable of on-board data logging, wireless transmission of data and performing real-time analysis. This device offers the unprecedented ability to perform comfortable, long-term (over multiple days), reliable and in situ assessment of EDA. It opens up opportunities for future investigations that were previously not feasible, and could have far-reaching implications for diagnosis and understanding of psychological or neurological conditions.

- I have validated the use of the distal forearm as an alternative site for EDA measurements. When compared to recordings from traditional palmar sites, high correlations were observed during physical, cognitive, as well as emotional stressors. The distal forearm provides an attractive alternative for long-term measurements because it is less encumbering and not as susceptible to motion artifacts as the palmar or plantar surfaces during normal activities of daily living.

- I have demonstrated the ability of the wearable biosensor to collect continuous recordings of EDA and accelerometry for a stretch of 1-7 days from patients with epilepsy

in a clinical environment (in-patient hospital). The device was tested on 95 patients and collected approximately 4500 (188 days) hours worth of EDA and ACM.

- I have characterized the alterations in both sympathetic (EDA) and parasympathetic activity (heart rate variability, HRV) that accompany complex partial and generalized tonic-clonic seizures in patients with epilepsy. The autonomic footprints revealed a period of prolonged autonomic imbalance involving sympathetic overactivation and parasympathetic suppression that is exacerbated after generalized tonic-clonic seizures. These findings may represent a critical window of vulnerability and may explain why generalized tonic-clonic seizures are a major risk factor for sudden unexpected death in epilepsy (SUDEP).

- I have presented the first evidence that the magnitude of autonomic alterations after generalized tonic-clonic seizures is associated with post-ictal EEG suppression, a possible biomarker related to the risk of SUDEP. The strong correlations between post-ictal EEG suppression and both sympathetic (e.g. amplitude of the EDA response) and vagal (e.g. maximal change in high-frequency HRV) alterations that act in opposite directions suggest that the intensity of a seizure may play a role in the pathophysiology of SUDEP. These results also raise the possibility that autonomic footprints of seizures could serve as biomarkers for the risk of SUDEP, as well as the possibility of a wearable device for round-the-clock monitoring to identify potentially dangerous seizures.

- I have presented a novel algorithm for generalized tonic-clonic seizure detection with the use of the wearable biosensor. This is the first demonstration of the utility of EDA to supplement ACM signals for seizure detection. The algorithm was tested on 80 patients containing a wide range of ordinary daily activities and achieved high sensitivity (94%) with a low rate of false alarms ($\leq$ 1 per 24 h). It is anticipated that the proposed wearable biosensor and seizure detection algorithm will provide an ambulatory seizure alarm and improve the quality of life of patients with uncontrolled tonic-clonic seizures.

6.2 Other Relevant Contributions

Beyond the scope of this thesis, during the time of work on my Ph.D., several other studies I have worked on have contributions in the broader field of mobile and pervasive health technologies. In particular, these efforts have sought to advance the state-of-the-art in measurements of cardiorespiratory function. These works have the following contributions:

- I designed a novel embodiment for wearable photoplethysmography (PPG) comprising a magnetic earring sensor and wireless earpiece. The miniaturized sensor can be worn comfortably on the earlobe and contains an embedded accelerometer to provide motion reference for adaptive noise cancellation. This system provides a platform for comfortable, robust, unobtrusive and discreet monitoring of heart rate. For more information, please refer to:

  Poh, M.Z., Swenson, N.C., and Picard, R.W., Motion Tolerant Magnetic Earring Sensor and Wireless Earpiece for Wearable Photoplethysmography. *IEEE Trans Inf Techol Biomed*, 14 (2010), 786-794.

- I designed a comfortable, even stylish system for measuring the bilateral blood volume pulse that fits inside ordinary earbuds. By adopting a smart phone as part of our platform, I exploited commonality in components such as microprocessors, memory, screen, keyboard and battery to reduce cost, weight and eliminate redundancy. Instead of having to carry additional gear, this system only relies on modified earphones and a cell phone, common pocket items, to provide measurements such as heart rate and beat-to-beat changes in heart rate (HRV). Since devices such as the iPhone and iPod touch tend to be very personal devices and are intended to be carried wherever people go, this system is a natural extension that adds the capability to track personal health. For more information, please refer to:

  Poh, M.Z., Kim K., Goessling, A., Swenson, N.C., and Picard, R.W., Cardiovascular Monitoring Using Earphones and a Mobile Device. *IEEE Pervasive Comput*, Epub ahead of print (2011).

- I developed a novel technique for automated, contact-free physiological measurements of heart rate, respiratory rate and HRV using a basic webcam. This methodology can be applied to color video recordings of the human face and is based on automatic face tracking along with blind source separation of the color channels into independent

components. As an example of an embodiment that fits seamlessly into the ambient home environment, the technology was integrated into a mirror interface to provide real-time measurements of heart rate. This interface is intended to offer a convenient means for people to track their daily health with minimal effort. For more information, please refer to:

Poh, M.Z., McDuff, D.J., and Picard, R.W., Non-contact, Automated Cardiac Pulse Measurements Using Video Imaging and Blind Source Separation. *Opt Express*, 18 (2010), 10762-10774.

Poh, M.Z., McDuff, D.J., and Picard, R.W., Advancements in Non-contact, Multiparameter Physiological Measurements Using a Webcam. *IEEE Trans Biomed Eng*, 58 (2011), 7-11.

Poh, M.Z., McDuff, D.J., and Picard, R.W., A Medical Mirror for Non-contact Health Monitoring. *ACM SIGGRAPH Emerging Technologies*, to appear (2011).

6.3 Future Work

6.3.1 Home-based, Ambulatory Studies

Even though the seizure detection algorithm presented in this thesis was tested on a wide range of everyday activities in the hospital, more studies are needed to validate the performance of this methodology in an outpatient setting, e.g. at home. This represents a crucial step in translating the technology to patients for everyday use. Patients with refractory epilepsy who are prescribed an ambulatory EEG system for use at home would be eligible for such a study. The feasibility of the wrist-worn biosensor for home-based ambulatory seizure monitoring can also be evaluated in terms of patient compliance, comfort levels and side effects. Another interesting experiment would be to explore alternative locations for attachment of the biosensors. For example, one could compare the performance of the seizure detection algorithm when the sensors are placed on the ankles instead of the wrists.

6.3.2 Off-line Seizure Detection and Classification

The thesis focused on *on-line* detection of ongoing seizures to allow timely notification of caregivers. Nonetheless, an *off-line* detector would still be valuable for tracking seizures for therapeutic purposes. It would provide an objective measure of seizure frequency, and improved outcome measures over currently used seizure diaries based on self-report. Because

latency is not an issue for an off-line detector, a much longer sliding window can be chosen. Given that the changes in EDA that accompany convulsive seizures last well into the post-ictal period, more EDA features could be utilized including the amplitude, area under the curve, rise time, fall time etc. It is likely that the detector's overall performance would improve, especially with regards to the false alarm rate, because the common false positive triggers such as hand flapping do not induce a prolonged EDA response.

It would also be worthwhile to evaluate the utility of a Bayesian approach using a Hidden Markov Model (HMM) for statistical modelling of the various stages of convulsive seizures. If stages such as the "tonic" and "clonic" phase could be well represented, this approach would provide further information beyond the occurrence of a seizure by allowing detailed classification of the seizure manifestation, e.g. clonic-tonic, tonic-clonic, clonic only, tonic only etc.

6.3.3 Detection of Complex Partial Seizures/Subclinical Seizures

The data indicate that changes in EDA do accompany certain complex partial seizures as well as subclinical seizures. However, larger studies will be needed to identify the epileptic foci that result in these autonomic alterations. Attempting to design a complex partial seizure detector based solely on EDA and ACM will be challenging, as the magnitude of EDA increase is low in general and not easily distinguished from other daily activities. It is unclear whether these focal seizures would result in an asymmetrical increase between bilateral measurements. If so, bilateral EDA measurements may provide useful information regarding seizure activity. Otherwise, incorporating information from other physiological recordings such as heart rate and heart rate variability parameters will provide a more promising approach.

6.3.4 Responsive, Closed-Loop Devices

Beyond providing notification to caregivers in the event of a seizure attack, there is also a need for intelligent devices that can respond promptly to deliver an intervention to abort the seizure. These closed-loop devices would require rapid detection algorithms as well as an effective treatment strategy. Interventions that could potentially abort seizures include electrical brain stimulation, vagus nerve stimulation and localized drug delivery. While the intervention devices may be implantable, wearable sensors that communicate with the

implanted devices could be used for seizure detection and triggering therapy. The success of these interventions is likely dependent on how soon a seizure can be detected, given the rapidity with which seizures may spread.

6.4 Outlook

This thesis has demonstrated the utility of a wearable EDA and ACM biosensor for the quantification of seizure intensity in terms of autonomic impact, as well as to provide a platform for timely detection of generalized tonic-clonic seizures. It also presented high correlation between autonomic measures such as EDA amplitude and post-ictal EEG suppression, a possible biomarker for SUDEP risk. It will be of great interest to establish whether or not these autonomic footprints could provide biomarkers to identify epilepsy patients who are at risk of SUDEP. Beyond the area of epilepsy, I envision that this wearable biosensor could aid in the diagnosis and understanding of other medical conditions such as schizophrenia, psychogenic non-epileptic seizures, hyperhidrosis and cystic fibrosis.

Appendix A

Supplementary Information on Design and Evaluation of Wearable Biosensor

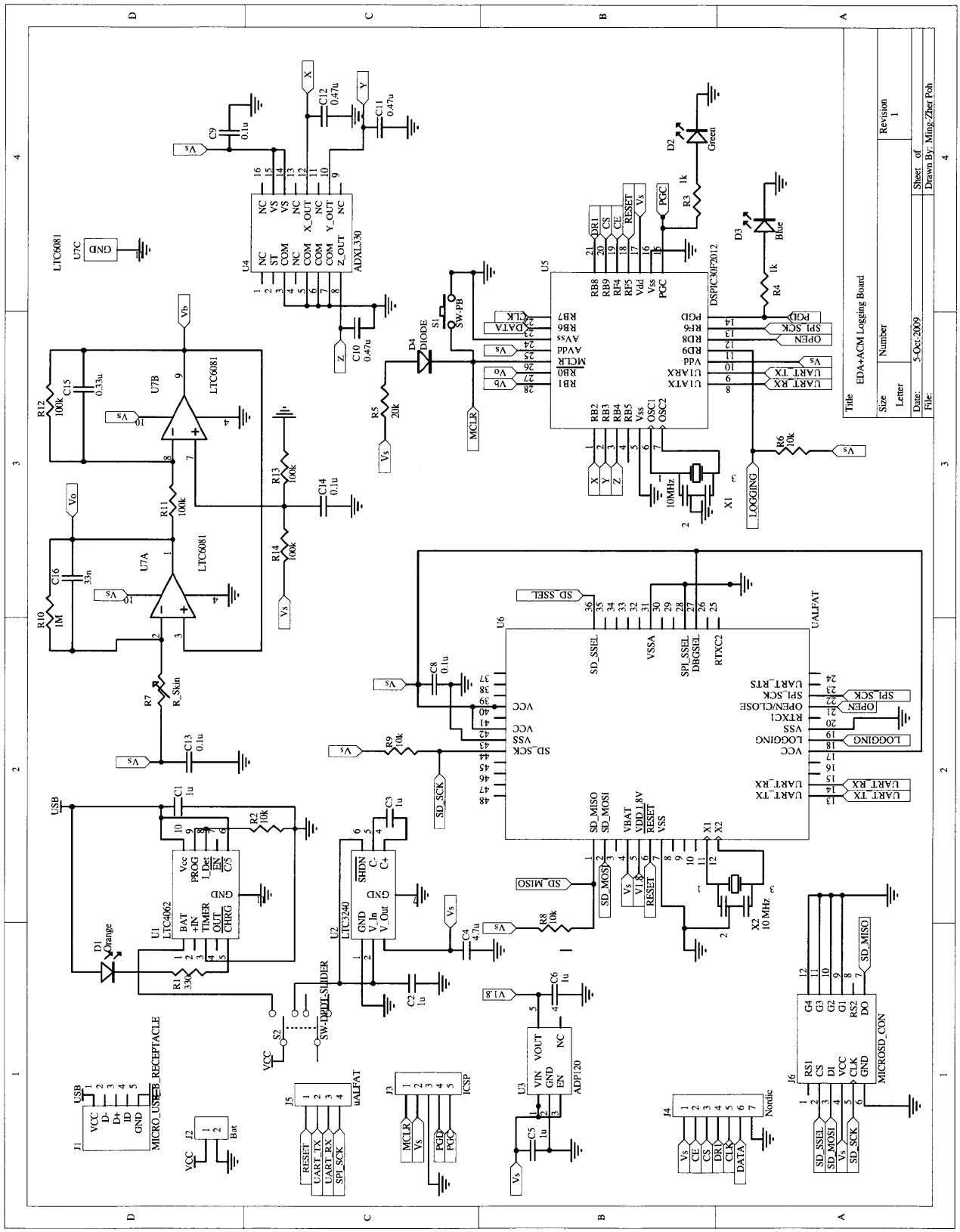

Figure A-1: *Layout of the EDA and ACM sensor board.*

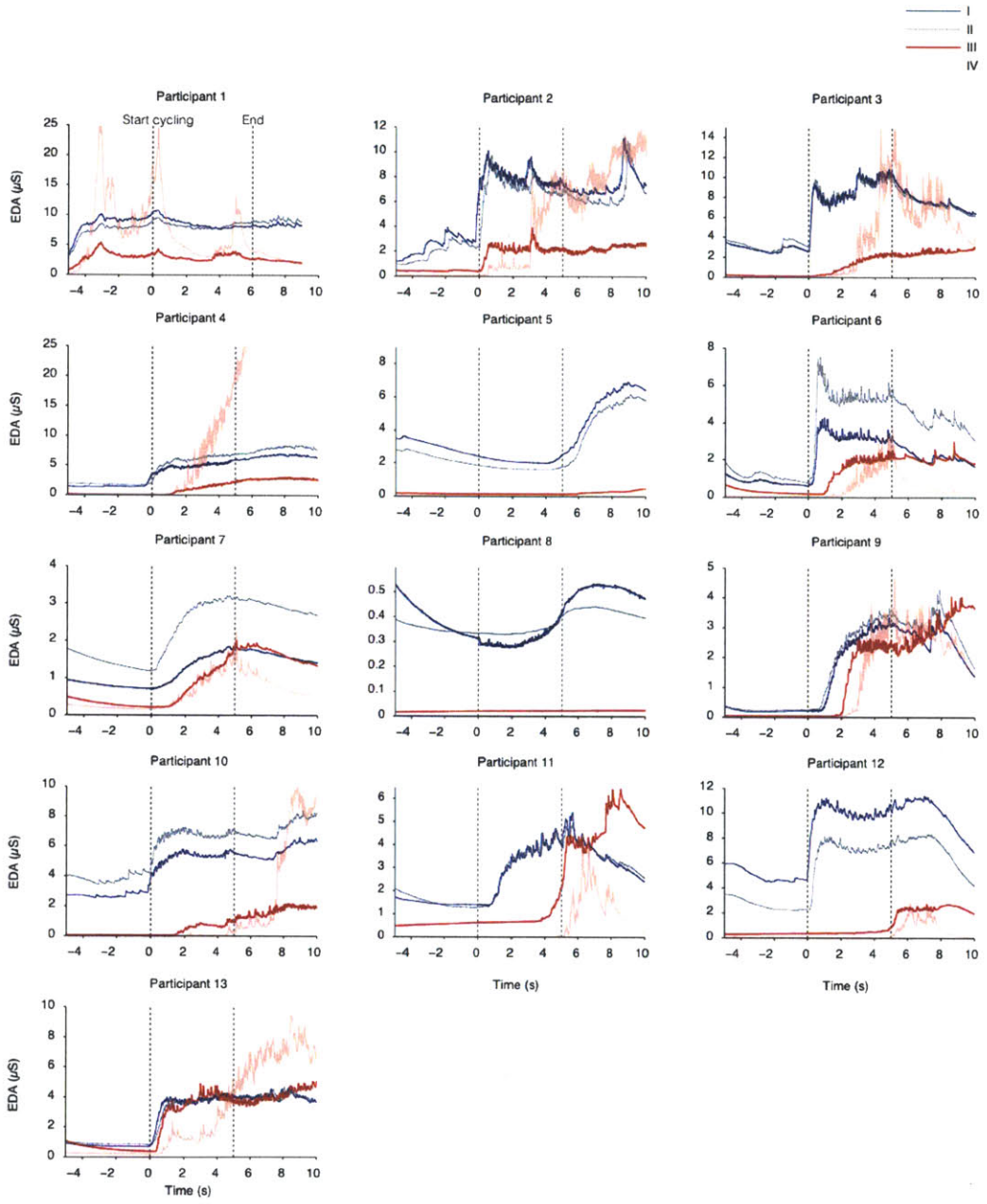

Figure A-2: *Individual EDA recordings of each participant during a physical task involving cycling. Measurements were made from (I) right fingers with Flexcomp, (II) left fingers with MIT sensor, (III) right distal forearm with MIT sensor using Ag/AgCl electrodes and (IV) left distal forearm with MIT sensor using conductive fabric electrodes*

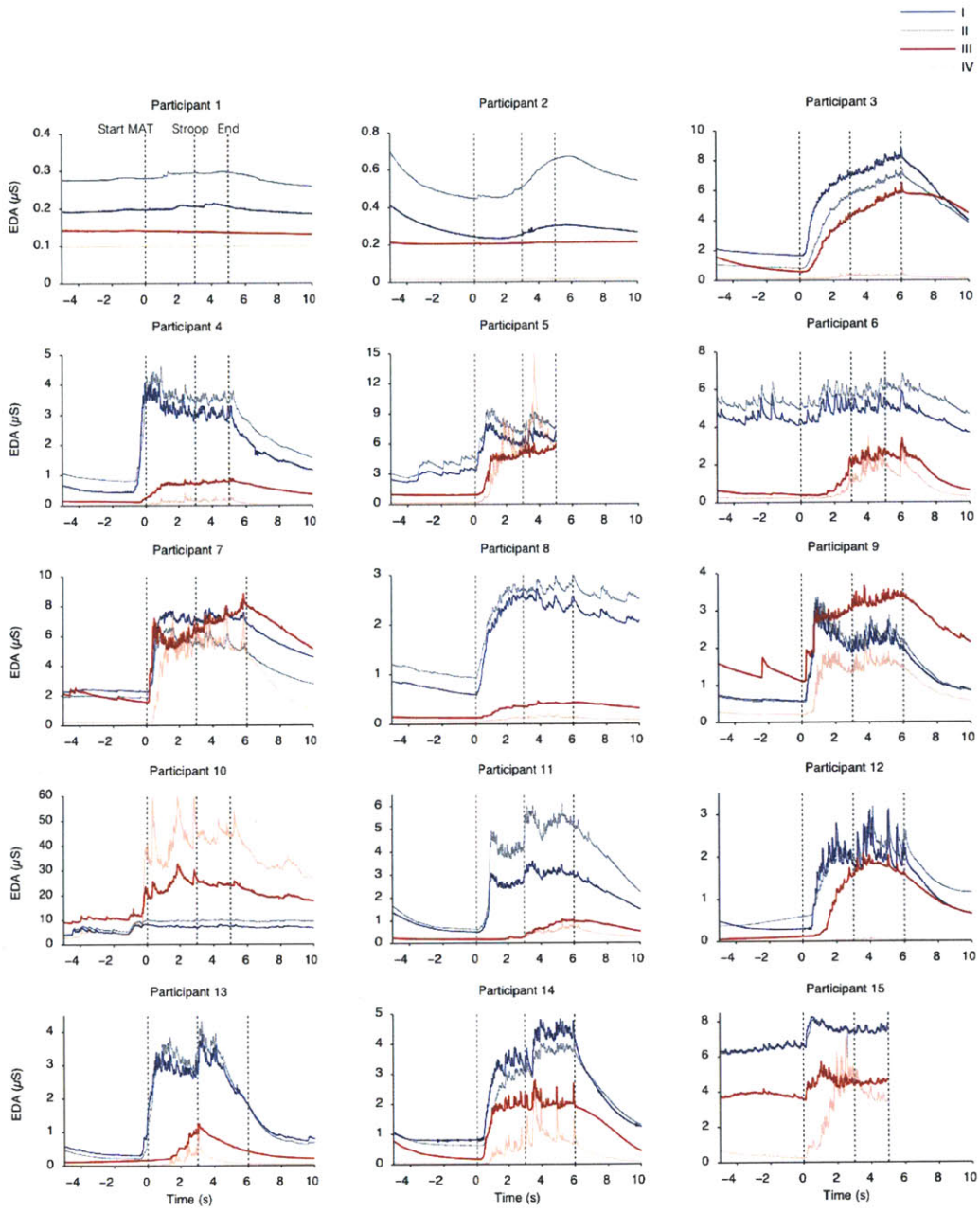

Figure A-3: *Individual EDA recordings of each participant during a cognitive task including a mental arithmetic test (MAT) and Stroop word-color matching test . Measurements were made from (I) right fingers with Flexcomp, (II) left fingers with MIT sensor, (III) right distal forearm with MIT sensor using Ag/AgCl electrodes and (IV) left distal forearm with MIT sensor using conductive fabric electrodes*

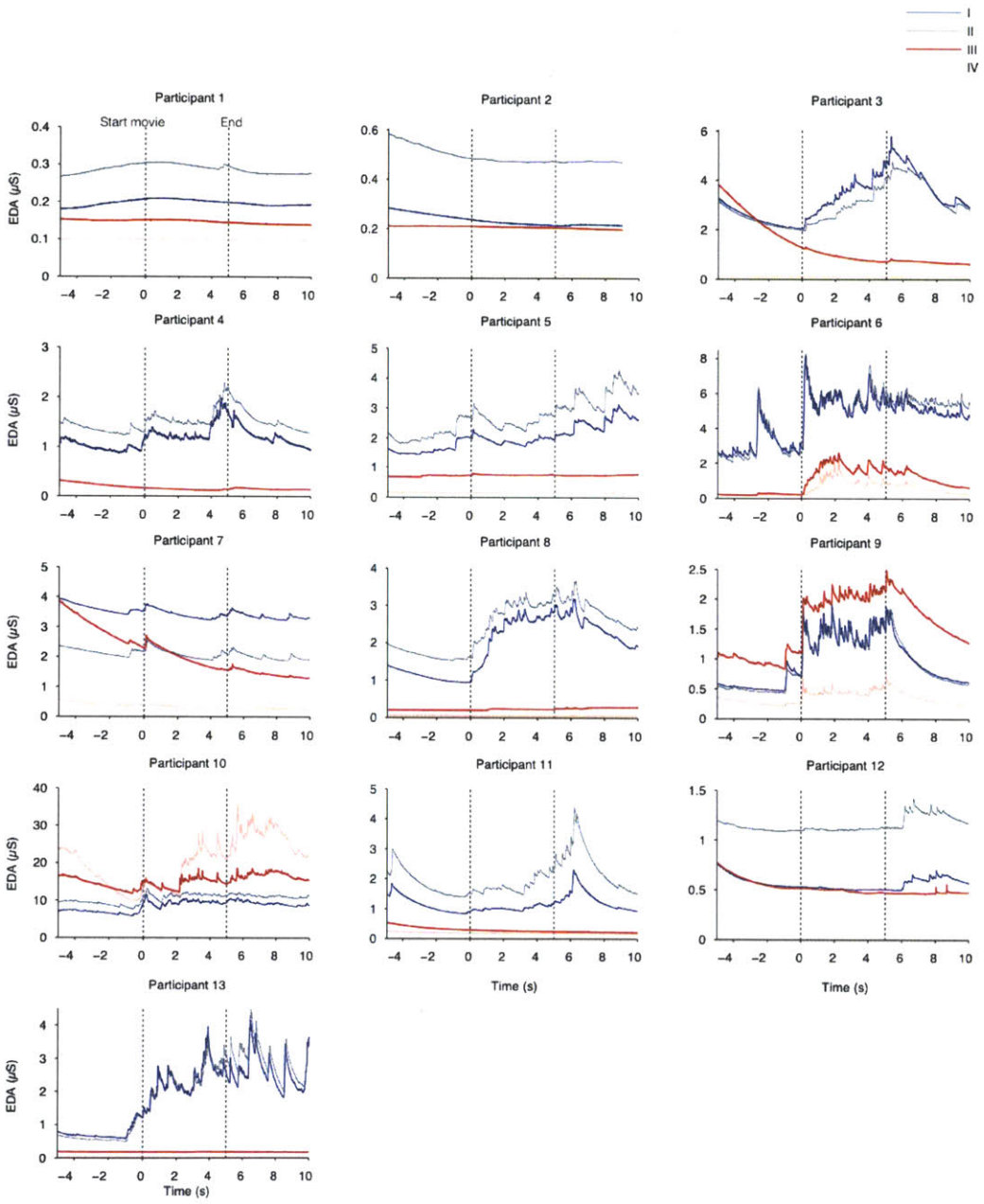

Figure A-4: *Individual EDA recordings of each participant during an emotional task consisting watching a horror movie clip. Measurements were made from (I) right fingers with Flexcomp, (II) left fingers with MIT sensor, (III) right distal forearm with MIT sensor using Ag/AgCl electrodes and (IV) left distal forearm with MIT sensor using conductive fabric electrodes*

Appendix B

Supplementary Information on Clinical Study

Figure B-1: *Data collection from patients with epilepsy staying at the long-term monitoring unit at Children's Hospital Boston. Continuous video, electroencephalographic (EEG), electrocardiographic (EKG), electrodermal activity (EDA) and 3-D accelerometry (ACM) recordings were obtained throughout the stay. Patients were not constrained to remaining in the bed as the EEG recording system was ambulatory (backpack). Video frames shown depict patients wearing the wrist-worn biosensors and performing a variety of daily activities*

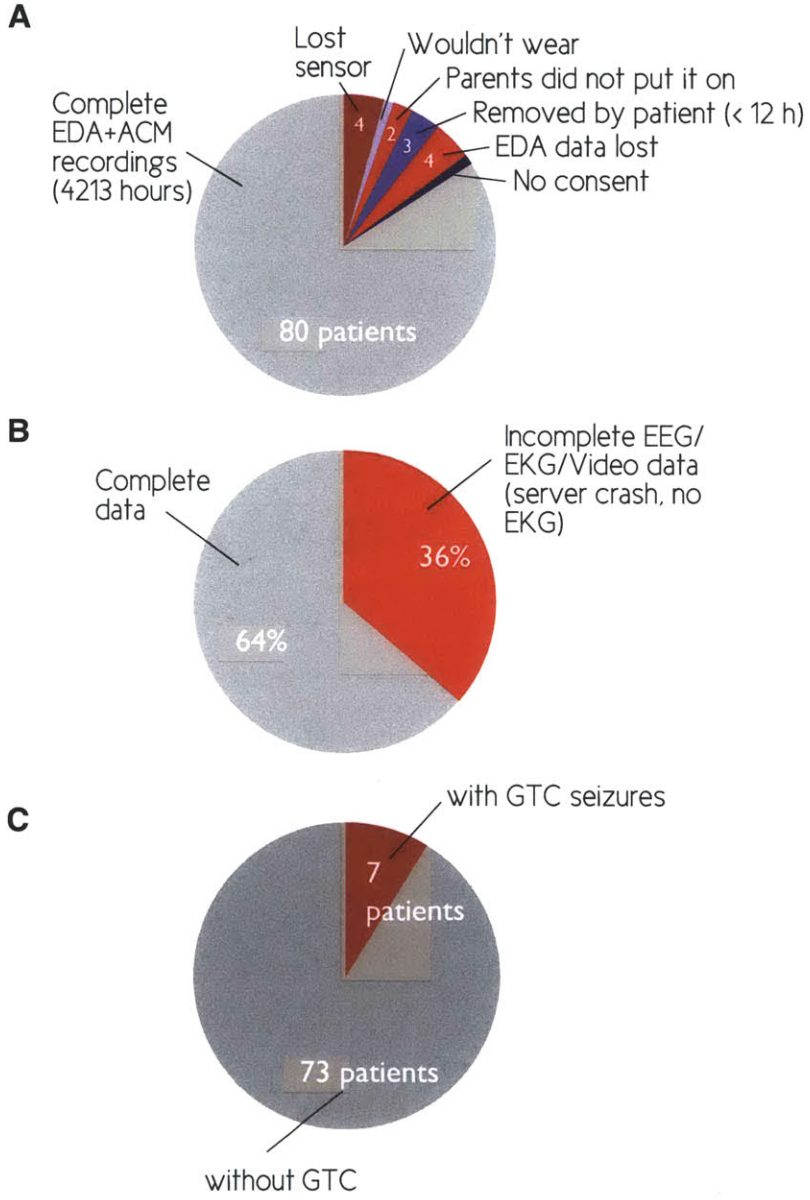

Figure B-2: *Summary of data collected from clinical study performed from Jan to September 2009. (A) 94 patients were enrolled and 80 provided over 12 hours of complete EDA and ACM recordings. (B) Due to a server crash, only 64% of those patients had complete EEG-EKG-video recordings. (C) 11 patients experienced at least one complex partial seizure (CPS) or generalized tonic-clonic (GTC) seizure. 7 patients experienced at least one GTC seizure.*

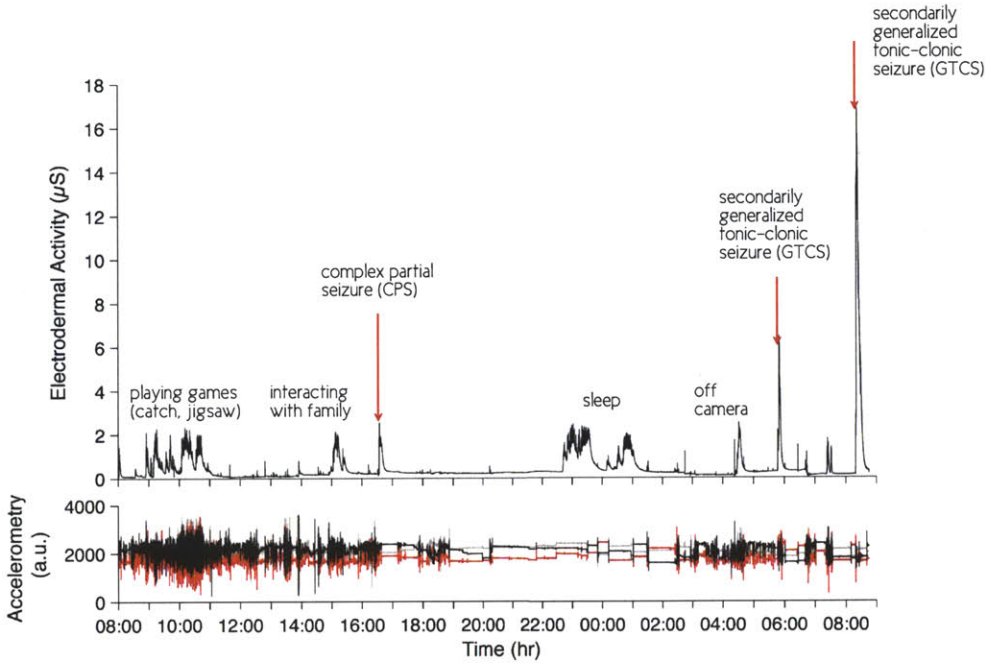

Figure B-3: *Example of a 24-hour recording from an 11-year-old female with refractory epilepsy. A single complex partial seizure and two GTC seizures that occurred during the monitoring period were accompanied by an increase in EDA.*

Appendix C

Supplementary Information on Autonomic Footprints of Epileptic Seizures

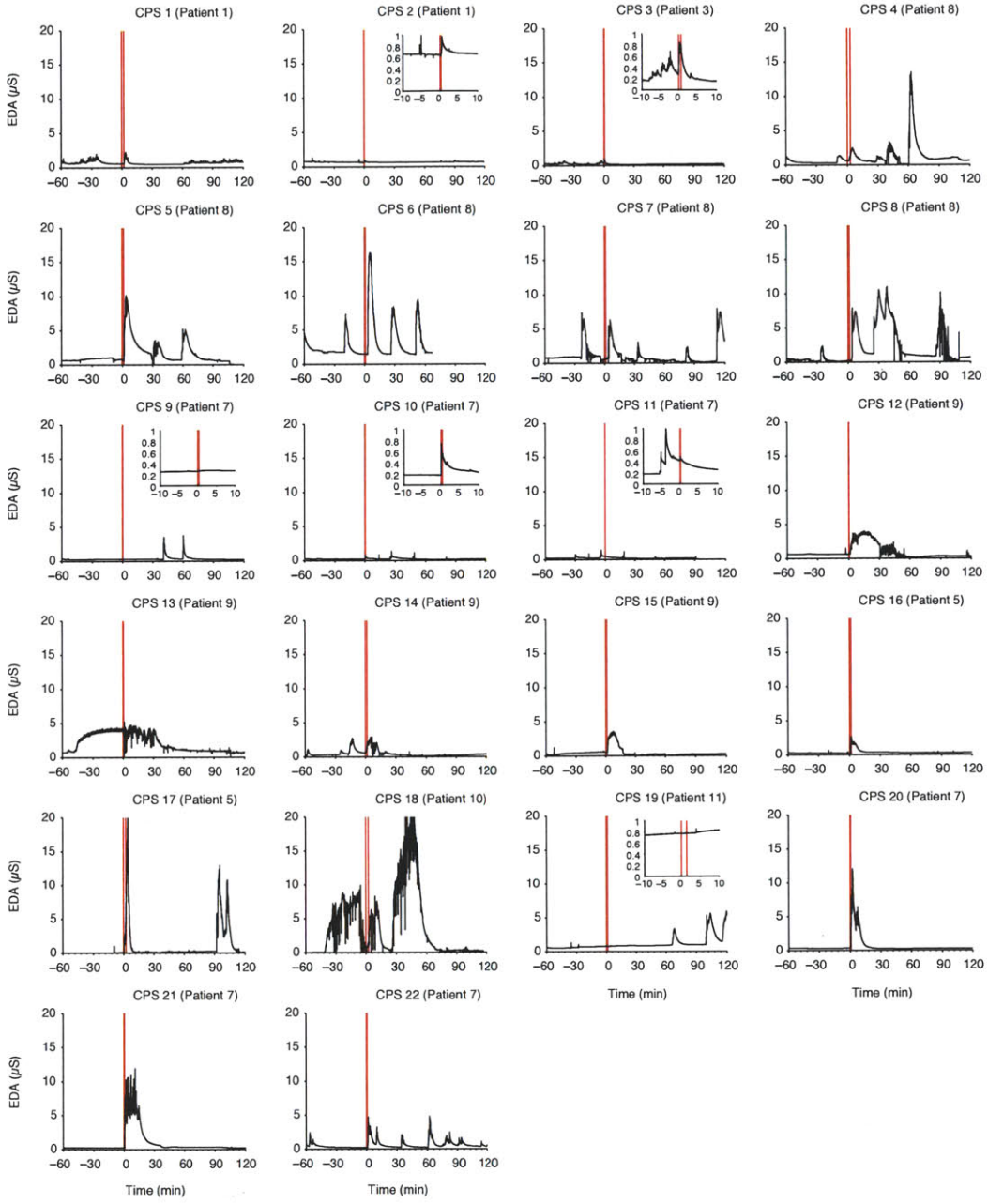

Figure C-1: *Peri-ictal EDA recordings (sympathetic) of individual complex partial seizures (CPS). Red lines denote seizure onset and offset*

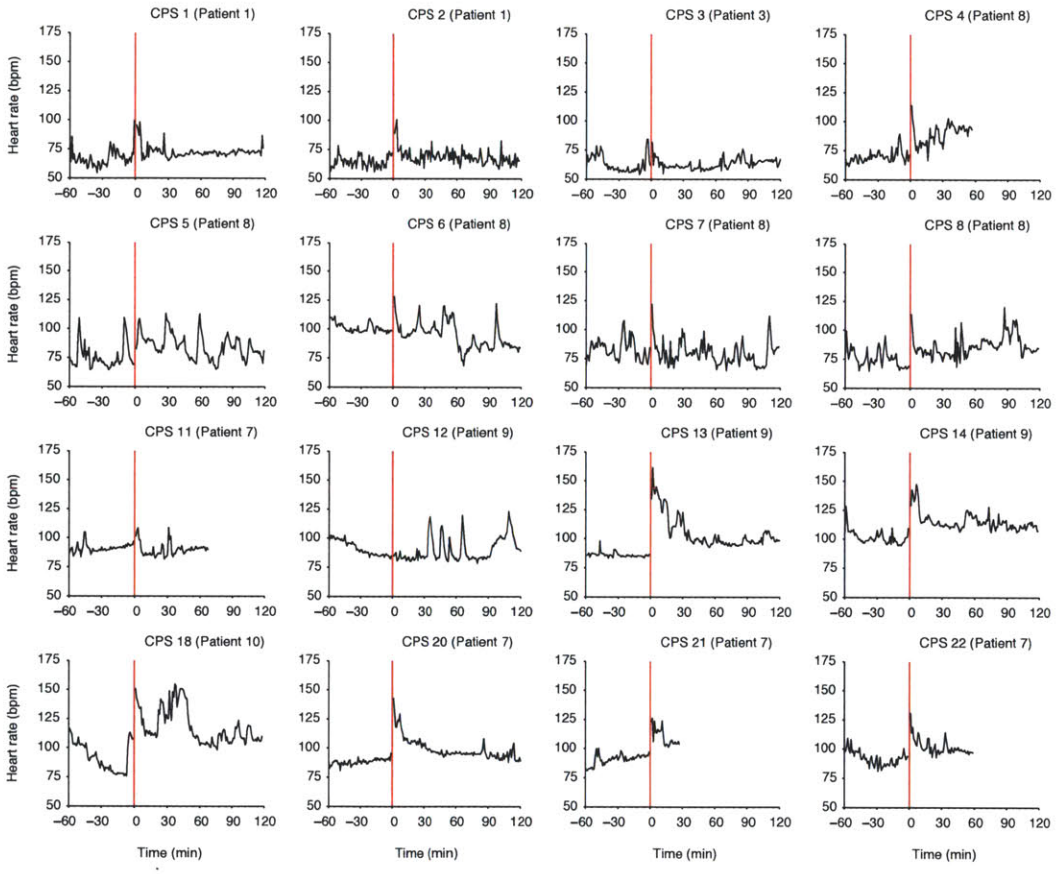

Figure C-2: *Peri-ictal heart rate recordings of individual complex partial seizures (CPS). Red line denotes CPS.*

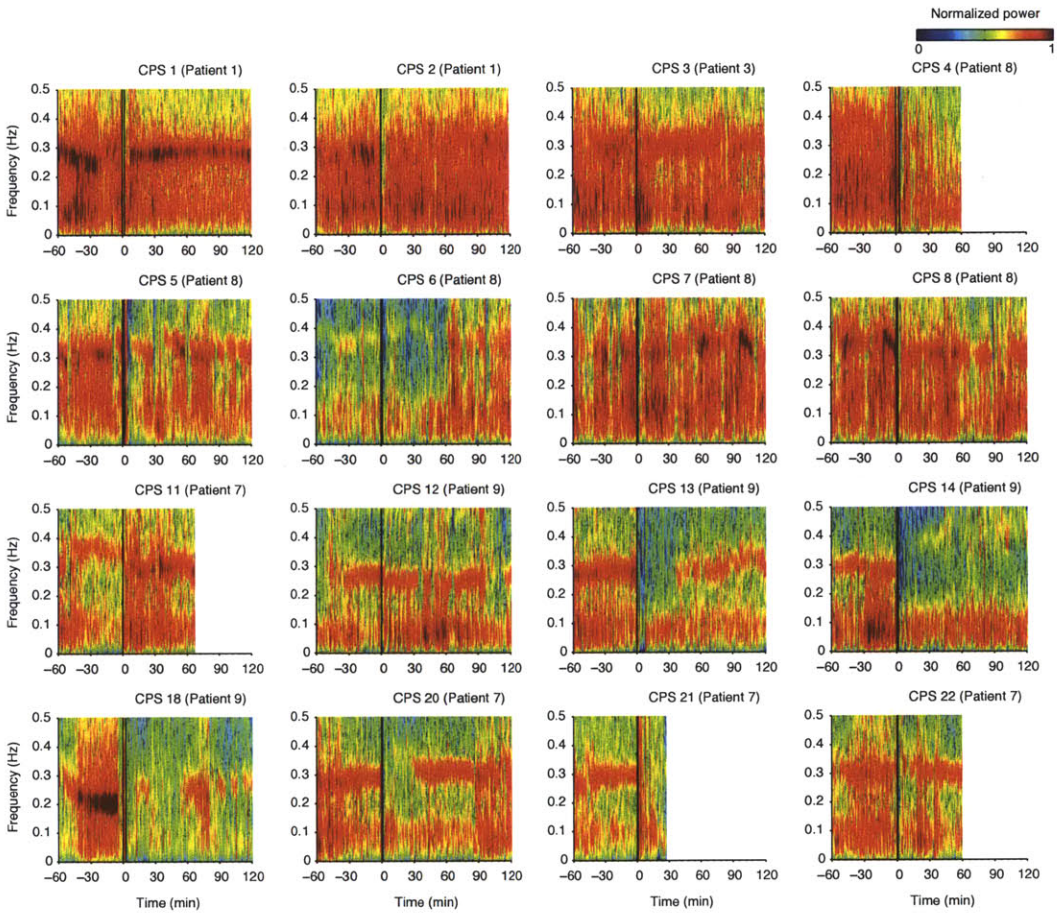

Figure C-3: *Time-frequency mapping of heart rate variability of individual complex partial seizures (CPS). Two main spectral components can be observed. The high frequency (HF: 0.15 - 0.4 Hz) component reflects vagal modulation of the heart rate; the low frequency (LF: 0.04 - 0.15 Hz) reflects a complex mixture of sympathetic and parasympathetic modulation. Black lines denote seizure onset and offset.*

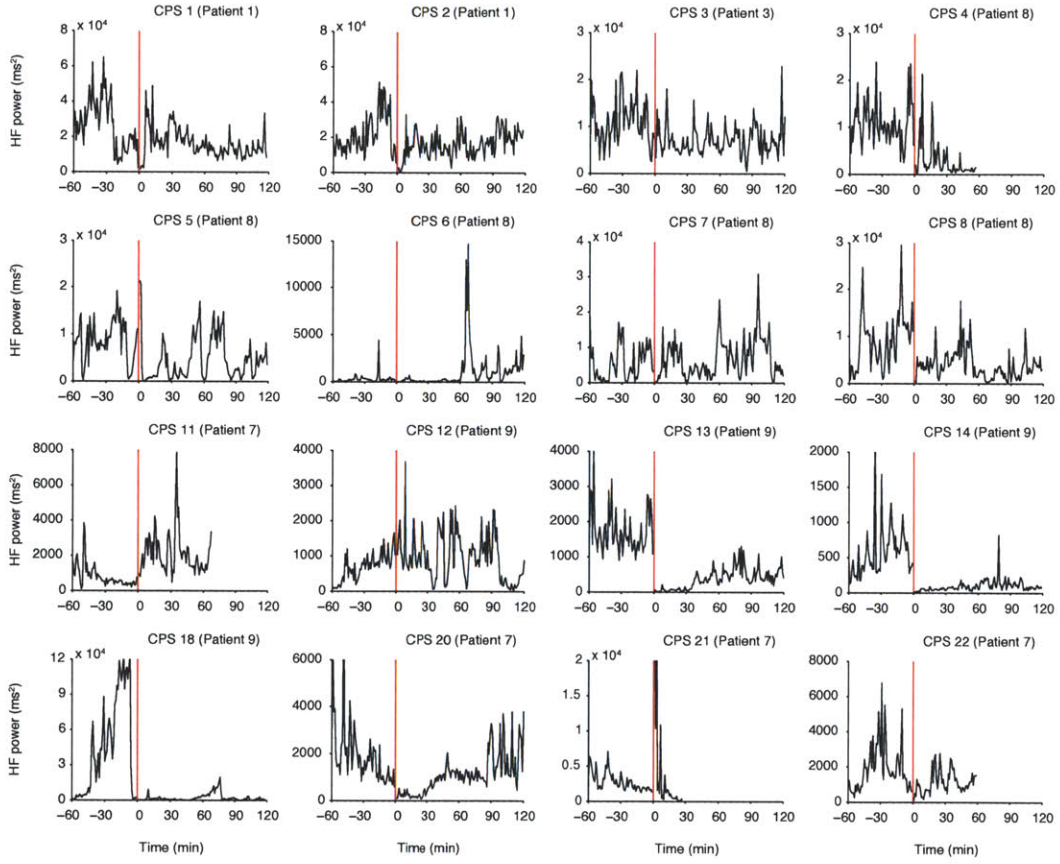

Figure C-4: *Peri-ictal high-frequency heart rate variability power (HF: 0.15-0.4 Hz; parasympathetic) of individual complex partial seizures (CPS). Red line denotes CPS.*

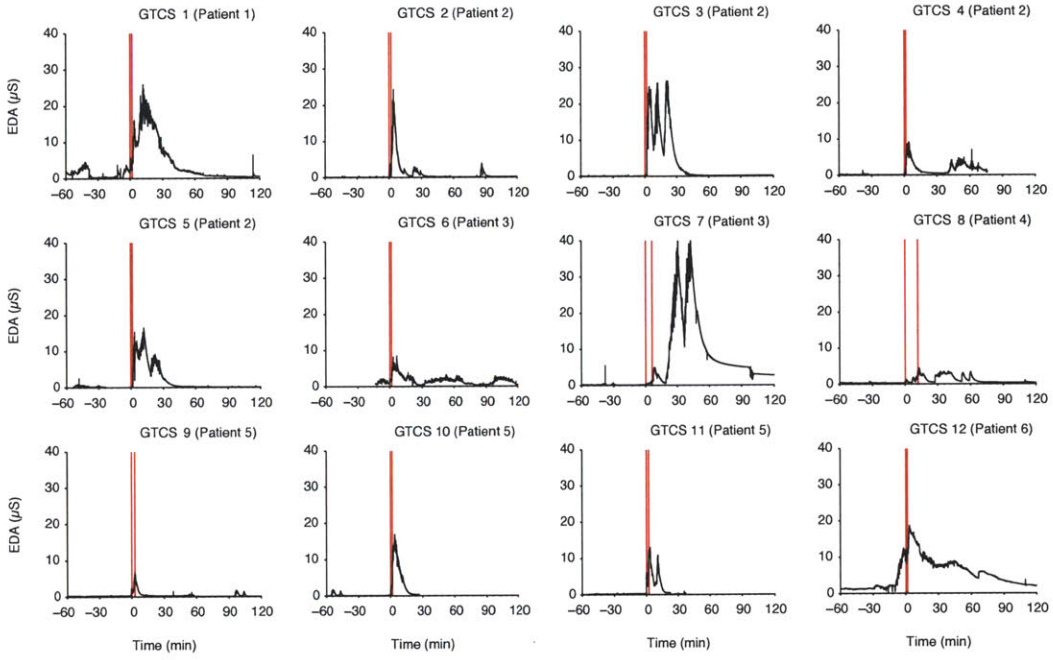

Figure C-5: *Peri-ictal EDA recordings(sympathetic) of individual generalized tonic-clonic seizures (GTCS). Red lines denote seizure onset and offset*

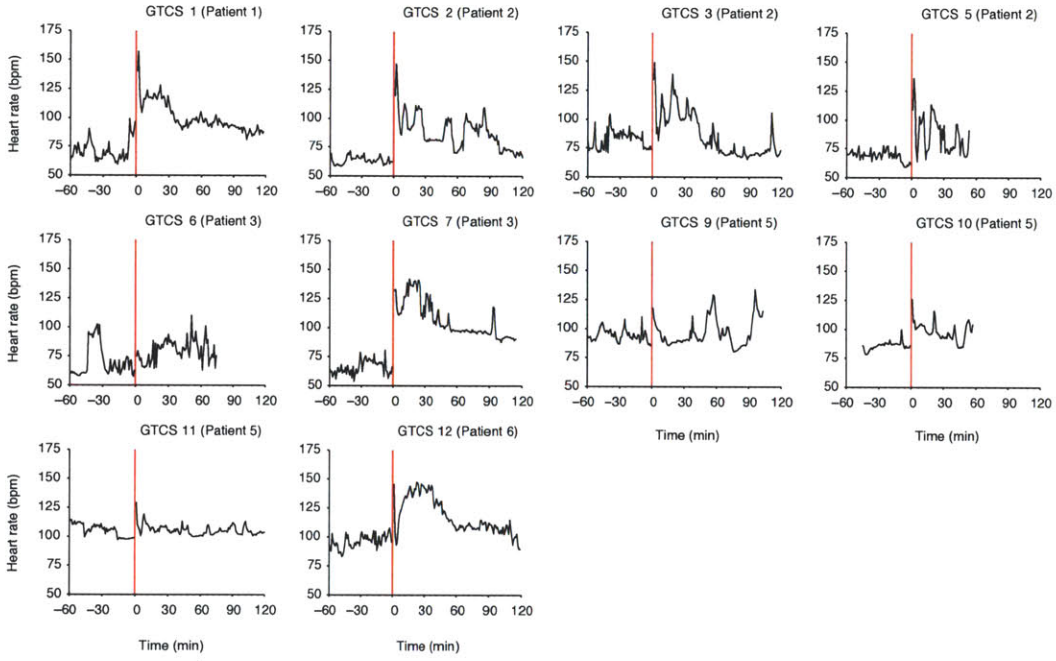

Figure C-6: *Peri-ictal heart rate recordings of individual generalized tonic-clonic seizures (GTCS). Red line denotes GTCS.*

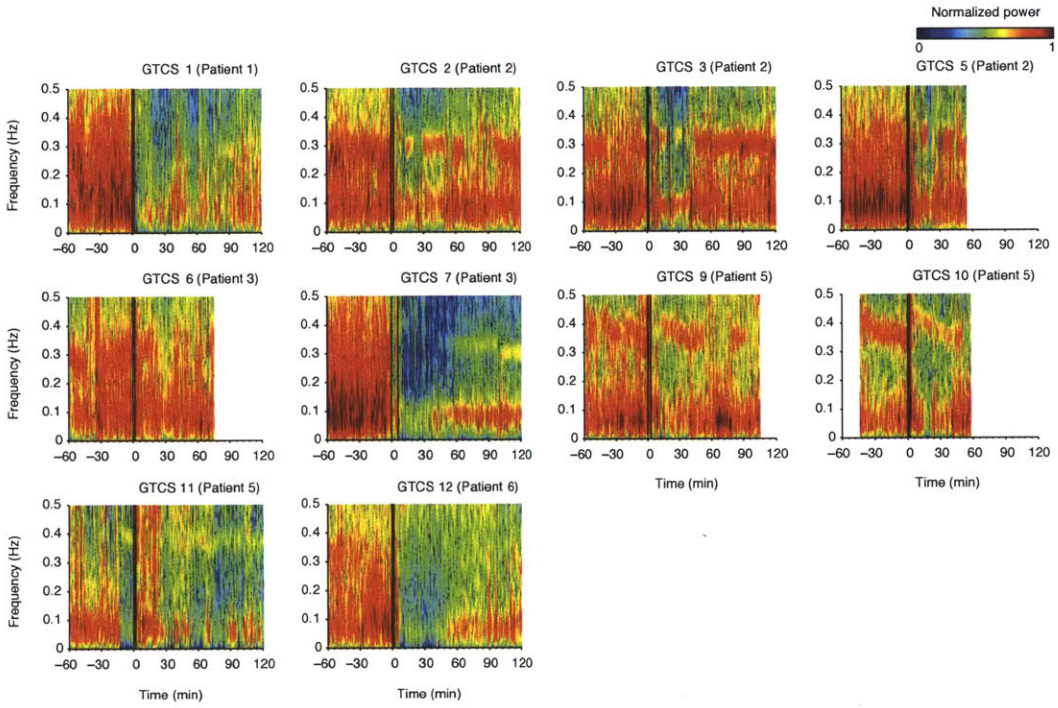

Figure C-7: *Time-frequency mapping of heart rate variability of individual generalized tonic-clonic seizures (GTCS). Two main spectral components can be observed. The high frequency (HF: 0.15 - 0.4 Hz) component reflects vagal modulation of the heart rate; the low frequency (LF: 0.04 - 0.15 Hz) reflects a complex mixture of sympathetic and parasympathetic modulation. Black lines denote seizure onset and offset.*

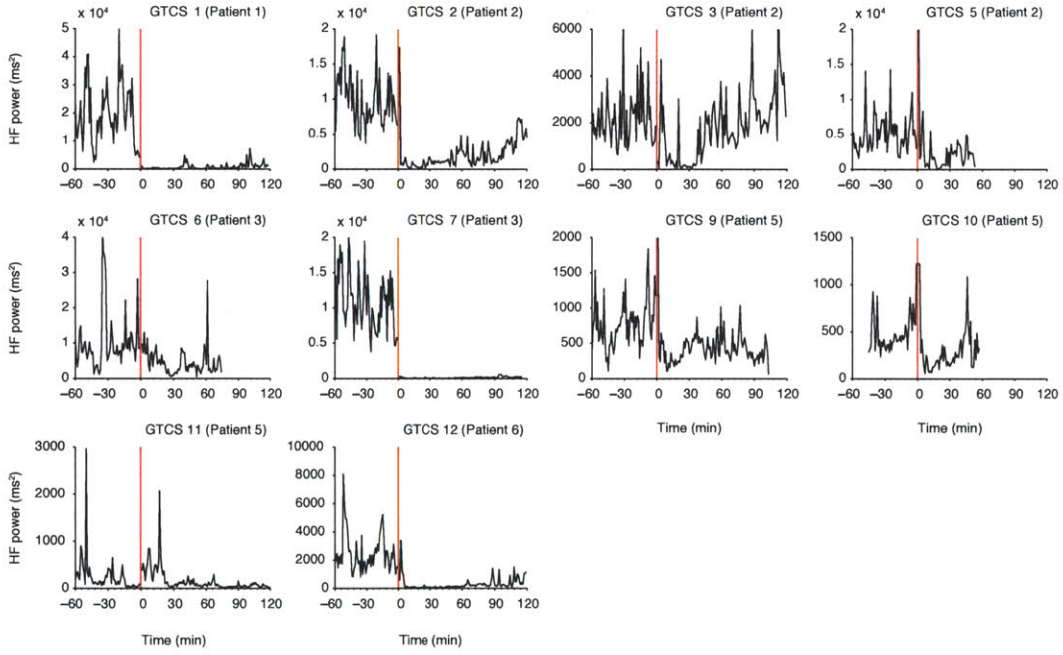

Figure C-8: *Peri-ictal high-frequency heart rate variability power (HF: 0.15-0.4 Hz; parasympathetic) of individual generalized tonic-clonic seizures (GTCS). Red line denotes GTCS.*

Appendix D

Supplementary Information on Convulsive Epileptic Seizure Detection

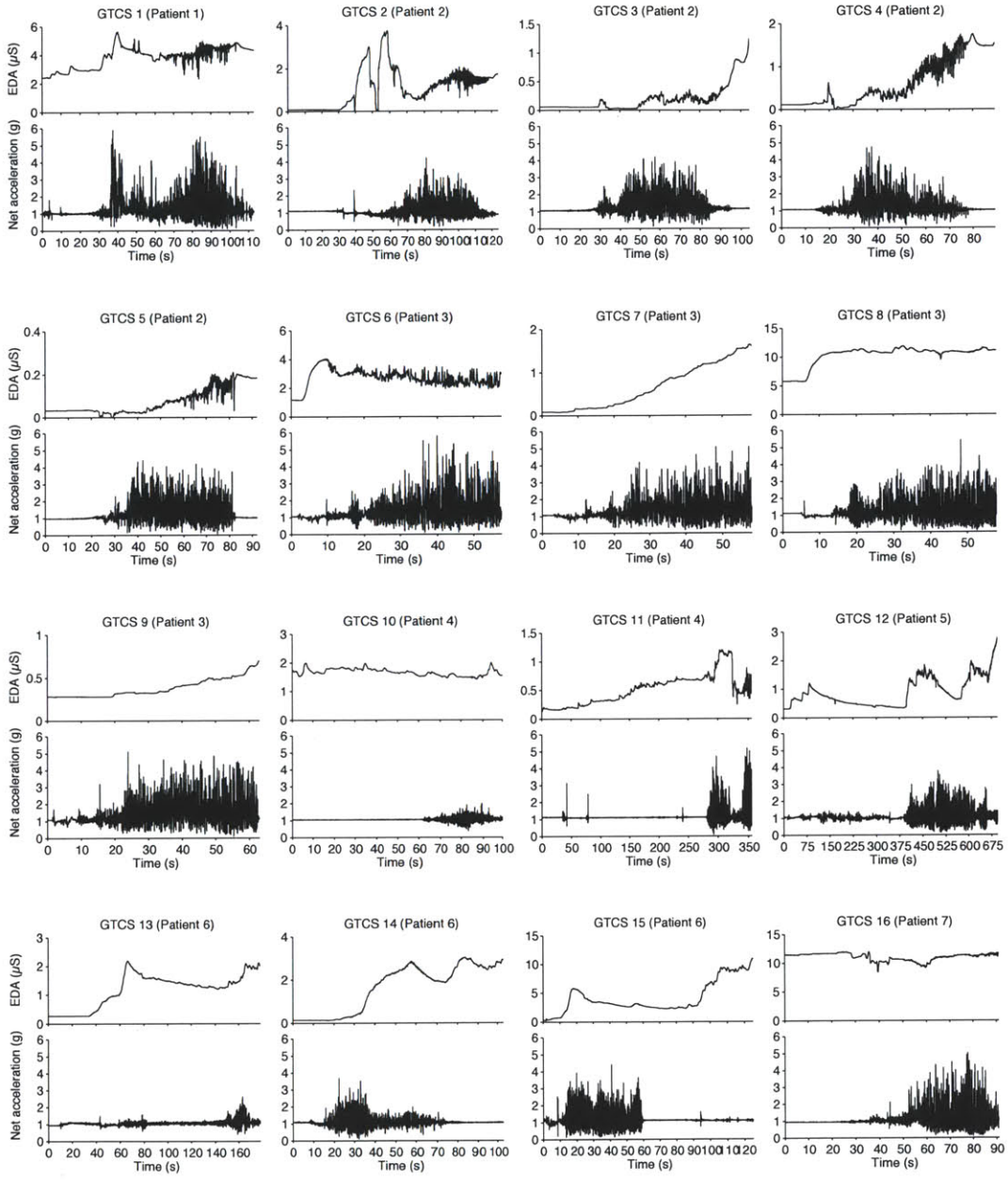

Figure D-1: *Electrodermal activity (EDA) and net acceleration recordings of individual generalized tonic-clonic seizures (GTCS) from seven patients included for seizure detection. This recordings are zoomed-in to highlight the ictal period. See Fig. D-2 for a broader view of the EDA changes surrounding each seizure.*

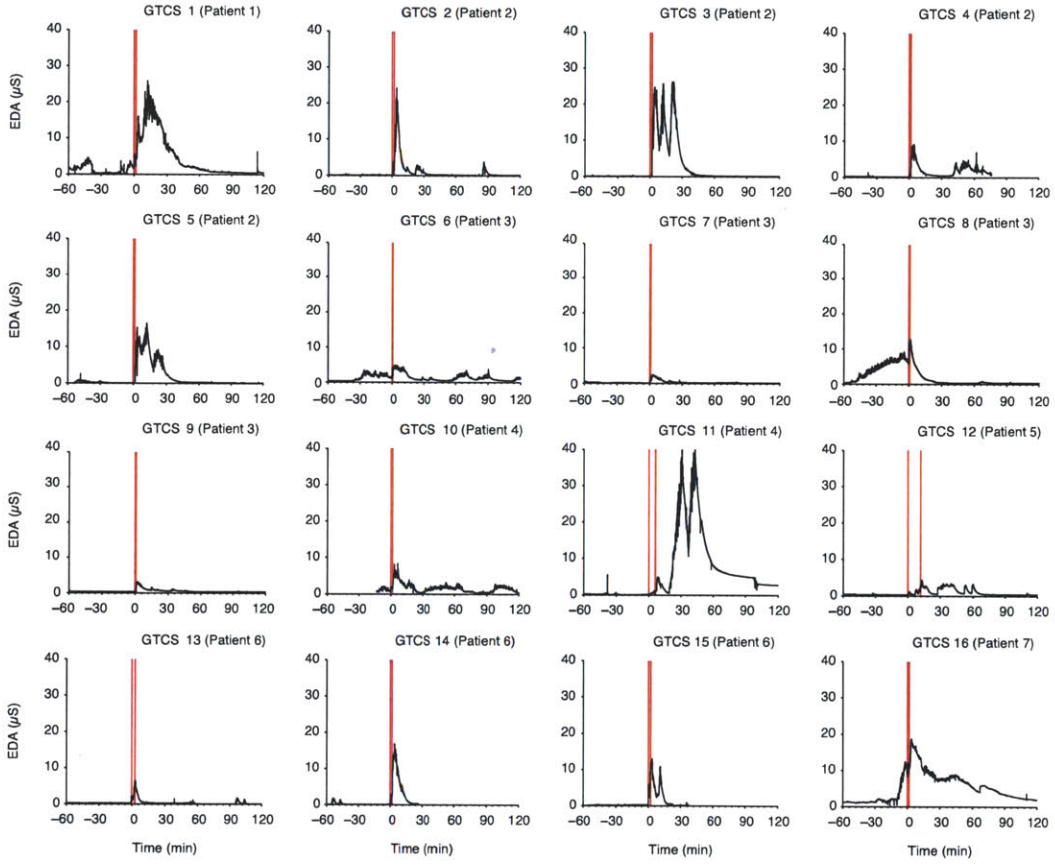

Figure D-2: *Electrodermal activity (EDA) recordings of individual generalized tonic-clonic seizures (GTCS) from seven patients included for seizure detection. Note: One new patient (patient 3) was included in this study so the numbering and ordering of seizures are different compared to Fig. C-5 from the previous study.*

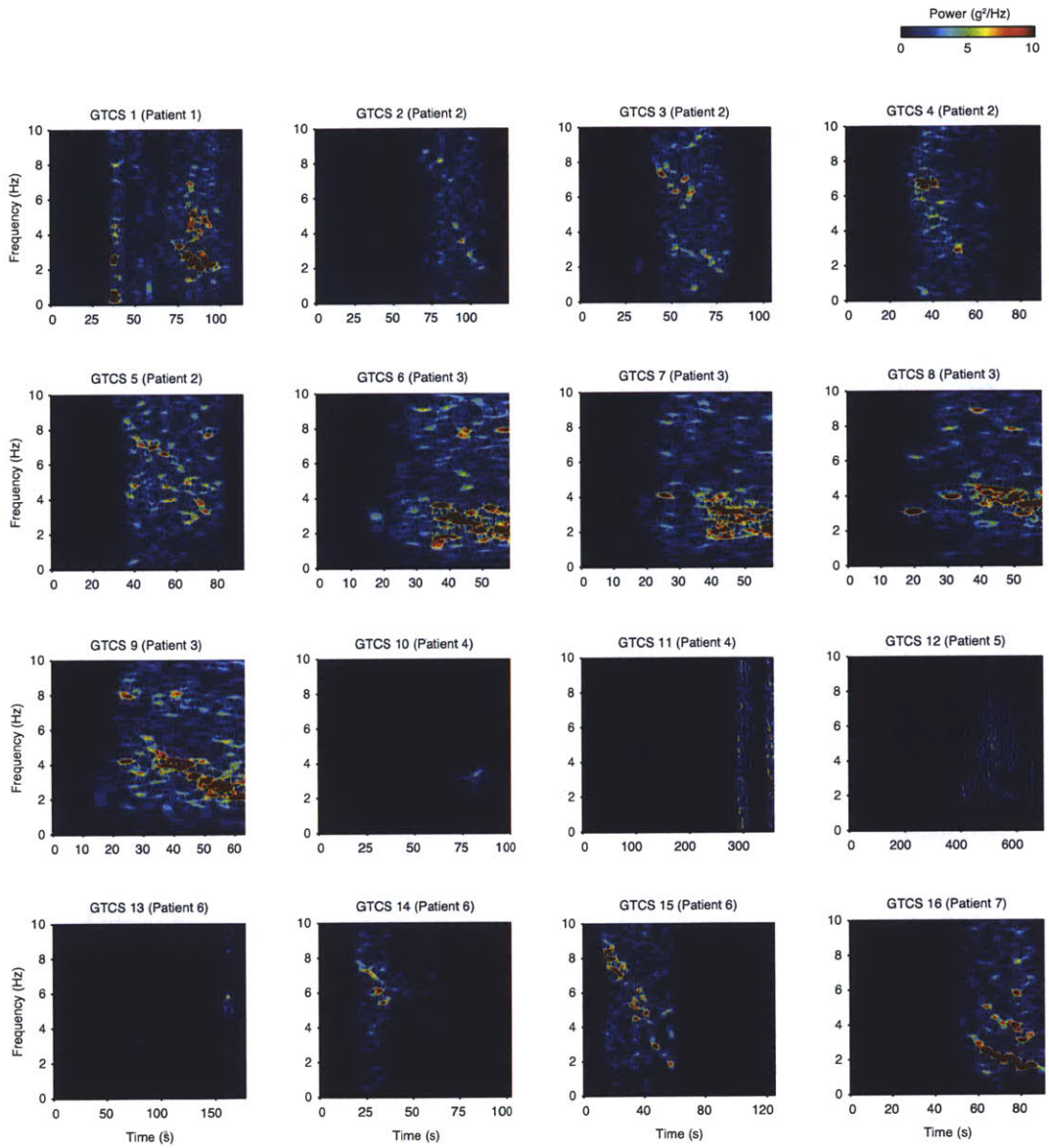

Figure D-3: *Time-frequency mapping of the net acceleration recordings of individual generalized tonic-clonic seizures (GTCS) from seven patients included for seizure detection.*

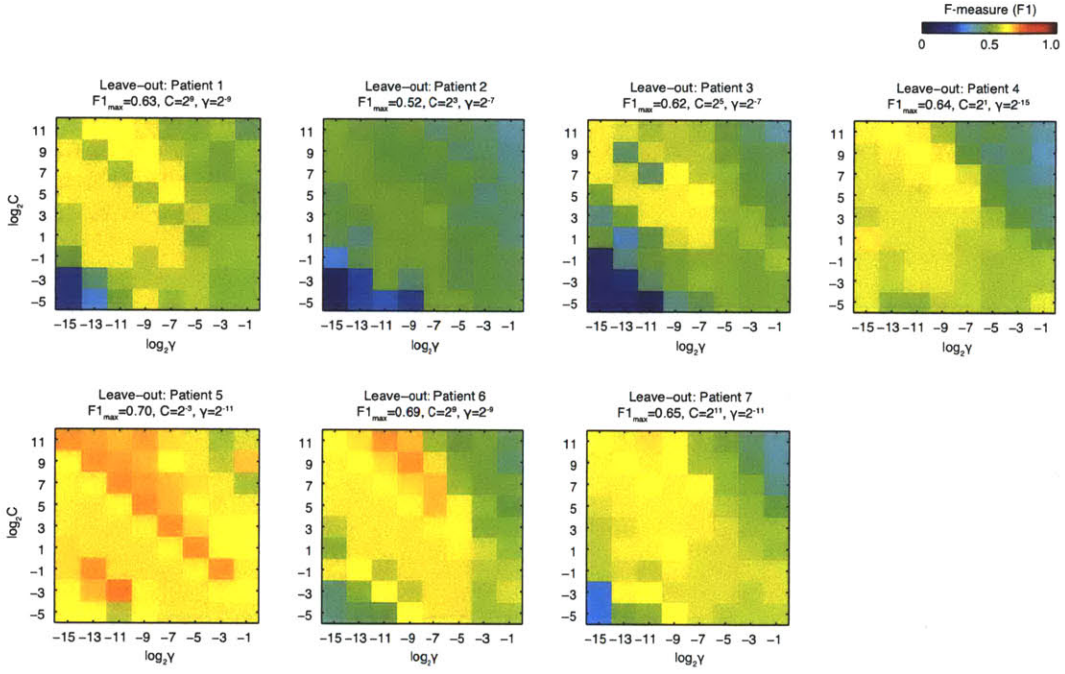

Figure D-4: *SVM parameter tuning for non-patient-specific seizure detection: Grid-search for optimal pair of C and γ values based on cross-validation of F-measure for (leave-one-patient-out using both EDA and ACM features).*

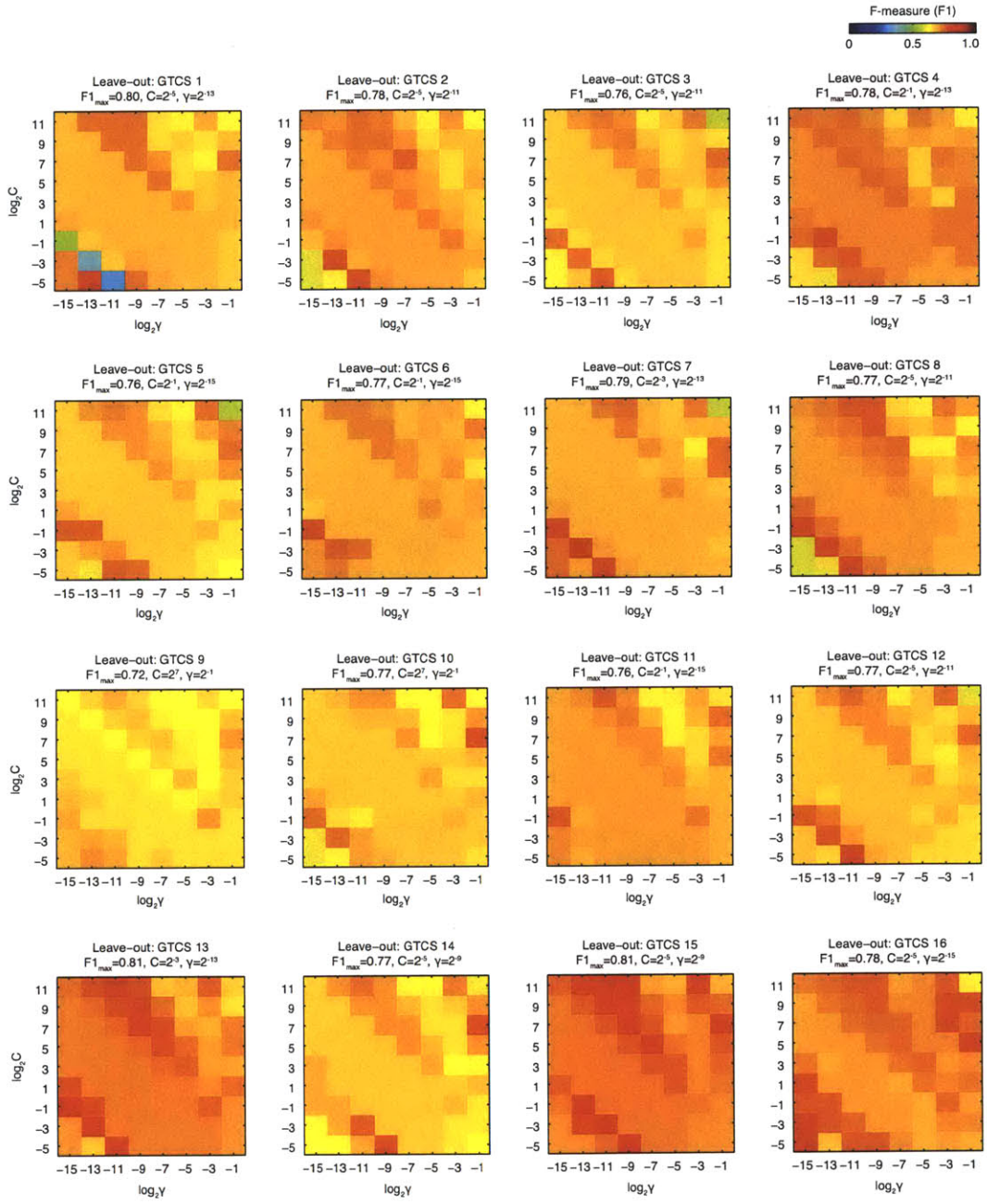

Figure D-5: *SVM parameter tuning for semi-patient-specific seizure detection: Grid-search for optimal pair of C and γ values based on cross-validation of F-measure for (leave-one-seizure-out using both EDA and ACM features).*

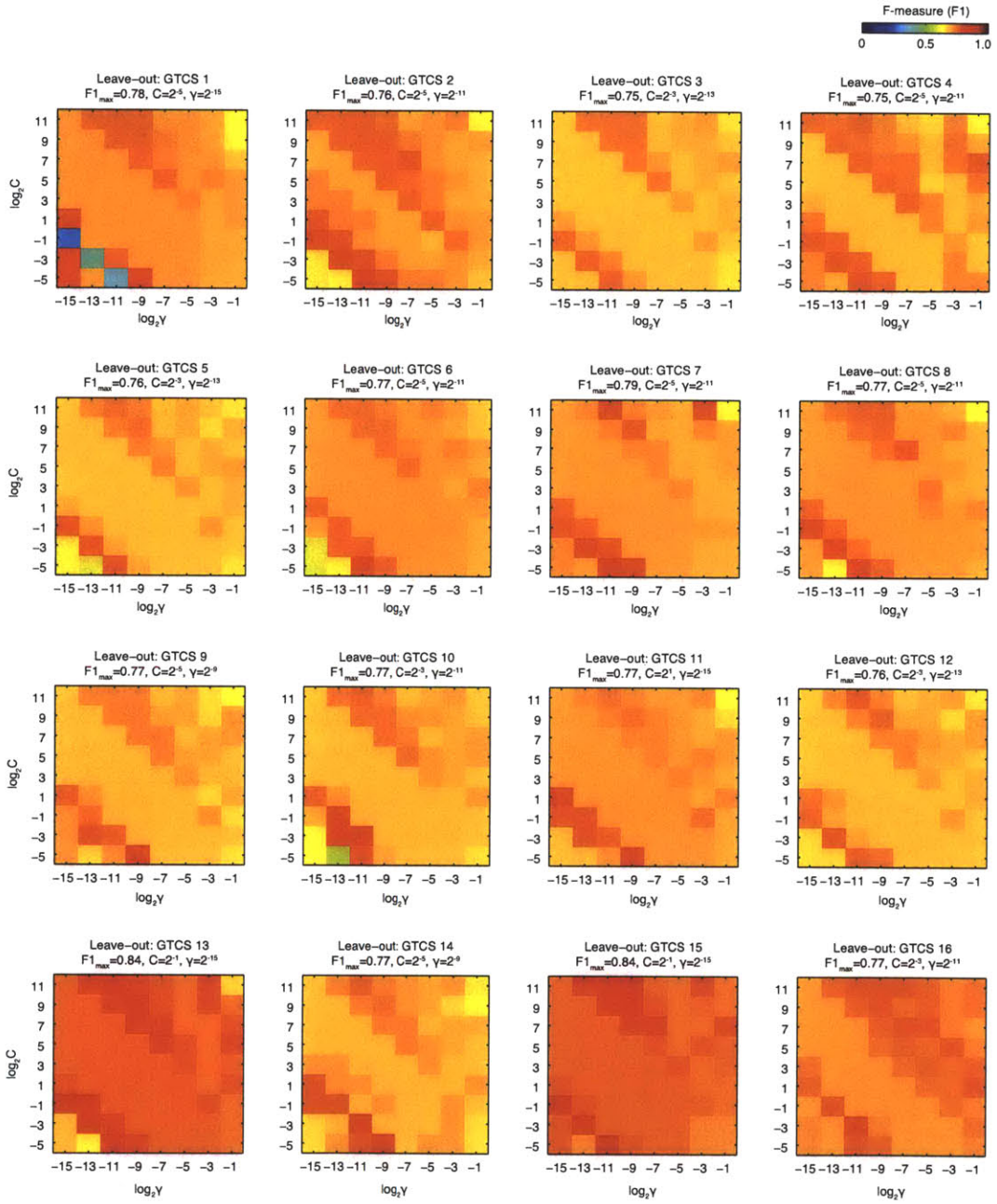

Figure D-6: *SVM parameter tuning for semi-patient-specific seizure detection: Grid-search for optimal pair of C and γ values based on cross-validation of F-measure for (leave-one-seizure-out using only ACM features).*

Bibliography

[1] *The writings of George Washington from the original manuscript sources: Volume 3.* http://etext.virginia.edu/etcbin/toccer-new2?id=WasFi03.xml&images=images/modeng&data=/texts/english/modeng/parsed&tag=public&part=96&division=div1, Accessed April 8, 2010.

[2] ADELSON, P., NEMOTO, E., SCHEUER, M., PAINTER, M., MORGAN, J., AND YONAS, H. Noninvasive continuous monitoring of cerebral oxygenation periictally using near-infrared spectroscopy: a preliminary report. *Epilepsia 40*, 11 (2005), 1484–1489.

[3] AFFECTIVA INC. *Q Sensor* (2011).

[4] AFONSO, V., TOMPKINS, W., NGUYEN, T., AND LUO, S. ECG beat detection using filter banks. *IEEE Transactions on Biomedical Engineering 46*, 2 (1999), 192–202.

[5] AKBANI, R., KWEK, S., AND JAPKOWICZ, N. Applying support vector machines to imbalanced datasets. *Machine Learning: ECML 2004* (2004), 39–50.

[6] AKSELROD, S., GORDON, D., UBEL, F., SHANNON, D., BARGER, A., AND COHEN, R. Power spectrum analysis of heart rate fluctuation: a quantitative probe of beat-to-beat cardiovascular control. *Science 213*, 4504 (1981), 220–222.

[7] AL-AWEEL, I., KRISHNAMURTHY, K., HAUSDORFF, J., MIETUS, J., IVES, J., BLUM, A., SCHOMER, D., AND GOLDBERGER, A. Postictal heart rate oscillations in partial epilepsy. *Neurology 53*, 7 (1999), 1590–1590.

[8] ALBINALI, F., GOODWIN, M., AND INTILLE, S. Recognizing stereotypical motor movements in the laboratory and classroom: a case study with children on the autism spectrum. In *Proceedings of the 11th international conference on Ubiquitous computing* (2009), ACM, pp. 71–80.

[9] ALLEN, J., ARMSTRONG, J., AND RODDIE, I. The regional distribution of emotional sweating in man. *The Journal of Physiology 235*, 3 (1973), 749.

[10] ANCOLI-ISRAEL, S., COLE, R., ALESSI, C., CHAMBERS, M., MOORCROFT, W., AND POLLAK, C. The role of actigraphy in the study of sleep and circadian rhythms. American Academy of Sleep Medicine Review Paper. *Sleep 26*, 3 (2003), 342–92.

[11] ANNEGERS, J., COAN, S., HAUSER, W., LEESTMA, J., DUFFELL, W., AND TARVER, B. Epilepsy, vagal nerve stimulation by the NCP system, mortality, and sudden, unexpected, unexplained death. *Epilepsia 39*, 2 (2005), 206–212.

[12] AXISA, F., GEHIN, C., DELHOMME, G., COLLET, C., ROBIN, O., AND DITTMAR, A. Wrist ambulatory monitoring system and smart glove for real time emotional, sensorial and physiological analysis. In *Engineering in Medicine and Biology Society, 2004. IEMBS'04. 26th Annual International Conference of the IEEE* (2004), vol. 1.

[13] BAO, L., AND INTILLE, S. Activity recognition from user-annotated acceleration data. *Pervasive Computing* (2004), 1–17.

[14] BATEMAN, L., SPITZ, M., AND SEYAL, M. Ictal hypoventilation contributes to cardiac arrhythmia and SUDEP: Report on two deaths in video-EEG–monitored patients. *Epilepsia 51*, 5 (2010), 916–920.

[15] BAUMGARTNER, C., LURGER, S., AND LEUTMEZER, F. Autonomic symptoms during epileptic seizures. *Epileptic Disorders 3* (2001), 103–116.

[16] BAUMGARTNER, C., SERLES, W., LEUTMEZER, F., PATARAIA, E., AULL, S., CZECH, T., PIETRZYK, U., RELIC, A., AND PODREKA, I. Preictal SPECT in temporal lobe epilepsy: regional cerebral blood flow is increased prior to electroencephalography-seizure onset. *Journal of Nuclear Medicine 39*, 6 (1998), 978.

[17] BECQ, G., BONNET, S., MINOTTI, L., ANTONAKIOS, M., GUILLEMAUD, R., AND KAHANE, P. Classification of epileptic motor manifestations using inertial and magnetic sensors. *Computers in Biology and Medicine* (2011).

[18] BENARROCH, E. The central autonomic network: functional organization, dysfunction, and perspective. *Mayo Clinic Proceedings 68*, 10 (1993), 988.

[19] BENJAMINI, Y., AND HOCHBERG, Y. Controlling the false discovery rate: a practical and powerful approach to multiple testing. *Journal of the Royal Statistical Society. Series B (Methodological) 57*, 1 (1995), 289–300.

[20] BERG, A., BERKOVIC, S., BRODIE, M., BUCHHALTER, J., CROSS, J., VAN EMDE BOAS, W., ENGEL, J., FRENCH, J., GLAUSER, T., MATHERN, G., ET AL. Revised terminology and concepts for organization of seizures and epilepsies: Report of the ILAE Commission on Classification and Terminology, 2005–2009. *Epilepsia 51*, 4 (2010), 676–685.

[21] BERNTSON, G., ET AL. Heart rate variability: origins, methods, and interpretive caveats. *Psychophysiology 34*, 6 (1997), 623–648.

[22] BILLMAN, G., AND HOSKINS, R. Time-series analysis of heart rate variability during submaximal exercise. Evidence for reduced cardiac vagal tone in animals susceptible to ventricular fibrillation. *Circulation 80*, 1 (1989), 146.

[23] BIRD, J., DEMBNY, K., SANDEMAN, D., AND BUTLER, S. Sudden unexplained death in epilepsy: an intracranially monitored case. *Epilepsia 38* (1997), S52–S56.

[24] BODY MEDIA INC. *SenseWear* (2010).

[25] BONATO, P. Wearable sensors/systems and their impact on biomedical engineering. *IEEE Engineering in Medicine and Biology Magazine 22*, 3 (2003), 18–20.

[26] BOUCSEIN, W. *Electrodermal activity*. Plenum Pub Corp, 1992.

[27] Bourke, A., O'Brien, J., and Lyons, G. Evaluation of a threshold-based tri-axial accelerometer fall detection algorithm. *Gait and Posture 26*, 2 (2007), 194–199.

[28] Bouten, C., Westerterp, K., Verduin, M., and Janssen, J. Assessment of energy expenditure for physical activity using a triaxial accelerometer. *Medicine & Science in Sports & Exercise 26*, 12 (1994), 1516.

[29] Brainquiry B.V. *QPET* (2010).

[30] Brodie, M., and Holmes, G. Should all patients be told about sudden unexpected death in epilepsy (SUDEP)? Pros and Cons. *Epilepsia 49*, s9 (2008), 99–101.

[31] Brown, M., Grundy, W., Lin, D., Cristianini, N., Sugnet, C., Furey, T., Ares, M., and Haussler, D. Knowledge-based analysis of microarray gene expression data by using support vector machines. *Proceedings of the National Academy of Sciences of the United States of America 97*, 1 (2000), 262.

[32] Cacioppo, J., Berntson, G., Binkley, P., Quigley, K., Uchino, B., and Fieldstone, A. Autonomic cardiac control. II. Noninvasive indices and basal response as revealed by autonomic blockades. *Psychophysiology 31*, 6 (1994), 586–598.

[33] Carlson, C., Arnedo, V., Cahill, M., and Devinsky, O. Detecting nocturnal convulsions: Efficacy of the MP5 monitor. *Seizure 18*, 3 (2009), 225–227.

[34] Casson, A., Smith, S., Duncan, J., and Rodriguez-Villegas, E. Wearable EEG: what is it, why is it needed and what does it entail? In *Engineering in Medicine and Biology Society, 2008. EMBS 2008. 30th Annual International Conference of the IEEE* (2008), IEEE, pp. 5867–5870.

[35] Chang, C.-C., and Lin, C.-J. *LIBSVM: a library for support vector machines*, 2001. Software available at `http://www.csie.ntu.edu.tw/~cjlin/libsvm`.

[36] Citizens United for Research in Epilepsy. *Epilepsy Facts* (2010).

[37] Critchley, H. Electrodermal responses: What happens in the brain. *The Neuroscientist* (2002).

[38] Cuppens, K., Lagae, L., Ceulemans, B., Van Huffel, S., and Vanrumste, B. Detection of nocturnal frontal lobe seizures in pediatric patients by means of accelerometers: A first study. In *Engineering in Medicine and Biology Society, 2009. EMBC 2009. Annual International Conference of the IEEE* (2009), IEEE, pp. 6608–6611.

[39] Dasheiff, R. Sudden unexpected death in epilepsy: a series from an epilepsy surgery program and speculation on the relationship to sudden cardiac death. *Journal of Clinical Neurophysiology 8*, 2 (1991), 216.

[40] Dasheiff, R., and Dickinson, L. Sudden unexpected death of epileptic patient due to cardiac arrhythmia after seizure. *Archives of Neurology 43*, 2 (1986), 194.

[41] De Chazal, P., O'Dwyer, M., and Reilly, R. Automatic classification of heartbeats using ECG morphology and heartbeat interval features. *IEEE Transactions on Biomedical Engineering 51*, 7 (2004), 1196–1206.

[42] De Ferrari, G., Salvati, P., Grossoni, M., Ukmar, G., Vaga, L., Patrono, C., and Schwartz, P. Pharmacologic modulation of the autonomic nervous system in the prevention of sudden cardiac death:: A study with propranolol, methacholine and oxotremorine in conscious dogs with a healed myocardial infarction. *Journal of the American College of Cardiology 22*, 1 (1993), 283–290.

[43] Deckers, C., Genton, P., Sills, G., and Schmidt, D. Current limitations of antiepileptic drug therapy: A conference review. *Epilepsy Research 53*, 1-2 (2003), 1–17.

[44] DeGiorgio, C., Miller, P., Meymandi, S., Chin, A., and Epps, J. RMSSD, a measure of vagus-mediated heart rate variability, is associated with risk factors for SUDEP: The SUDEP-7 Inventory. *Epilepsy & Behavior 19*, 1 (2010), 78–81.

[45] Delamont, R., Julu, P., and Jamal, G. Changes in a measure of cardiac vagal activity before and after epileptic seizures. *Epilepsy research 35*, 2 (1999), 87–94.

[46] Devinsky, O. Effects of seizures on autonomic and cardiovascular function. *Epilepsy Currents 4*, 2 (2004), 43.

[47] Doherty, M. The sudden death of Patsy Custis, or George Washington on sudden unexplained death in epilepsy. *Epilepsy & Behavior 5*, 4 (2004), 598–600.

[48] Dolu, N., Ozesmi, C., Comu, N., Süer, C., and Gölgeli, A. Effect of hyperglycemia on electrodermal activity in diabetic rats. *International Journal of Neuroscience 116*, 6 (2006), 715–729.

[49] Duller, P., and Gentry, W. Use of biofeedback in treating chronic hyperhidrosis: a preliminary report. *British Journal of Dermatology 103*, 2 (1980), 143–146.

[50] Eckmann, J., Kamphorst, S., and Ruelle, D. Recurrence plots of dynamical systems. *Europhysics Letters 4* (1987), 973.

[51] Edelberg, R. Electrodermal recovery rate, goal-orientation, and aversion. *Psychophysiology 9*, 5 (1972), 512–520.

[52] Edelberg, R., Greiner, T., and Burch, N. Some membrane properties of the effector in the galvanic skin response. *Journal of Applied Physiology 15*, 4 (1960), 691.

[53] Elger, C. Future trends in epileptology. *Current Opinion in Neurology 14*, 2 (2001), 185.

[54] Elliott, I., Lach, L., and Smith, M. I just want to be normal: a qualitative study exploring how children and adolescents view the impact of intractable epilepsy on their quality of life. *Epilepsy & Behavior 7*, 4 (2005), 664–678.

[55] Epilepsy Foundation. *Epilepsy and Seizure Statistics* (2010).

[56] Espinosa, P., Lee, J., Tedrow, U., Bromfield, E., and Dworetzky, B. Sudden unexpected near death in epilepsy: malignant arrhythmia from a partial seizure. *Neurology 72*, 19 (2009), 1702.

[57] Eydgahi, H. Design and evaluation of iCalm: a novel, wrist-worn, low-power, low-cost, wireless physiological sensor module. *MIT SM Thesis* (2008).

[58] FEDERICO, P., ABBOTT, D., BRIELLMANN, R., HARVEY, A., AND JACKSON, G. Functional MRI of the pre-ictal state. *Brain 128*, 8 (2005), 1811.

[59] FENDER, F. Foerster's scheme of the dermatomes. *Archives of Neurology & Psychiatry 41*, 4 (1939), 688.

[60] FERE, C. Note sur les modifications de la résistance électrique sous l'influence des excitations sensorielles et des émotions. *Comptes Rendus Société de Biologie 5* (1888), 217–219.

[61] FICKER, D., SO, E., SHEN, W., ANNEGERS, J., O'BRIEN, P., CASCINO, G., AND BELAU, P. Population-based study of the incidence of sudden unexplained death in epilepsy. *Neurology 51*, 5 (1998), 1270.

[62] FISHER, R., BOAS, W., BLUME, W., ELGER, C., GENTON, P., LEE, P., AND ENGEL, J. Epileptic seizures and epilepsy: Definitions proposed by the International League Against Epilepsy (ILAE) and the International Bureau for Epilepsy (IBE). *Epilepsia 46*, 4 (2005), 470–472.

[63] FISHER, S. Body image and asymmetry of body reactivity. *Journal of Abnormal and Social Psychology 57*, 3 (1958), 292–298.

[64] FLETCHER, R., DOBSON, K., GOODWIN, M., EYDGAHI, H., WILDER-SMITH, O., FERNHOLZ, D., KUBOYAMA, Y., HEDMAN, E., POH, M., AND PICARD, R. iCalm: Wearable sensor and network architecture for wirelessly communicating and logging autonomic activity. *IEEE Transactions on Information Technology in Biomedicine 14*, 2 (2010), 215–223.

[65] FORSGREN, L., HAUSER, W., OLAFSSON, E., SANDER, J., SILLANPÄÄ, M., AND TOMSON, T. Mortality of epilepsy in developed countries: a review. *Epilepsia 46*, s11 (2005), 18–27.

[66] FOWLES, D., CHRISTIE, M., EDELBERG, R., GRINGS, W., LYKKEN, D., AND VENABLES, P. Publication recommendations for electrodermal measurements. *Psychophysiology 18*, 3 (1981), 232–239.

[67] FRASER, A., AND SWINNEY, H. Independent coordinates for strange attractors from mutual information. *Physical Review A 33*, 2 (1986), 1134.

[68] FRIIS, M., AND LUND, M. Stress convulsions. *Archives of Neurology 31*, 3 (1974), 155.

[69] FROST JR, J., HRACHOVY, R., KELLAWAY, P., AND ZION, T. Quantitative analysis and characterization of infantile spasms. *Epilepsia 19*, 3 (1978), 273–282.

[70] FRUCHT, M., QUIGG, M., SCHWANER, C., AND FOUNTAIN, N. Distribution of seizure precipitants among epilepsy syndromes. *Epilepsia 41*, 12 (2000), 1534–1539.

[71] GOTMAN, J. Automatic recognition of epileptic seizures in the EEG. *Electroencephalography and Clinical Neurophysiology 54*, 5 (1982), 530–540.

[72] GRAVELING, R. A., AND BROOKE, J. D. Hormonal and cardiac response of autistic children to changes in environmental stimulation. *Journal of Autism and Childhood Schizophrenia 8*, 4 (Dec 1978), 441–55.

[73] GUYON, I., WESTON, J., BARNHILL, S., AND VAPNIK, V. Gene selection for cancer classification using support vector machines. *Machine lLarning 46*, 1 (2002), 389–422.

[74] HILZ, M., DEVINSKY, O., DOYLE, W., MAUERER, A., AND DUTSCH, M. Decrease of sympathetic cardiovascular modulation after temporal lobe epilepsy surgery. *Brain 125*, 5 (2002), 985.

[75] HITIRIS, N., SURATMAN, S., KELLY, K., STEPHEN, L., SILLS, G., AND BRODIE, M. Sudden unexpected death in epilepsy: a search for risk factors. *Epilepsy & Behavior 10*, 1 (2007), 138–141.

[76] HOPF, H., SKYSCHALLY, A., HEUSCH, G., AND PETERS, J. Low-frequency spectral power of heart rate variability is not a specific marker of cardiac sympathetic modulation. *Anesthesiology 82*, 3 (1995), 609.

[77] HULL JR, S., EVANS, A., VANOLI, E., ADAMSON, P., STRAMBA-BADIALE, M., ALBERT, D., AND FOREMAN, R. Heart rate variability before and after myocardial infarction in conscious dogs at high and low risk of sudden death. *Journal of the American College of Cardiology 16*, 4 (1990), 978–985.

[78] HULL JR, S., VANOLI, E., ADAMSON, P., VERRIER, R., FOREMAN, R., AND SCHWARTZ, P. Exercise training confers anticipatory protection from sudden death during acute myocardial ischemia. *Circulation 89*, 2 (1994), 548.

[79] ILAE. Proposal for revised clinical and electroencephalographic classification of epileptic seizures. *Epilepsia 22*, 4 (Aug 1981), 489–501.

[80] JALLON, P. A Bayesian approach for epileptic seizures detection with 3D accelerometers sensors. In *Engineering in Medicine and Biology Society (EMBC), 2010 Annual International Conference of the IEEE* (2010), IEEE, pp. 6325–6328.

[81] JARDINE, D., CHARLES, C., FORRESTER, M., WHITEHEAD, M., AND NICHOLLS, M. A neural mechanism for sudden death after myocardial infarction. *Clinical Autonomic Research 13*, 5 (2003), 339–341.

[82] JAY, G., AND LEESTMA, J. Sudden death in epilepsy. A comprehensive review of the literature and proposed mechanisms. *Acta Neurologica Scandinavica. Supplementum 82* (1981), 1–66.

[83] JEAN-LOUIS, G., KRIPKE, D., COLE, R., ASSMUS, J., AND LANGER, R. Sleep detection with an accelerometer actigraph: comparisons with polysomnography. *Physiology & behavior 72*, 1-2 (2001), 21–28.

[84] JOHANSEN, J., LINDAHL, G., AND SANDSTEDT, P. Home-video observation of seizures in children with epilepsy-impact on quality of family life. *Seizure 8*, 6 (1999), 356.

[85] JOHNSON, L., AND LUBIN, A. Spontaneous electrodermal activity during waking and sleeping. *Psychophysiology* (1966).

[86] KARAYIANNIS, N., TAO, G., XIONG, Y., SAMI, A., VARUGHESE, B., FROST JR, J., WISE, M., AND MIZRAHI, E. Computerized motion analysis of videotaped neonatal seizures of epileptic origin. *Epilepsia 46*, 6 (2005), 901–917.

[87] KEEGAN, J., AND GARRETT, F. The segmental distribution of the cutaneous nerves in the limbs of man. *The Anatomical Record 102*, 4 (1948), 409–437.

[88] KENNEL, M., BROWN, R., AND ABARBANEL, H. Determining embedding dimension for phase-space reconstruction using a geometrical construction. *Physical Review A 45*, 6 (1992), 3403.

[89] KEREM, D., AND GEVA, A. Forecasting epilepsy from the heart rate signal. *Medical and Biological Engineering and Computing 43*, 2 (2005), 230–239.

[90] KRAMER, U., KIPERVASSER, S., SHLITNER, A., AND KUZNIECKY, R. A Novel Portable Seizure Detection Alarm System: Preliminary Results. *Journal of Clinical Neurophysiology 28*, 1 (2011), 36.

[91] KUNO, Y. *Human Perspiration.* Thomas, 1956.

[92] KWAN, P., AND BRODIE, M. Early identification of refractory epilepsy. *New England Journal of Medicine 342*, 5 (2000), 314.

[93] LANGAN, Y., NASHEF, L., AND SANDER, J. Sudden unexpected death in epilepsy: a series of witnessed deaths. *Journal of Neurology, Neurosurgery & Psychiatry 68*, 2 (2000), 211.

[94] LANGAN, Y., NASHEF, L., AND SANDER, J. Case-control study of SUDEP. *Neurology 64*, 7 (2005), 1131.

[95] LANTEAUME, L., KHALFA, S., RÉGIS, J., MARQUIS, P., CHAUVEL, P., AND BARTOLOMEI, F. Emotion induction after direct intracerebral stimulations of human amygdala. *Cerebral Cortex 17*, 6 (2007), 1307.

[96] LATHERS, C., AND SCHRAEDER, P. Autonomic dysfunction in epilepsy: characterization of autonomic cardiac neural discharge associated with pentylenetetrazol-induced epileptogenic activity. *Epilepsia 23*, 6 (2007), 633–647.

[97] LATHERS, C., SCHRAEDER, P., AND BUNGO, M. The mystery of sudden death: mechanisms for risks. *Epilepsy & Behavior 12*, 1 (2008), 3–24.

[98] LEE, H., HONG, S., TAE, W., SEO, D., AND KIM, S. Partial seizures manifesting as apnea only in an adult. *Epilepsia 40*, 12 (2005), 1828–1831.

[99] LEE, M. EEG video recording of sudden unexpected death in epilepsy (SUDEP). *Epilepsia 39*, Suppl 6 (1998), 123.

[100] LEE, Y., YOON, S., LEE, C., AND LEE, M. Wearable EDA sensor gloves using conducting fabric and embedded system. In *World Congress on Medical Physics and Biomedical Engineering 2006*, Springer, pp. 883–888.

[101] LEESTMA, J., WALCZAK, T., HUGHES, J., KALELKAR, M., AND TEAS, S. A prospective study on sudden unexpected death in epilepsy. *Annals of Neurology 26*, 2 (1989), 195–203.

[102] LEMKE, D., HUSSAIN, S., WOLFE, T., TORBEY, M., LYNCH, J., CARLIN, A., FITZSIMMONS, B., AND ZAIDAT, O. Tako-Tsubo cardiomyopathy associated with seizures. *Neurocritical Care 9*, 1 (2008), 112–117.

[103] LEPPIK, I. E. *Contemporary Diagnosis and Management of the Patient with Epilepsy.* Handbooks in Health Care, Newton, Pennsylvania, USA, 2000.

[104] LHATOO, S., FAULKNER, H., DEMBNY, K., TRIPPICK, K., JOHNSON, C., AND BIRD, J. An electroclinical case-control study of sudden unexpected death in epilepsy. *Annals of neurology.*

[105] LI, Z., DA SILVA, A., AND CUNHA, J. Movement quantification in epileptic seizures: a new approach to video-EEG analysis. *IEEE Transactions on Biomedical Engineering 49*, 6 (2002), 565–573.

[106] LITT, B., AND ECHAUZ, J. Prediction of epileptic seizures. *The Lancet Neurology 1*, 1 (2002), 22–30.

[107] LOCKMAN, J., FISHER, R., AND OLSON, D. Detection of seizure-like movements using a wrist accelerometer. *Epilepsy & Behavior 20*, 4 (2011), 638–641.

[108] LODDENKEMPER, T., KELLINGHAUS, C., GANDJOUR, J., NAIR, D., NAJM, I., BINGAMAN, W., AND LÜDERS, H. Localising and lateralising value of ictal piloerection. *Journal of Neurology, Neurosurgery & Psychiatry 75*, 6 (2004), 879.

[109] LODDENKEMPER, T., AND KOTAGAL, P. Lateralizing signs during seizures in focal epilepsy. *Epilepsy & Behavior 7*, 1 (2005), 1–17.

[110] MALIK, M., BIGGER, J., CAMM, A., KLEIGER, R., MALLIANI, A., MOSS, A., AND SCHWARTZ, P. Heart rate variability: Standards of measurement, physiological interpretation, and clinical use. *European Heart Journal 17*, 3 (1996), 354.

[111] MANGINA, C., AND BEUZERON-MANGINA, J. Direct electrical stimulation of specific human brain structures and bilateral electrodermal activity. *International Journal of Psychophysiology 22*, 1-2 (1996), 1–8.

[112] MARTIN, G., MAGID, N., MYERS, G., BARNETT, P., SCHAAD, J., WEISS, J., LESCH, M., AND SINGER, D. Heart rate variability and sudden death secondary to coronary artery disease during ambulatory electrocardiographic monitoring. *The American Journal of Cardiology 60*, 1 (1987), 86–89.

[113] MARWAN, N., CARMEN ROMANO, M., THIEL, M., AND KURTHS, J. Recurrence plots for the analysis of complex systems. *Physics Reports 438*, 5-6 (2007), 237–329.

[114] MATHIE, M., COSTER, A., LOVELL, N., AND CELLER, B. Accelerometry: Providing an integrated, practical method for long-term, ambulatory monitoring of human movement. *Physiological Measurement 25* (2004), R1.

[115] MCLEAN, B., AND WIMALARATNA, S. Sudden death in epilepsy recorded in ambulatory EEG. *British Medical Journal 78*, 12 (2007), 1395.

[116] MESBAH, M. Newborn seizure detection based on heart rate variability. *IEEE Transactions on Biomedical Engineering* (Jan 2009).

[117] MIRKIN, A., AND COPPEN, A. Electrodermal activity in depression: Clinical and biochemical correlates. *The British Journal of Psychiatry 137*, 1 (1980), 93–97.

[118] MOHANRAJ, R., NORRIE, J., STEPHEN, L., KELLY, K., HITIRIS, N., AND BRODIE, M. Mortality in adults with newly diagnosed and chronic epilepsy: a retrospective comparative study. *The Lancet Neurology 5*, 6 (2006), 481–487.

[119] MØLGAARD, H., SØRENSEN, K., AND BJERREGAARD, P. Attenuated 24-h heart rate variability in apparently healthy subjects, subsequently suffering sudden cardiac death. *Clinical Autonomic Research 1*, 3 (1991), 233–237.

[120] MORMANN, F., ANDRZEJAK, R., ELGER, C., AND LEHNERTZ, K. Seizure prediction: the long and winding road. *Brain 130*, 2 (2007), 314.

[121] NAGAI, Y., GOLDSTEIN, L., FENWICK, P., AND TRIMBLE, M. Clinical efficacy of galvanic skin response biofeedback training in reducing seizures in adult epilepsy: a preliminary randomized controlled study. *Epilepsy & Behavior 5*, 2 (2004), 216–223.

[122] NAKAGAWA, M., SAIKAWA, T., AND ITO, M. Progressive reduction of heart rate variability with eventual sudden death in two patients. *British Medical Journal 71*, 1 (1994), 87.

[123] NASHEF, L. Sudden unexpected death in epilepsy: terminology and definitions. *Epilepsia 38*, s11 (2007), S6–S8.

[124] NASHEF, L., FISH, D., GARNER, S., SANDER, J., AND SHORVON, S. Sudden death in epilepsy: a study of incidence in a young cohort with epilepsy and learning difficulty. *Epilepsia 36*, 12 (2005), 1187–1194.

[125] NASHEF, L., FISH, D., SANDER, J., AND SHORVON, S. Incidence of sudden unexpected death in an adult outpatient cohort with epilepsy at a tertiary referral centre. *British Medical Journal 58*, 4 (1995), 462.

[126] NASHEF, L., GARNER, S., SANDER, J., FISH, D., AND SHORVON, S. Circumstances of death in sudden death in epilepsy: interviews of bereaved relatives. *Journal of Neurology, Neurosurgery & Psychiatry 64*, 3 (1998), 349.

[127] NIJSEN, T., AARTS, R., ARENDS, J., AND CLUITMANS, P. Automated detection of tonic seizures using 3-D accelerometry. In *4th European Conference of the International Federation for Medical and Biological Engineering* (2009), Springer, pp. 188–191.

[128] NIJSEN, T., AARTS, R., CLUITMANS, P., AND GRIEP, P. Time-Frequency Analysis of Accelerometry Data for Detection of Myoclonic Seizures. *IEEE Transactions on Information Technology in Biomedicine 14*, 5 (2010), 1197–1203.

[129] NIJSEN, T., ARENDS, J., GRIEP, P., AND CLUITMANS, P. The potential value of three-dimensional accelerometry for detection of motor seizures in severe epilepsy. *Epilepsy & Behavior 7*, 1 (2005), 74–84.

[130] NILSSON, L., AHLBOM, A., FARAHMAND, B., AND TOMSON, T. Mortality in a population-based cohort of epilepsy surgery patients. *Epilepsia 44*, 4 (2003), 575–581.

[131] NILSSON, L., FARAHMAND, B., PERSSON, P., THIBLIN, I., AND TOMSON, T. Risk factors for sudden unexpected death in epilepsy: a case control study. *The Lancet 353*, 9156 (1999), 888–893.

[132] NOBLE, W. What is a support vector machine? *Nature Biotechnology 24*, 12 (2006), 1565–1567.

[133] NOVAK, P., AND NOVAK, V. Time/frequency mapping of the heart rate, blood pressure and respiratory signals. *Medical and Biological Engineering and Computing 31*, 2 (Mar 1993), 103–10.

[134] NOVAK, V., REEVES, A., NOVAK, P., LOW, P., AND SHARBROUGH, F. Time-frequency mapping of RR interval during complex partial seizures of temporal lobe origin. *Journal of the Autonomic Nervous System 77*, 2-3 (1999), 195–202.

[135] OBRIST, P. Skin resistance levels and galvanic skin response: Unilateral differences. *Science 139*, 3551 (1963), 227.

[136] PAPEZ, J., AND NEYLAN, T. A proposed mechanism of emotion. *Journal of Neuropsychiatry and Clinical Neurosciences 7*, 1 (1995), 102–112.

[137] PATEL, S., LORINCZ, K., HUGHES, R., HUGGINS, N., GROWDON, J., STANDAERT, D., AKAY, M., DY, J., WELSH, M., AND BONATO, P. Monitoring motor fluctuations in patients with Parkinson's disease using wearable sensors. *IEEE Transactions on Information Technology in Biomedicine 13*, 6 (2009), 864–873.

[138] PATEL, S., MANCINELLI, C., DALTON, A., PATRITTI, B., PANG, T., SCHACHTER, S., AND BONATO, P. Detecting epileptic seizures using wearable sensors. In *Bioengineering Conference, 2009 IEEE 35th Annual Northeast* (2009), IEEE, pp. 1–2.

[139] PEZZELLA, M., STRIANO, P., CIAMPA, C., ERRICHIELLO, L., PENZA, P., AND STRIANO, S. Severe pulmonary congestion in a near miss at the first seizure: Further evidence for respiratory dysfunction in sudden unexpected death in epilepsy. *Epilepsy & Behavior 14*, 4 (2009), 701–702.

[140] PICARD, R., AND SCHEIRER, J. The galvactivator: A glove that senses and communicates skin conductivity. In *Proceedings from the 9th International Conference on Human-Computer Interaction, New Orleans* (2001), Citeseer.

[141] POH, M., SWENSON, N., AND PICARD, R. A Wearable Sensor for Unobtrusive, Long-Term Assessment of Electrodermal Activity. *IEEE Transactions on Biomedical Engineering 57*, 5 (2010), 1243–1252.

[142] POMERANZ, B., MACAULAY, R., CAUDILL, M., KUTZ, I., ADAM, D., GORDON, D., KILBORN, K., BARGER, A., SHANNON, D., COHEN, R., ET AL. Assessment of autonomic function in humans by heart rate spectral analysis. *American Journal of Physiology-Heart and Circulatory Physiology 248*, 1 (1985), H151.

[143] POP-JORDANOVA, N., ZORCEC, T., AND DEMERDZIEVA, A. Electrodermal biofeedback in treating psychogenic nonepileptic seizures. *Prilozi 26* (2005), 43–51.

[144] PURVES, S., WILSON-YOUNG, M., AND SWEENEY, V. Sudden death in epilepsy: single case report with video-EEG documentation. *Epilepsia 33*, suppl 3 (1992), 123.

[145] QU, H., AND GOTMAN, J. A patient-specific algorithm for the detection of seizure onset in long-term EEG monitoring: possible use as a warning device. *IEEE Transactions on Biomedical Engineering 44*, 2 (2002), 115–122.

[146] RAUSCHER, G., DEGIORGIO, A., MILLER, P., AND DEGIORGIO, C. Sudden unexpected death in epilepsy associated with progressive deterioration in heart rate variability. *Epilepsy & Behavior* (2011), Epub ahead of print.

[147] RICKLES JR, W., AND DAY, J. Electrodermal activity in non-palmer skin sites. *Psychophysiology 4*, 4 (2007), 421–435.

[148] RONKAINEN, E., ANSAKORPI, H., HUIKURI, H., MYLLYLÄ, V., ISOJÄRVI, J., AND KORPELAINEN, J. Suppressed circadian heart rate dynamics in temporal lobe epilepsy. *Journal of Neurology, Neurosurgery & Psychiatry 76*, 10 (2005), 1382.

[149] SAAB, M., AND GOTMAN, J. A system to detect the onset of epileptic seizures in scalp EEG. *Clinical Neurophysiology 116*, 2 (2005), 427–442.

[150] SAFFITZ, J. E. Sympathetic neural activity and the pathogenesis of sudden cardiac death. *Heart Rhythm 5*, 1 (2008), 140 – 141.

[151] SAKAMOTO, K., SAITO, T., ORMAN, R., KOIZUMI, K., LAZAR, J., SALCICCIOLI, L., AND STEWART, M. Autonomic consequences of kainic acid-induced limbic cortical seizures in rats: peripheral autonomic nerve activity, acute cardiovascular changes, and death. *Epilepsia 49*, 6 (Jun 2008), 982–96.

[152] SATO, K., KANG, W., SAGA, K., AND SATO, K. Biology of sweat glands and their disorders. i. normal sweat gland function. *Journal of the American Academy of Dermatology 20*, 4 (1989), 537.

[153] SATO, K., KANG, W., SAGA, K., AND SATO, K. Biology of sweat glands and their disorders. ii. disorders of sweat gland function. *Journal of the American Academy of Dermatology 20*, 5 Pt 1 (1989), 713.

[154] SCANAILL, C., CAREW, S., BARRALON, P., NOURY, N., LYONS, D., AND LYONS, G. A review of approaches to mobility telemonitoring of the elderly in their living environment. *Annals of Biomedical Engineering 34*, 4 (2006), 547–563.

[155] SCHELL, A., DAWSON, M., RISSLING, A., VENTURA, J., SUBOTNIK, K., GITLIN, M., AND NUECHTERLEIN, K. Electrodermal predictors of functional outcome and negative symptoms in schizophrenia. *Psychophysiology 42*, 4 (2005), 483–492.

[156] SCHLIACK, H., AND SCHIFFTER, R. Neurophysiologie und Pathophysiologie der Schweißsekretion. *Handbuch der Haut-und Geschlechtskrankheiten, Bd 1*, 4 (1979), 349–458.

[157] SCHRAEDER, P., AND LATHERS, C. Paroxysmal autonomie dysfunction, epileptogenic activity and sudden death. *Epilepsy Research 3*, 1 (1989), 55–62.

[158] SCHULC, E., UNTERBERGER, I., SABOOR, S., HILBE, J., ERTL, M., AMMENWERTH, E., TRINKA, E., AND THEM, C. Measurement and quantification of generalized tonic-clonic seizures in epilepsy patients by means of accelerometry-An explorative study. *Epilepsy Research* (2011).

[159] SCHULZE-BONHAGE, A., SALES, F., WAGNER, K., TEOTONIO, R., CARIUS, A., SCHELLE, A., AND IHLE, M. Views of patients with epilepsy on seizure prediction devices. *Epilepsy & Behavior* (2010).

[160] SEVCENCU, C., AND STRUIJK, J. Autonomic alterations and cardiac changes in epilepsy. *Epilepsia 51*, 5 (2010), 725–737.

[161] SHASTRI, D., MERLA, A., TSIAMYRTZIS, P., AND PAVLIDIS, I. Imaging Facial Signs of Neurophysiological Responses. *IEEE Transactions on Biomedical Engineering 56*, 2 (2009), 477.

[162] SHIELDS, S., MACDOWELL, K., FAIRCHILD, S., AND CAMPBELL, M. Is mediation of sweating cholinergic, adrenergic, or both? A comment on the literature. *Psychophysiology 24*, 3 (2007), 312–319.

[163] SHOEB, A., EDWARDS, H., CONNOLLY, J., BOURGEOIS, B., TED TREVES, S., AND GUTTAG, J. Patient-specific seizure onset detection. *Epilepsy & Behavior 5*, 4 (2004), 483–498.

[164] SILLANPÄÄ, M., AND SHINNAR, S. Long-Term Mortality in Childhood-Onset Epilepsy. *New England Journal of Medicine 363*, 26 (2010), 2522–2529.

[165] SIMON, R., AMINOFF, M., AND BENOWITZ, N. Changes in plasma catecholamines after tonic-clonic seizures. *Neurology 34*, 2 (1984), 255.

[166] SLEIGHT, P., LA ROVERE, M., MORTARA, A., PINNA, G., MAESTRI, R., LEUZZI, S., BIANCHINI, B., TAVAZZI, L., AND BERNARDI, L. Physiology and pathophysiology of heart rate and blood pressure variability in humans: is power spectral analysis largely an index of baroreflex gain? *Clinical Science 88*, 1 (1995), 103.

[167] SO, E. What is known about the mechanisms underlying SUDEP? *Epilepsia 49* (2008), 93–98.

[168] SO, E., SAM, M., AND LAGERLUND, T. Postictal central apnea as a cause of SUDEP: evidence from near-SUDEP incident. *Epilepsia 41*, 11 (2000), 1494–1497.

[169] SO, E. L. What is known about the mechanisms underlying sudep? *Epilepsia 49* (Dec 2008), 93–98.

[170] SPERLING, M., HARRIS, A., NEI, M., LIPORACE, J., AND O'CONNOR, M. Mortality after epilepsy surgery. *Epilepsia 46*, s11 (2005), 49–53.

[171] STEIN, P., AND KLEIGER, M. Insights from the study of heart rate variability. *Annual Review of Medicine 50*, 1 (1999), 249–261.

[172] STÖLLBERGER, C., HUBER, J., ENZELSBERGER, B., AND FINSTERER, J. Fatal outcome of epileptic seizure-induced takotsubo syndrome with left ventricular rupture. *European Journal of Neurology 16*, 6 (2009), e116–e117.

[173] STRAUSS, M., REYNOLDS, C., HUGHES, S., PARK, K., MCDARBY, G., AND PICARD, R. The handwave bluetooth skin conductance sensor. *Affective Computing and Intelligent Interaction* (2005), 699–706.

[174] SUN, M., AND HILL, J. A method for measuring mechanical work and work efficiency during human activities. *Journal of Biomechanics 26*, 3 (1993), 229–241.

[175] SURGES, R., SCOTT, C. A., AND WALKER, M. C. Enhanced qt shortening and persistent tachycardia after generalized seizures. *Neurology 74*, 5 (Feb 2010), 421–6.

[176] SURGES, R., STRZELCZYK, A., SCOTT, C., WALKER, M., AND SANDER, J. Postictal generalized electroencephalographic suppression is associated with generalized seizures. *Epilepsy & Behavior* (2011).

[177] SURGES, R., THIJS, R. D., TAN, H. L., AND SANDER, J. W. Sudden unexpected death in epilepsy: risk factors and potential pathomechanisms. *Nature Reviews Neurology 5*, 9 (Sep 2009), 492–504.

[178] SWALLOW, R., HILLIER, C., AND SMITH, P. Sudden unexplained death in epilepsy (SUDEP) following previous seizure-related pulmonary oedema: case report and review of possible preventative treatment. *Seizure 11*, 7 (2002), 446–448.

[179] TAPIA, E., INTILLE, S., AND LARSON, K. Activity recognition in the home using simple and ubiquitous sensors. *Pervasive Computing* (2004), 158–175.

[180] TARCHANOFF, J. Décharges électriques dans la peau de lhomme sous linfluence de lexcitation des organes des sens et de différentes formes dactivité psychique. *Comptes Rendus des séances de la Société de Biologie 9* (1889), 447–51.

[181] TARVAINEN, M., KOISTINEN, A., VALKONEN-KORHONEN, M., PARTANEN, J., AND KARJALAINEN, P. Analysis of galvanic skin responses with principal components and clustering techniques. *IEEE Transactions on Biomedical Engineering 48*, 10 (2001), 1071–1079.

[182] TARVAINEN, M. P., RANTA-AHO, P. O., AND KARJALAINEN, P. A. An advanced detrending method with application to HRV analysis. *IEEE Transactions on Biomedical Engineering 49*, 2 (2002), 172–5.

[183] TÉLLEZ-ZENTENO, J., RONQUILLO, L., AND WIEBE, S. Sudden unexpected death in epilepsy: Evidence-based analysis of incidence and risk factors. *Epilepsy Research 65*, 1-2 (2005), 101–115.

[184] TEMEC INSTRUMENTS. *Vitaport* (2010).

[185] TERRENCE, C., RAO, G., AND PERPER, J. Neurogenic pulmonary edema in unexpected, unexplained death of epileptic patients. *Annals of Neurology 9*, 5 (1981), 458–464.

[186] THOMAS, P., LANDRE, E., SUISSE, G., BRELOIN, J., DOLISI, C., AND CHATEL, M. Syncope anoxo-ischémique par dyspnée obstructive au cours d'une crise partielle complexe temporale droite. *Epilepsies 8*, 4 (1996), 339–346.

[187] THOUGHT TECHNOLOGY INC. *Flexcomp* (2010).

[188] TOMSON, T., ERICSON, M., IHRMAN, C., AND LINDBLAD, L. Heart rate variability in patients with epilepsy1. *Epilepsy Research 30*, 1 (1998), 77–83.

[189] TOMSON, T., NASHEF, L., AND RYVLIN, P. Sudden unexpected death in epilepsy: current knowledge and future directions. *Lancet Neurology 7*, 11 (2008), 1021–1031.

[190] TOMSON, T., WALCZAK, T., SILLANPAA, M., AND SANDER, J. Sudden unexpected death in epilepsy: a review of incidence and risk factors. *Epilepsia 46*, s11 (2005), 54–61.

[191] TOTH, V., HEJJEL, L., FOGARASI, A., GYIMESI, C., ORSI, G., SZUCS, A., KOVACS, N., KOMOLY, S., EBNER, A., AND JANSZKY, J. Periictal heart rate variability analysis suggests long-term postictal autonomic disturbance in epilepsy. *European Journal of Neurology 17*, 6 (2010), 780–787.

[192] TRONSTAD, C., GJEIN, G., GRIMNES, S., MARTINSEN, G., KROGSTAD, A., AND FOSSE, E. Electrical measurement of sweat activity. *Physiological Measurement 29*, 6 (2008), 407.

[193] VAEZMOUSAVI, S., BARRY, R., RUSHBY, J., AND CLARKE, A. Arousal and activation effects on physiological and behavioral responding during a continuous performance task. *Acta Neurobiologiae Experimentalis 67*, 4 (2007), 461.

[194] VAN BUREN, J. Some autonomic concomitants of ictal automatism; a study of temporal lobe attacks. *Brain 81*, 4 (1958), 505.

[195] VANOLI, E., DE FERRARI, G., STRAMBA-BADIALE, M., HULL JR, S., FOREMAN, R., AND SCHWARTZ, P. Vagal stimulation and prevention of sudden death in conscious dogs with a healed myocardial infarction. *Circulation Research 68*, 5 (1991), 1471.

[196] VAPNIK, V. *The nature of statistical learning theory.* Springer Verlag, 2000.

[197] VENABLES, P. Autonomic activity. *Annals of the New York Academy of Sciences 620*, 1 (1991), 191–207.

[198] VIGLIONE, S., AND WALSH, G. Proceedings: Epileptic seizure prediction. *Electroencephalography and Clinical Neurophysiology 39*, 4 (1975), 435.

[199] VIGOUROUX, R. Sur le role de la resistance electrique des tissues dans lelectrodiagnostic. *Comptes Rendes Societe de Biologie 31* (1879), 336–9.

[200] VILA, J., PALACIOS, F., PRESEDO, J., FERNANDEZ-DELGADO, M., FELIX, P., AND BARRO, S. Time-frequency analysis of heart-rate variability. *IEEE Engineering in Medicine and Biology Magazine 16*, 5 (1997), 119–126.

[201] VLACHOS, M., MEEK, C., VAGENA, Z., AND GUNOPULOS, D. Identifying similarities, periodicities and bursts for online search queries. In *Proceedings of the 2004 ACM SIGMOD International Conference on Management of Data* (2004), ACM, pp. 131–142.

[202] WALCZAK, T., LEPPIK, I., DAMELIO, M., RARICK, J., SO, E., AHMAN, P., RUGGLES, K., CASCINO, G., ANNEGERS, J., AND HAUSER, W. Incidence and risk factors in sudden unexpected death in epilepsy. *Neurology 56*, 4 (2001), 519.

[203] WALLIN, B. Sympathetic Nerve Activity Underlying Electrodermal and Cardiovascular Reactions in Man. *Psychophysiology 18*, 4 (1981), 470–476.

[204] WEINAND, M., CARTER, L., EL-SAADANY, W., SIOUTOS, P., LABINER, D., AND OOMMEN, K. Cerebral blood flow and temporal lobe epileptogenicity. *Neurosurgical Focus 1*, 5 (1996), 5.

[205] WILLIAMSON, P., FOWLES, D., AND WEINBERGER, M. Electrodermal potential and conductance measurements clinically discriminate between cystic fibrosis and control patients. *Pediatric Research 19*, 8 (1985), 810.

[206] WORLD HEALTH ORGANIZATION. *Atlas: Epilepsy Care in the World* (2005).

[207] YOKOTA, T., AND FUJIMORI, B. Effects of brain-stem stimulation upon hippocampal electrical activity, somatomotor reflexes and autonomic functions. *Electroencephalography and Clinical Neurophysiology 16*, 4 (1964), 375–382.

[208] YOKOTA, T., SATO, A., AND FUJIMORI, B. Inhibition of sympathetic activity by stimulation of limbic system. *The Japanese Journal of Physiology 13* (1963), 138.

[209] ZHOU, S., JUNG, B., TAN, A., TRANG, V., GHOLMIEH, G., HAN, S., LIN, S., FISHBEIN, M., CHEN, P., AND CHEN, L. Spontaneous stellate ganglion nerve activity and ventricular arrhythmia in a canine model of sudden death. *Heart Rhythm 5*, 1 (2008), 131–139.